Production of γ-valerolactone from the hydrogenation of levulinic acid or alkyl levulinates : calorimetry and kinetic study

Yanjun Wang

Normandie Université

THESE

Pour obtenir le diplôme de doctorat

Spécialité Génie des Procédé

Préparée au sein de « l'Institut National des Sciences Appliquées de Rouen Normandie »

Production of γ-valerolactone from the hydrogenation of levulinic acid or alkyl levulinates: Calorimetry and Kinetic study

Présentée et soutenue par
Yanjun WANG

Thèse soutenue publiquement le 20/03/2020 devant le jury composé de		
Igor PLAZL	Professor, University of Ljublijana, Slovenia	Rapporteur
Henrik GRÉNMAN	Professor, Åbo Akademi University, Finland	Rapporteur
Claude DE BELLEFON	Directeur de recherche CNRS, Laboratoire de Génie des Procédés Catalytiques, France.	Examinateur
Tapio SALMI	Professor, Åbo Akademi University, Finland	Examinateur
Vincenzo RUSSO	Assistant professor, University of Naples Federico II Naples, Italy	Examinateur
Lamiae VERNIÈRES-HASSIMI	MCF, LSPC, INSA Rouen, France	Encadrante de thèse
Sébastien LEVENEUR	MCF-HDR, LSPC, INSA Rouen, France	Directeur de thèse

Thèse dirigée par

Dr. HDR Sébastien LEVENEUR, **laboratoire LSPC EA 4704**

CHINA SCHOLARSHIP COUNCIL

INSA INSTITUT NATIONAL DES SCIENCES APPLIQUÉES ROUEN NORMANDIE

ED PSIME

LSPC Laboratoire de sécurité des procédés chimiques

“士不可以不弘毅，

任重而道远”

《论语·泰伯章》

WANG Yanjun

Born in 17/11/1989, Wendeng, China

Education:

2016.10-2020.4	Ph.D candidate in chemical engineering in LSPC (Laboratoire de Sécurité des Procédés Chimiques), INSA Rouen, France.
2013.9-2016.9	Master of Engineering in Chemical Engineering for Energy, Biomass Catalytic Conversion Lab, College of Energy, Xiamen university, China.

Research experience: Synthesis of value-added products from biomass raw materials and its derivatives such as bamboo pulp, C6 sugars and levulinic acid, e.g., reductive amination of levulinic acid.

2008.9-2012.6	Bachelor in Environmental Science, College of Environmental Science & Engineering, Nanjing University of Information Science & Technology, China.

Supporting program:

- 2016 UT/INSA-CSC program (42months, Chinese government scholarship);
- AMED project funded with the support from the European Union with the European

Regional Development Fund (ERDF) and from the Regional Council of Normandie;

- Project PHC Galileo "Emergency response in 2nd generation biomass valorization processes";
- Finnish-French project: Biomass valorization: Process Safety & Process intensification

Teaching and supervision experiences:

a) 54 hours teaching and practice in analytical and calorimetry courses for engineer students.
b) 2018.2-2018.7 Supervision of research project (Mariasole Cipolletta, Bologna University) on "Structure-reactivity study on hydrogenation of levulinic acid and its esters to γ-valerolactone".
c) 2019.6-2019.9 Participation to the supervision of bachelor thesis (Bastien Baclawski, INSA Rouen) on "Simulation of thermal behavior for production of γ-valerolactone under adiabatic conditions".
d) 2019.4-2019.6 Participation to the supervision of bachelor thesis (Quentin Gregoire, INSA Rouen) on "Henry's constant measurement for hydrogen in water and alcohols".
e) 2017.4-2017.6 Participation to the supervision of bachelor thesis (Marta Lazúen Muros, José Luis Vidal Castaño, INSA Rouen) on "Hydrogenation of levulinic acid with formic acid to γ-valerolactone in water".

Acknowledgements

The research for my doctoral thesis is supported by the cooperation program between China scholarship council (CSC) and the UTs and INSAs (France). The work is performed at the Laboratoire de Sécurité des Procédés Chimiques in INSA Rouen Normandie during the years of 2016-2020.

I would like to say that my study in INSA Rouen Normandie is an impressive experience. I have experienced so much that I do believe this wonderful period leaves me a huge spiritual wealth. I would like to thank all the people and all the things I experienced that enrich my study life and makes me progress all the time.

I would like to thank China Scholarship Council (CSC) for providing me the opportunity to study in France with scholarship. The cooperation program between CSC and UTs and INSAs in France provided so interesting project about biomass valorization that I would like to express my sincere gratitude to this program.

I would like to thank my supervisor Dr. Sébastien Leveneur for his supervision on my study and also on my life. His enthusiasm, preciseness, diligent, efficiency on my PhD project impressed me a lot. Each time I encounter problems for experiments, he is always there to listen to me and give me advices immediately. His huge storage of knowledge and wide horizon induce me to get more interests in research for biomass valorization and obtain more technic skills and study methods. I would like to say that he is so kind that he always stands with me and helps me. Besides the project, he also helps me a lot for my family. I would like to sincerely appreciate all his helps.

I would like to thank Lamiae Vernières-Hassimi as my encadrant for the doctoral thesis. She gives me lots of advices on safety aspect of my study. I would also like to thank all the staffs from LSPC. They are very kind to me and help me when I need. The activities organized by the Lab LSPC leave me a beautiful memory. In particular, I would like to thank Béchara Taouk, the director of LSPC for his gentilesse and help. I would like to

thank Bruno Daronat, Sylvie Poubelle and Jean-Pierre Hébert for their help for my experiments. I would like to thank CSI member Isabelle Polaert and Valeria Casson Moreno. For lots of affaires, I would like to thank Pereira De Araujo Maria for her kindness, caring and help. I would also express my sincere gratitude to Stéphane Marcotte, Christine Devouge-Boyer, Mélanie Mignot from COBRA for your help in chemical analysis.

I would like to thank all my PhD and master colleagues in LSPC. Working with you is a wonderful experience and I'm happy to know more about cultures and funny stories from you all. Specially, I would like to thank Xiaoshuang Cai, Chetna Mohabeer, Elizabeth Garcia Hernandez, Xiaojia Lu, Jundong Wang, Jie Xu for your kindness, help and encouragements during these years. You paint a special color for my life in France and the memory with you is so lovely.

I would like to thank all of jury members of my doctoral thesis defense: Igor Plazl, Henrik Grénman, Claude De Bellefon, Tapio Salmi, Vincenzo Russo for your time and availability for my defense.

Finally, I would like to thank my wife Liwen CHEN and my little son Zhiyuan WANG, the life with you is so bright that I can encounter with troubles bravely and firmly. You bring me so much happiness that I really appreciate your accompany and understanding. Thanks to strong support of my wife, I can focus more on work. Without you and our son, I can't imagine how the life will be. I love you!

Yanjun Wang
Rouen, France
March, 2020

Remerciements

Les recherches pour ma thèse sont soutenues par le programme de coopération entre le China scholarship council (CSC) et les UTs et INSAs (France). Les travaux sont réalisés au Laboratoire de Sécurité des Procédés Chimiques de l'INSA de Rouen Normandie pendant les années 2016-2020. Je voudrais dire que mon étude à l'INSA de Rouen Normandie est une expérience impressionnante. J'ai tellement vécu que je crois que cette période merveilleuse me laisse une immense richesse spirituelle. Je tiens à remercier toutes les personnes et toutes les choses que j'ai vécues qui enrichissent ma vie d'étudiant et me font progresser sans cesse.

Je tiens à remercier le China Scholarship Council (CSC) de m'avoir donné la possibilité d'étudier en France grâce à une bourse. Le programme de coopération entre le CSC et les UTs et les INSAs en France a permis de réaliser un projet si intéressant sur la valorisation de la biomasse que je tiens à exprimer ma sincère gratitude à ce programme.

Je tiens à remercier mon superviseur, Dr Sébastien Leveneur, pour sa supervision de mon étude et de ma vie. Son enthousiasme, sa précision, son assiduité et son efficacité dans mon projet m'ont beaucoup impressionné. Chaque fois que je rencontre des problèmes pour des expériences, il est toujours là pour m'écouter et me donner des conseils immédiatement. Son immense réservoir de connaissances et son large horizon m'incitent à m'intéresser davantage à la recherche pour la valorisation de la biomasse et à acquérir plus de compétences techniques et de méthodes d'étude. Je voudrais dire qu'il est si gentil qu'il est toujours à mes côtés et qu'il m'aide. Outre le projet, il m'aide aussi beaucoup pour ma famille. J'aimerais sincèrement apprécier toute son aide.

Je tiens à remercier Lamiae Vernières-Hassimi, mon encadrante pour la thèse. Elle me donne beaucoup de conseils sur l'aspect sécurité de mon étude. Je tiens également à remercier l'ensemble du personnel du LSPC. Ils sont très gentils avec moi et m'aident quand j'en ai besoin. Les activités organisées par le Lab LSPC me laissent un beau souvenir. Je

voudrais remercier en particulier Béchara Taouk, le directeur du LSPC pour sa gentillesse et son aide. Je tiens à remercier Bruno Daronat, Sylvie Poubelle et Jean-Pierre Hébert pour leur aide sur mes expériences. Je tiens à remercier Isabelle Polaert et Valeria Casson Moreno, membres du CSI. Pour beaucoup d'affaires, je voudrais remercier Pereira De Araujo Maria pour sa gentillesse, son attention et son aide. Je voudrais également exprimer ma sincère gratitude à Stéphane Marcotte, Christine Devouge-Boyer, Mélanie Mignot du COBRA pour votre aide sur l'analyse chimique.

Je tiens à remercier tous mes collègues et maîtrises du LSPC. Travailler avec vous est une expérience merveilleuse et je suis heureux d'en savoir plus sur les cultures et les histoires drôles de vous tous. Je tiens à remercier tout particulièrement Xiaoshuang Cai, Chetna Mohabeer, Elizabeth Garcia Hernandez, Xiaojia Lu, Jundong Wang, Jie Xu pour votre gentillesse, votre aide et vos encouragements au cours de ces années. Vous peignez une couleur spéciale pour ma vie en France et le souvenir que j'ai de vous est si beau.

Je tiens à remercier tous les membres du jury de ma soutenance: Igor Plazl, Henrik Grénman, Claude De Bellefon, Tapio Salmi, Vincenzo Russo pour votre temps et votre disponibilité pour ma soutenance.

Enfin, je voudrais remercier ma femme Liwen CHEN et mon petit fils Zhiyuan WANG, la vie avec vous est si brillante que je peux affronter les problèmes avec courage et fermeté. Vous m'apportez tellement de bonheur que j'apprécie vraiment votre accompagnement et votre compréhension. Grâce au soutien de ma femme, je peux me concentrer davantage sur mon travail. Sans toi et notre fils, je ne peux pas imaginer comment sera la vie. Je vous aime !

Yanjun Wang
Rouen, France
Mars, 2020

Abstract

With the development of society and economy all over the world, fossil energy plays a fundamental role in the economy, society and politics. Till now, different renewable energy are explored to be an alternative for energy supply, such as wind, solar, hydro- and biomass energy. Among these renewable energy, biomass has been regarded as the organic carbon source which can be applied for production of fuels, chemicals, materials to substitute the corresponding petroleum-based products. Although the structure and composition of biomass are complex, significant efforts have been done in developing biorefineries as the bio-based products have shown attractive characteristics such as sustainable, biodegradable and biocompatible.

Among the bio-based chemicals, production of platform molecules such as levulinic acid (LA) and its esters and its further upgrading to γ-valerolactone (GVL) is one of attractive way for biomass valorization. Levulinic acid and its esters can be obtained through hydrolysis and alcoholysis reactions by using cellulose and hemicellulose. By further hydrogenation reaction, γ-valerolactone is produced and it is also regarded as a platform molecule for further upgrading to biofuels and chemicals with wide application. To scale-up the hydrogenation reaction and to find the optimum operating conditions towards safety and cost, the following questions should be answered:

-What is the thermal risk of this reaction?
-Which starting materials to choose (LA or esters)?
-For a better energy integration of this process, how to measure the reaction enthalpies?

Herein, at first, thermal risk assessment for hydrogenation of levulinic acid to γ-valerolactone catalyzed by Ru/C in water was performed. A simplified kinetic model including energy balance under near-adiabatic conditions was developed. Experiments at different operating conditions were performed in calorimeter ARSST (Advanced Reactive System Screening Tool) to estimate the kinetic constants of this reaction system. Two thermal risk parameters TMR_{ad} (Time to reach the Maximum temperature Rate under

adiabatic condition), which characterizes the probability of thermal runaway, and ΔT_{ad} (the difference between the maximum and initial reaction temperature), which characterizes the severity of thermal runaway, were used to assess the thermal risk of this reaction system with the aid of a risk matrix. Based on the model built, these two risk parameters were estimated and the thermal risk was assessed depending on different operating conditions, such as temperature, LA concentration, hydrogen pressure and catalyst loading. Through this thermal risk assessment, it was possible to know the safe operation conditions for this reaction system.

Secondly, based on the experiments, it was noticed that levulinic acid is quite corrosive. Thus, it is important to compare the kinetics of GVL production from different starting materials. Application of the concept of Linear Free Energy Relationships, i.e., Taft equation, to hydrogenation of levulinic acid and its corresponding esters to γ-valerolactone catalyzed by Ru/C was performed. The goal of this study was to find the relationships between reactant structure and their reactivity. A kinetic model including gas-liquid mass transfer phenomenon and Taft equation was developed. Experiments with different initial conditions were performed in a batch reactor under isothermal and isobaric conditions to estimate the kinetic constants and Taft parameters. γ-valerolactone was used as a solvent to allow the solubility of the different reactants, namely, LA, methyl levulinate (ML), ethyl levulinate (EL) and n-butyl levulinate (BL). These four substrates are the most common produced levulinate derived chemicals. It was demonstrated that the kinetics of the first step, i.e., hydrogenation of LA, ML, EL or BL to the corresponding intermediates and the kinetics of the second step, i.e., ring-closure follow Taft equation. The kinetics were compared and the overall reaction rate follow the order: $r_{GVL\ from\ LA} > r_{GVL\ from\ ML} > r_{GVL\ from\ EL} > r_{GVL\ from\ BL}$. The polar and steric effect of the substituents were studied according to the Taft equation and it is shown that polar effect governs the kinetics of both reaction steps.

Thirdly, the knowledge of reaction enthalpies is important to optimize the energy consumption in a chemical process. Thus, this part is also fundamental to estimate the operating cost and capital investment. The estimation of such thermodynamic constants by using different thermodynamic models can be hazardous, because in this study GVL was

used as a solvent and there are no data concerning the intermediates. Hence, experimental determination of reaction enthalpy for production of γ-valerolactone was performed. Hydrogenation of methyl levulinate (ML) to GVL catalyzed by Ru/C was selected for this study. A method which links calorimetry measurement with composition analysis was developed to determine the reaction enthalpy of the overall reaction and two consecutive steps. The calorimeter RC1 and Tian-Calvet calorimeter C80 were used to measure the heat released or absorbed by the reaction system. Combined with Gas-Chromatography analysis, it is possible to determine the reaction enthalpy for the overall reaction and two consecutive steps. It was found that the overall reaction enthalpy was -51.5 $kJ.mol^{-1}$, which indicates that the reaction for production of GVL from ML is exothermic. The reaction enthalpy for the first hydrogenation step was calculated to be -58.66 $kJ.mol^{-1}$, and the reaction enthalpy for the second ring-closure step was calculated to be +7.16 $kJ.mol^{-1}$.

A brief summary of this doctoral thesis work is shown in the figure below:

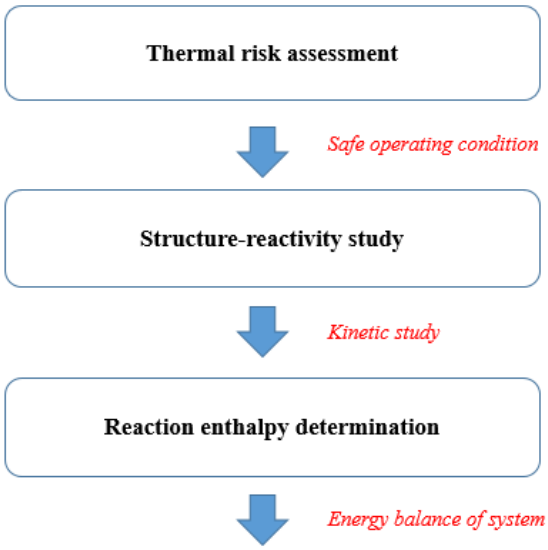

Graphical abstract for the doctoral thesis of Yanjun WANG.

Résumé

Avec le développement de la société et de l'économie dans le monde entier, l'énergie fossile joue un rôle fondamental dans l'économie, la société et la politique. Jusqu'à présent, différentes énergies renouvelables sont explorées pour constituer une alternative à l'approvisionnement énergétique, comme l'énergie éolienne, solaire, hydraulique et celle issue de la biomasse. Parmi ces énergies renouvelables, la biomasse a été considérée comme la source de carbone organique qui peut être utilisée pour la production de carburants, de produits chimiques, de matériaux pour remplacer les produits similaires issus de la pétrochimie. Bien que la structure et la composition de la biomasse soient complexes, des efforts importants ont été faits pour développer les bioraffineries, car les produits à base de biomasse ont montré des caractéristiques attrayantes telles que la durabilité, la biodégradabilité et la biocompatibilité.

Parmi les produits chimiques d'origine biologique, la production de molécules plates-formes telles que l'acide lévulinique (LA) et ses esters et le γ-valérolactone (GVL) est l'un des moyens intéressants de valorisation de la biomasse. L'acide lévulinique et ses esters peuvent être obtenus par des réactions d'hydrolyse et d'alcoolyse en utilisant de la cellulose et de l'hémicellulose. Par une réaction d'hydrogénation supplémentaire, on obtient la γ-valérolactone. Cette molécule est également considérée comme une plateforme pour la valorisation en biocarburants et de produits chimiques ayant de nombreuses applications. Pour intensifier la réaction d'hydrogénation et pour trouver les conditions opératoires optimales en termes de sécurité et de coût, il convient de répondre aux questions suivantes :

-Quel est le risque thermique de cette réaction ?
-Quelles matières premières à choisir (LA ou esters) ?
-Pour une meilleure intégration énergétique de ce processus, comment mesurer les enthalpies de réaction ?

Dans un premier temps, une évaluation du risque thermique pour l'hydrogénation de l'acide lévulinique en γ-valérolactone catalysée par le Ru/C dans l'eau a été réalisée. Un modèle cinétique simplifié incluant le bilan énergétique dans le condition quasi-adiabatique a été développé. Des expériences dans des différentes conditions opératoires ont été réalisées dans le calorimètre ARSST (Advanced Reactive System Screening Tool) pour estimer les constantes cinétiques de ce système de réaction. Deux paramètres de risque thermique TMR_{ad} (Temps nécessaire pour atteindre le taux maximal de température en condition adiabatique), qui caractérise la probabilité d'emballement thermique, et ΔT_{ad} (différence entre la température maximale et la température initiale de la réaction), qui caractérise la gravité de l'emballement thermique, ont été utilisés pour évaluer le risque thermique de ce système de réaction à l'aide d'une matrice de risque. Sur la base de ce modèle, ces deux paramètres de risque ont été estimés et le risque thermique a été évalué en fonction de différentes conditions opératoires, telles que la température, la concentration en acide lévulinique, la pression d'hydrogène et la charge de catalyseur. Grâce à cette évaluation du risque thermique, il a été possible de connaître les conditions opératoires sûres de ce système de réaction.

Deuxièmement, sur la base des expériences, on a constaté que l'acide lévulinique est assez corrosif. Il est donc important de comparer la cinétique de la production de GVL à partir de différentes matières premières. On a appliqué le concept de relations linéaires d'énergie libre, i.e., l'équation de Taft, à l'hydrogénation de l'acide lévulinique et de ses esters correspondants en γ-valérolactone catalysée par Ru/C. Le but de cette étude était de trouver les relations entre les structures des réactifs et leur réactivité. Un modèle cinétique incluant le phénomène de transfert de masse gaz-liquide et l'équation de Taft a été développé. Des expériences avec différentes conditions initiales ont été réalisées dans un réacteur à fonctionnement discontinu dans des conditions isothermes et isobares pour estimer les constantes cinétiques et les paramètres de Taft. Le γ-valérolactone a été utilisé comme solvant pour permettre la solubilité des réactifs différents, LA, le lévulinate de méthyle (ML), le lévulinate d'éthyle (EL) et le lévulinate de n-butyle (BL). Ces quatre substrats sont les produits chimiques dérivés du lévulinate les plus couramment produit. Il a été démontré que la cinétique de la première étape, i.e., l'hydrogénation de LA, ML, EL ou BL en les

intermédiaires correspondants et la cinétique de la deuxième étape, i.e., la fermeture du cycle, suivent l'équation de Taft. Les cinétiques ont été comparées et la vitesse de réaction globale suit l'ordre suivant : $r_{GVL\ de\ LA} > r_{GVL\ de\ ML} > r_{GVL\ de\ EL} > r_{GVL\ de\ BL}$. Les effets polaires et stériques des substituants ont été étudiés selon l'équation de Taft et il est montré que l'effet polaire régit la cinétique des deux étapes de la réaction.

Troisièmement, la connaissance des enthalpies de réaction est importante pour optimiser la consommation d'énergie dans un processus chimique. Ainsi, cette partie est également fondamentale pour estimer les frais de fonctionnement et l'investissement en capital. L'estimation de ces constantes thermodynamiques en utilisant différents modèles thermodynamiques peut être dangereuse, car dans cette étude, le GVL a été utilisé comme solvant et il n'y a pas de données concernant les intermédiaires. C'est pourquoi une détermination expérimentale de l'enthalpie de réaction pour la production de γ-valérolactone a été réalisée. L'hydrogénation du lévulinate de méthyle (ML) en GVL catalysée par Ru/C a été choisie pour cette étude. Une méthode qui lie la mesure calorimétrique à l'analyse de la composition a été développée pour déterminer l'enthalpie de la réaction globale et deux étapes consécutives. Le calorimètre RC1 et le calorimètre Tian-Calvet C80 ont été utilisés pour mesurer la chaleur libérée ou absorbée par le système réactionnel. Combiné à l'analyse par chromatographie en phase gazeuse, il est possible de déterminer l'enthalpie de réaction pour la réaction globale et deux étapes consécutives. Il a été constaté que l'enthalpie globale de la réaction était de -51,5 $kJ.mol^{-1}$, ce qui indique que la réaction pour la production de GVL à partir de ML est exothermique. L'enthalpie de la réaction pour la première étape d'hydrogénation a été calculée à -58,66 $kJ.mol^{-1}$, et l'enthalpie de la réaction pour la deuxième étape de fermeture du cycle a été calculée à +7,16 $kJ.mol^{-1}$.

Un résumé de ce travail de thèse est présenté par la figure ci-dessous :

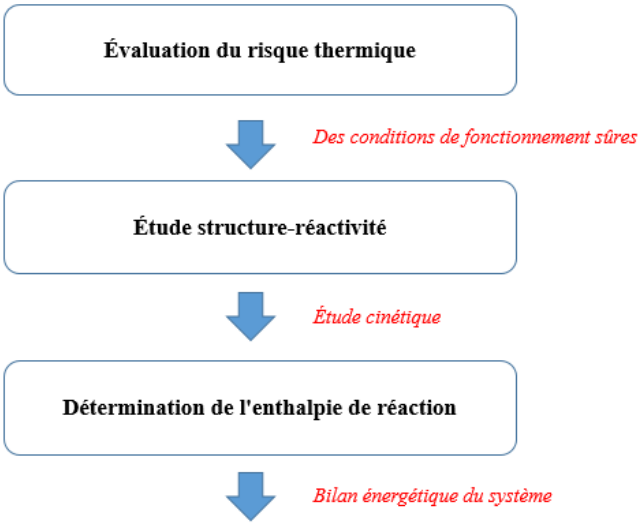

Résumé graphique pour la thèse de Yanjun WANG

Publications and Communications related to thesis

List of Publications:

1. Application of the concept of Linear Free Energy Relationships to the Hydrogenation of Levulinic acid and its corresponding esters. Wang Y, Cipolletta M, Vernières-Hassimi L, Casson-Moreno V, Leveneur S. Chemical Engineering Journal, 374 (2019): 822-831.
2. Thermal risk assessment of levulinic acid hydrogenation to γ-valerolactone. Wang Y, Vernières-Hassimi L, Casson-Moreno V, Hébert JP, Leveneur S. Organic Process Research & Development, 2018, 22(9): 1092-1100.

List of Communications:

Oral presentation

A.-L. Garbetti, V. Casson Moreno, S. Leveneur, L. Vernières-Hassimi, G. Antonioni, L. Abdelouahed, A. Tugnoli, Y. Wang, E. Salzano, L. Estel, V. Cozzani, "Risk assessment of levulinic acid production process from lignocellulosic biomass and upgrading to gamma-valerolactone"
Oral presentation for the 10th World Congress of Chemical Engineering, 1st-5th October 2017, Barcelona, Spain

Poster presentations

Y. Wang, M. Cipolletta, L. Vernières-Hassimi, V. Casson-Moreno, S. Leveneur, T. Salmi, "Kinetic modelling for hydrogenation of levulinic acid and its esters"
Poster presentation for ECCE 10 - European Congress of Chemical Engineering 15th-19th September, 2019, Florence, Italy

Y. Wang, L. Vernières-Hassimi, V. Casson-Moreno, S. Leveneur, "Intrinsic kinetic

constants versus safety parameters: hydrogenation of levulinic acid to γ-valerolactone”
Poster presentation for the 25th International Conference on Chemical Reaction Engineering ISCRE25, 20th-23rd May 2018, Florence, Italy.

Y. Wang, L. Vernières-Hassimi, S. Leveneur, “Production de γ-valerolactone: développement d’un procédé sûr et vert”
Poster presentation for the SFGP 2017 conference, 11th-13th July, 2017, Nancy, France.

Résumé étendu de la thèse

Production de γ-valérolactone par hydrogénation d'acide lévulinique ou de lévulinates d'alkyles : Étude calorimétrique et cinétique

Contenu

Chapitre I. Contexte de l'étude

La valorisation de l'énergie est l'une des questions les plus importantes dans le monde entier, car l'énergie soutient le développement de tous les aspects de notre société humaine. En effet, la localisation géographique des réserves de pétrole, considérées comme le "sang" de l'industrie moderne, n'est pas équilibrée à l'échelle mondiale et leur stockage diminue en raison de l'augmentation de la consommation d'énergie. Le pétrole a donc fortement influencé le développement de l'économie et de la société de chaque pays. Bien que l'industrie pétrolière offre un moyen facile et efficace d'approvisionnement en énergie, il est nécessaire de chercher une alternative pour remplacer le pétrole en raison de ses caractéristiques non durables et non renouvelables. Par ailleurs, l'utilisation du pétrole entraîne également l'émission de gaz à effet de serre qui est considérée comme la principale cause du changement climatique.

En tant que source de carbone renouvelable, la valorisation de la biomasse a suscité un grand intérêt dans le monde entier, avec des caractéristiques attrayantes car elle est abondante, durable et renouvelable. La biomasse lignocellulosique de deuxième génération n'a pas de concurrence avec le secteur alimentaire et a fait l'objet d'une plus grande attention au cours des dernières décennies. D'énormes quantités de produits peuvent être obtenues à partir de la biomasse lignocellulosique . Ainsi, des bioraffineries basées sur cette biomasse sont apparues et se sont développées régulièrement (Figure 1). Parmi ces produits dérivés de la biomasse, l'acide lévulinique (LA) et ses esters ont montré un grand potentiel en tant que molécules plateformes pour synthétiser et remplacer les produits correspondants à base de pétrole. Par exemple, on peut valoriser ces molécules, par hydrogénation, en une autre molécule plateforme : le γ-valérolactone (GVL).

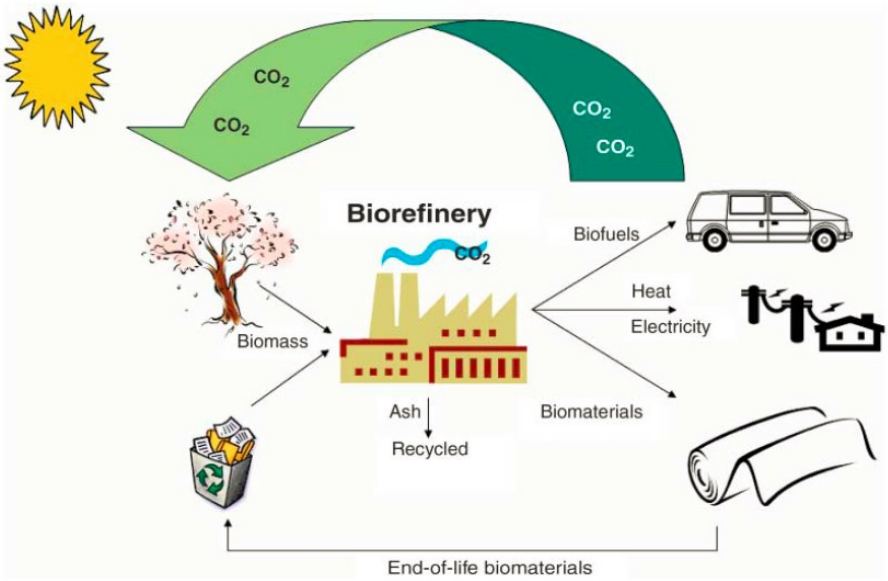

Figure 1. Le cycle totalement intégré agro-biocarburants-biomatériaux-biopuissance pour des technologies durables [11].

L'acide lévulinique (LA) est considéré comme l'une des 12 molécules plateformes d'origine biologique par le ministère de l'énergie américain en 2004. L'acide lévulinique et ses esters peuvent être obtenus par hydrolyse ou alcoolyse à partir de la cellulose de la biomasse lignocellulosique (Figure 2). Ils peuvent également être obtenus à partir d'hémicellulose. Avec deux groupes actifs, le groupe hydroxyle et le groupe carboxyle dans la molécule, l'acide lévulinique est une molécule plateforme polyvalente et facilement soluble dans l'eau, l'éthanol, l'acétone, l'éther diéthylique et d'autres solvants organiques. Par ailleurs, il possède un grand potentiel de conversion en de nombreuses molécules exceptionnelles telles que l'acide diphénolique (DPA), l'acide succinique, le méthyltétrahydrofurane (THF), le γ-valérolactone (GVL), l'acide succinique, les pyrrolidones, etc. par différents types de réactions (Figure 3). Ces séries de produits chimiques peuvent être largement utilisées comme polymères, herbicides, produits pharmaceutiques, biocarburants, plastifiants, solvants, etc. en remplaçant les produits chimiques à base de pétrole en raison de leurs caractéristiques biocompatibles et biodégradables. Les esters de l'acide lévulinique sont considérés comme une molécule alternative de cet acide pour produire les produits à forte valeur ajoutée et sont également utilisés comme composants d'additifs pour les mélanges de carburants et comme biolubrifiants.

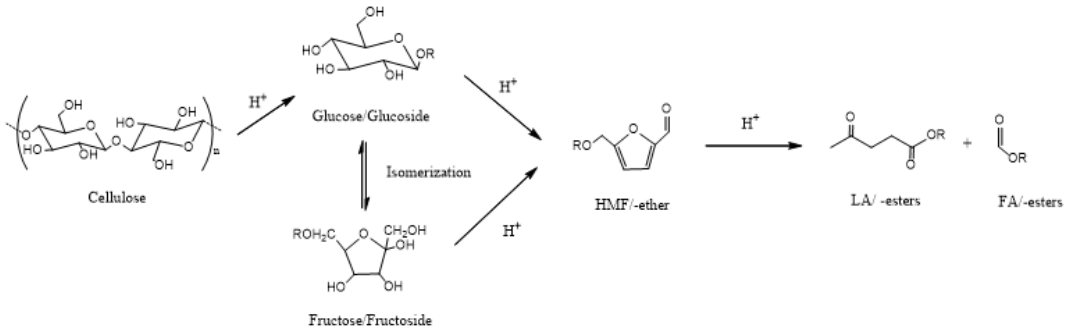

Figure 2. Mécanisme proposé d'hydrolyse de la cellulose en LA et ses esters.

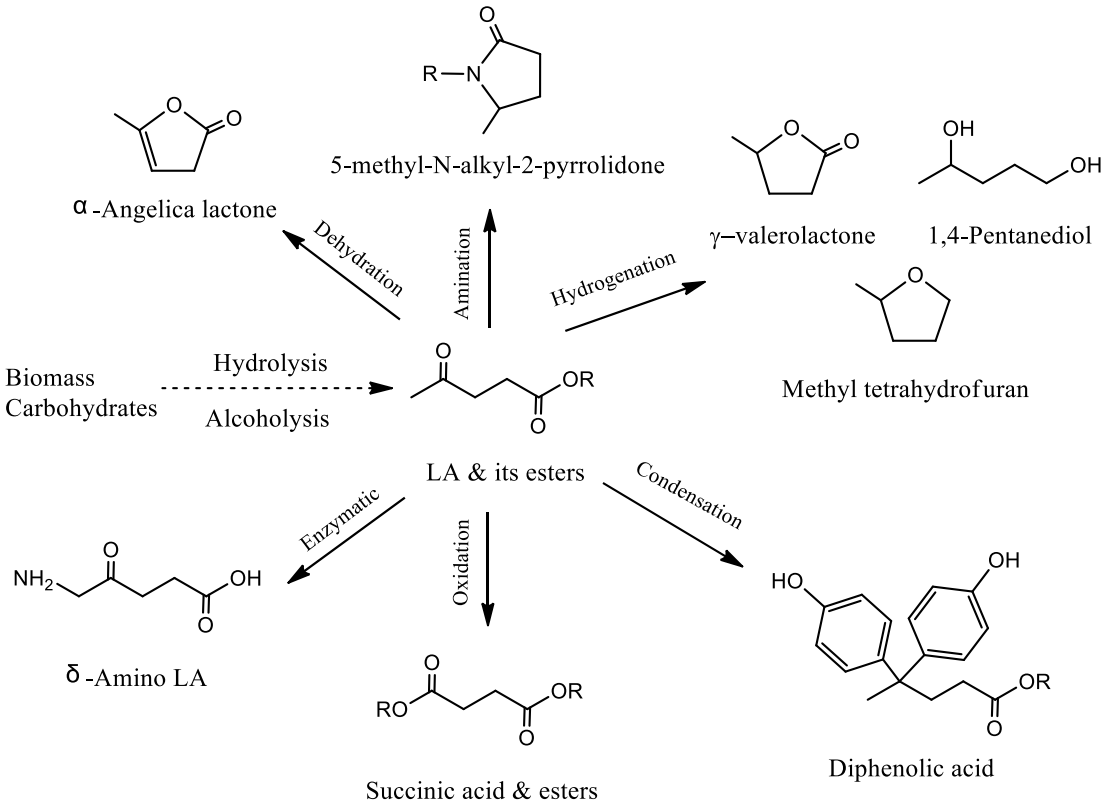

Figure 3. Produits de LA et de ses esters par différentes réactions.

Le γ-valérolactone (GVL), obtenu par hydrogénation d'acide lévulinique ou de lévulinates, peut être principalement utilisée comme additifs pour carburants et solvants et a un grand potentiel pour être transformée en produits chimiques de valeur, en biodiesel et en

carburants pour avions en tant que molécule plateforme importante (Figure 4). Ainsi, la production de GVL suscite un grand intérêt dans le monde entier.

En fonction des différents donneurs d'hydrogène, il existe trois voies de conversion de l'acide lévulinique ou de ses esters en GVL: l'utilisation directe d'hydrogène moléculaire (H_2) pour l'hydrogénation; l'utilisation d'acide formique pour la décomposition en H_2; l'utilisation d'alcools pour l'hydrogénation par transfert catalytique par la réaction de Meerwein-Ponndorf-Verley (MPV) (Figure 5). L'utilisation d'hydrogène moléculaire permet d'hydrogéner directement l'acide lévulinique ou ses esters, ce qui permet une réaction facile, rapide et efficace. Comme il est produit avec le LA à un rapport molaire de 1:1 dans le rendement théorique par hydrolyse de la cellulose, l'acide formique peut être utilisé comme donneur d'hydrogène sans séparation en suivant le principe de l'économie d'atomes. Ces dernières années, en utilisant la réaction réductrice MPV, les aldéhydes et les cétones peuvent être réduits en alcools correspondants, qui peuvent être appliqués pour l'hydrogénation du groupe carbonyle dans LA et de ses esters en GVL. Les progrès récents des technologies de production de GVL à partir de dérivés de la biomasse, en particulier de LA et de ses esters, sont passés en revue en fonction des différents donneurs d'hydrogène et catalyseurs.

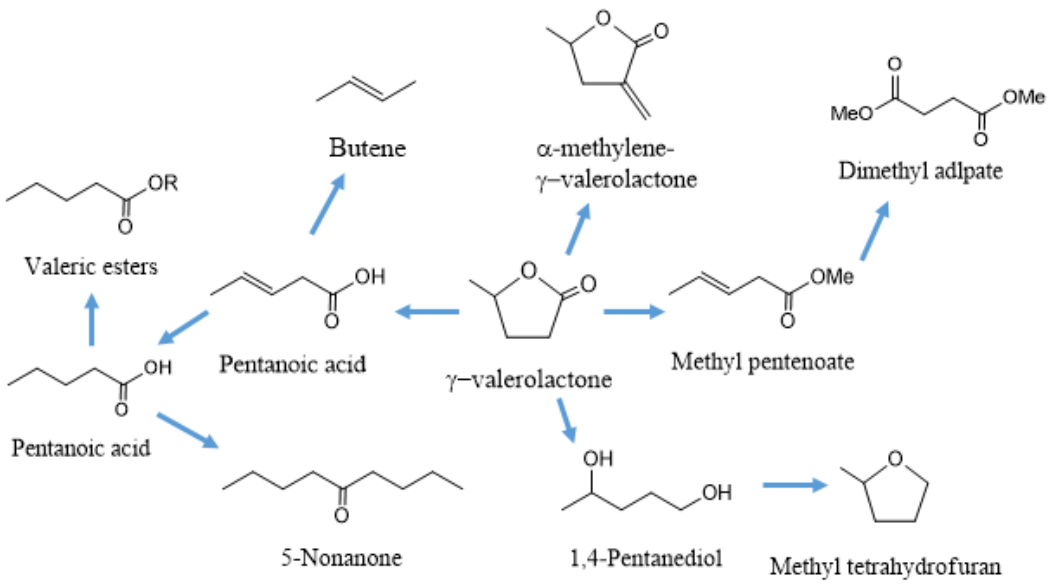

Figure 4. Conversion de GVL en biocarburants et en produits chimiques.

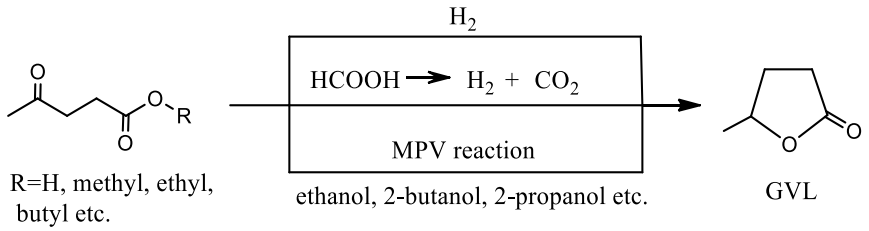

Figure 5. Hydrogénation de LA et de ses esters en GVL avec différents donneurs d'hydrogène.

D'après l'analyse de la littérature sur la production de γ-valérolactone, beaucoup d'efforts ont été faits sur le catalyseur, mais il reste encore des besoins à combler. En effet, pour intensifier ce processus, il convient de répondre aux questions suivantes : Dans quelle mesure cette réaction d'hydrogénation est-elle sûre ? Quelles sont les enthalpies de réaction pour ce système ? Quels sont les meilleurs réactifs parmi l'acide lévulinique ou ses esters ?

L'objectif de cette thèse est d'étudier la cinétique et la thermodynamique de l'hydrogénation de l'acide lévulinique (LA) et de ses esters en GVL. Cette thèse est divisée en trois parties :

- Évaluation du risque thermique pour l'hydrogénation de l'acide lévulinique en γ-valérolactone.
- Étude de la structure-réactivité de l'hydrogénation de l'acide lévulinique et de ses esters correspondants.
- Détermination expérimentale des enthalpies de réaction pour la production de γ-valérolactone.

Chapitre II. Évaluation du risque thermique pour l'hydrogénation de l'acide lévulinique en γ-valérolactone

Pour développer un procédé sûr de production de GVL, il faut procéder à une évaluation du risque thermique de la production de GVL à partir de l'hydrogénation de l'acide lévulinique. Comme souligné dans l'introduction, certains modèles cinétiques ont été développés pour cette synthèse, mais aucun d'entre eux n'a étudié son comportement thermique. L'hydrogénation de molécules insaturées étant connue pour être exothermique, le risque d'emballement thermique ne peut être négligé. L'emballement thermique pourrait se produire en cas de défaillance du refroidissement pendant le processus. La réaction se déroulera en condition adiabatique et la température augmente rapidement pour provoquer des accidents si aucune barrières de sécurité n'est mise en place. Cette étude permettra de déterminer les conditions opératoires sûres pour une application industrielle ultérieure. Cette étude est particulièrement importante pour les réacteurs à fonctionnement discontinu dans lesquels l'accumulation thermique est plus importante que dans les systèmes à fonctionnement semi-continu ou continu.

Dans ce chapitre, une évaluation du risque thermique pour l'hydrogénation de LA en GVL catalysée par le Ru/C dans l'eau a été réalisée. Pour évaluer le risque thermique, un modèle cinétique dans le condition quasi-adiabatique a été développé et deux paramètres de risque thermique ΔT_{ad} et TMR_{ad} ont été déterminés. Le paramètre de risque thermique TMR_{ad} définit le temps nécessaire pour atteindre le taux maximum de température et caractérise la probabilité d'emballement thermique. Le paramètre de risque thermique ΔT_{ad} est la différence entre la température maximale et la température de réaction initiale et caractérise la gravité de l'emballement thermique. En cas de défaillance du refroidissement, la réaction se déroulera en condition adiabatique. Il est donc important de connaître les valeur de TMR_{ad} et ΔT_{ad} pour évaluer le risque thermique du système réactionnel. La définition des TMR_{ad} et ΔT_{ad} est présentée par la Figure 6. Les expériences en mode adiabatique ont été réalisées dans l'ARSST (Advanced Reactive System Screening Tool).

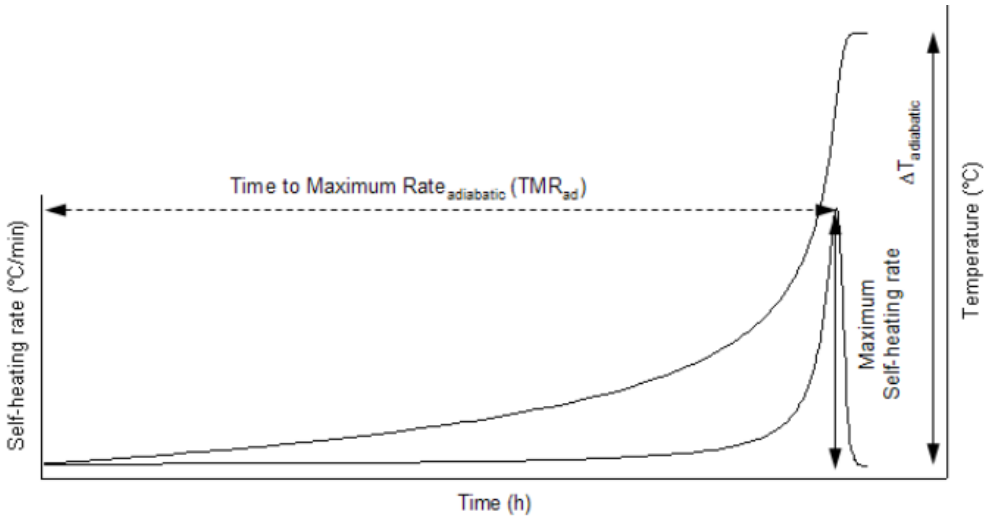

Figure 6. La définition de TMR_{ad} et ΔT_{ad}

En général, pour estimer ces paramètres, on utilise l'approche d'ordre zéro car elle est la plus conservatiste. Dans cette étude, nous avons pris en compte les deux étapes de réactions pour estimer le TMR_{ad}. Enfin, nous avons développé une matrice de risque thermique en multipliant la gravité et la probabilité du risque afin d'évaluer le risque thermique de cette réaction. La méthodologie de cette évaluation du risque thermique est illustrée par la Figure 7.

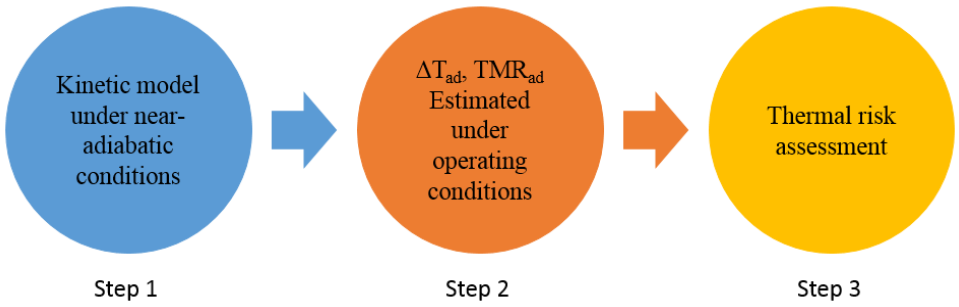

Figure 7. Méthodologie d'évaluation du risque thermique pour l'hydrogénation de LA en GVL.

L'hydrogénation de l'acide lévulinique en γ-valerolactone comprend deux étapes : la première étape est l'hydrogénation du groupe cétonique de LA conduisant à la formation d'acide 4-hydroxypentanoïque (HPA). La deuxième étape est la réaction de fermeture

réversible du cycle de l'HPA en GVL. Le mécanisme d'hydrogénation de l'acide lévulinique est illustré par la Figure 8.

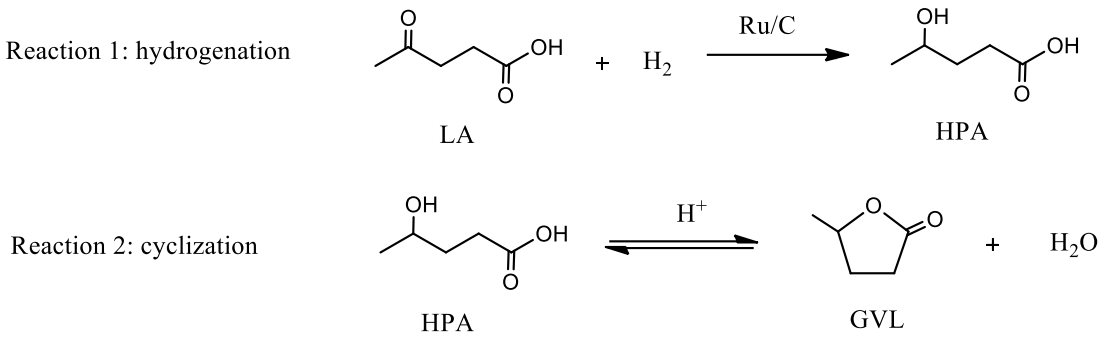

Figure 8. Mécanisme de réaction pour l'hydrogénation de LA en GVL catalysée par Ru/C dans de l'eau.

L'hydrogénation de LA en HPA à la surface du catalyseur est décrite par un modèle de Langmuir-Hinshelwood :

$$R_1 = \frac{k_1.P_{H_2}.K_{LA}.[LA]}{(1 + K_{LA}.[LA] + K_{GVL}.[GVL] + K_{HPA}.[HPA])^2} \quad (1)$$

Pour la seconde réaction, la transformation réversible du HPA en GVL se produit en phase de masse et est catalysée par les acides de Brönsted dû à LA et HPA. La deuxième réaction peut être exprimée comme suit :

$$R_2 = k_2.[H^+]\left([HPA] - \frac{1}{K_2}[GVL]\right) \quad (2)$$

Le bilan énergétique de la phase liquide s'exprime sous la forme :

$$\frac{dT}{dt} = \frac{q_{rx} + q_{el}}{m_{LA}(t).C_{P_{LA}}(T) + m_W(t).C_{P_W}(T) + m_{GVL}(t).C_{P_{GVL}}(T) + m_{HPA}(t).C_{P_{HPA}}(T) + m_{cat}.C_{P_{cat}}(T) + m_{insert}.C_{P_{insert}}(T)}$$

$$= \frac{q_{rx}}{m_{LA}(t).C_{P\,LA}(T)+m_W(t).C_{P\,W}(T)+m_{GVL}(t).C_{P\,GVL}(T)+m_{HPA}(t).C_{P\,HPA}(T)+m_{cat}.C_{P\,cat}(T)+m_{insert}.C_{P\,insert}(T)} + \beta \quad (3)$$

Le bilan thermique du système ARSST comprend l'énergie libérée par les réactions exothermiques q_{rx} et l'énergie fournie par le chauffage électrique q_{el}. La rampe de température dépend de l'énergie totale de q_{rx} et q_{el}, de la masse et des capacités thermiques spécifiques de toutes les compositions connexes, y compris le mélange réactionnel et les inserts. La détermination de β, qui est la vitesse de chauffage électrique de fond, est estimée à partir de l'étape initiale de la rampe de température par chauffage électrique sans réaction. Ce paramètre a été fixé pour chaque expérience.

L'énergie q_{rx} due aux réactions chimiques exothermiques peut être exprimée sous la forme:

$$q_{rx} = \left(-R_1.\Delta H_{R,1}.\frac{m_{cat}}{V_{liq}} - R_2.\Delta H_{R,2}\right).V_{liq} \quad (4)$$

Une méthode de régression non linéaire a été utilisée pour estimer les constantes cinétiques en utilisant la température de la réaction comme observable. Une bonne concordance entre les données expérimentales et le modèle a été obtenue (Figure 9).

Ensuite, sur la base des critères pour les valeurs de ΔT_{ad} et TMR_{ad}, il est possible de créer une matrice de risque d'emballement thermique présentée dans le Tableau 1 conformément aux lignes directrices pour la conception des matrices de risque.

Pour étudier l'évaluation des risques thermiques de ce système de réaction, les effets de la concentration en LA, de la température, de la charge du catalyseur et de la pression de l'hydrogène ont été étudiés. Les deux paramètres de risque TMR_{ad} et ΔT_{ad} ont été déterminés en utilisant le modèle cinétique développé dans ce chapitre dans le condition quasi-adiabatique par simulation en faisant varier la charge du catalyseur de 0,0001 à 0,14

kg.L^{-1}, la température du processus de 100 à 130°C, la concentration initiale de LA de 0,62 à 6,75 mol.L^{-1} et la pression d'hydrogène de 15 à 50 bars.

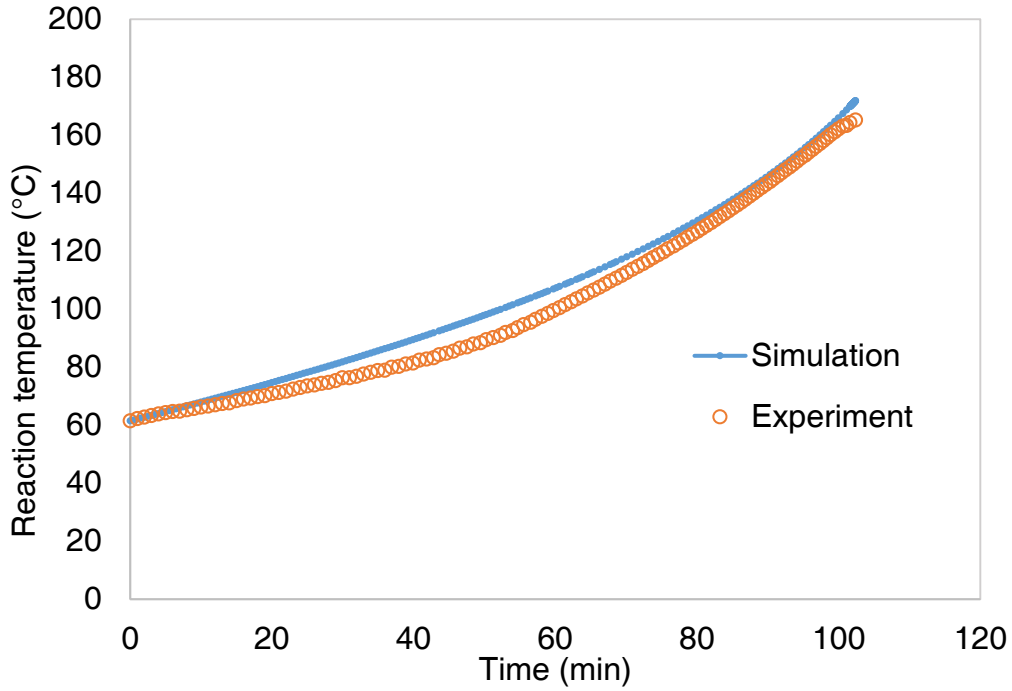

Figure 9. Ajustement du modèle aux données expérimentales (par example).

Tableau 1. Matrice de risque pour un emballement thermique.

Probability	Severity Factor	Negligible *1*	Medium *2*	Critical *3*	Catastrophic *4*
Frequent	*6*	6	12	18	24
Probable	*5*	5	10	15	20
Occasional	*4*	4	8	12	16
Seldom	*3*	3	6	9	12
Remote	*2*	2	4	6	8
Impossible	*1*	1	2	3	4

Non-acceptable Medium Negligible

Il convient de noter que le risque thermique est moyen dans la majorité des cas et que des barrières de sécurité devraient être incluses pour prévenir une situation d'emballement

thermique (Tableau 2 par exemple). L'augmentation de la pression de l'hydrogène peut également accroître le risque thermique.

Tableau 2. Évolution du risque thermique en fonction de la température du procédé et de la concentration en LA pour une charge de catalyseur de 0,014 kg.L^{-1} sous 35 bar H_2 (**Medium** **Negligible**)

RISK	*[LA] mol.L^{-1}*									
Tp °C	*0.62*	*1.25*	*1.90*	*2.55*	*3.22*	*3.90*	*4.59*	*5.30*	*6.02*	*6.75*
100	**6**	**6**	**6**	**10**	**10**	**10**	**10**	**10**	**10**	**10**
110	**6**	**6**	**6**	**12**	**10**	**10**	**10**	**10**	**10**	**10**
115	**6**	**6**	**6**	**12**	**10**	**10**	**10**	**10**	**10**	**10**
120	**6**	**6**	**6**	**12**	**12**	**12**	**10**	**10**	**10**	**10**
125	**6**	**6**	**6**	**12**	**12**	**12**	**10**	**10**	**10**	**10**
126	**6**	**6**	**6**	**12**	**12**	**12**	**12**	**10**	**10**	**10**
127	**6**	**6**	**6**	**12**	**12**	**12**	**12**	**10**	**10**	**10**
128	**6**	**6**	**6**	**12**	**12**	**12**	**12**	**10**	**10**	**10**
129	**6**	**6**	**6**	**12**	**12**	**12**	**12**	**12**	**10**	**10**
130	**6**	**6**	**6**	**12**	**12**	**12**	**12**	**12**	**10**	**10**

Enfin, L'évaluation du risque thermique de ce système de réaction pourrait permettre d'identifier une plage de conditions opératoires sûres qui pourrait être appliquée à l'optimisation des conditions opératoires de ce procédé en fonction du bilan massique et énergétique et de la conception chimique du réacteur.

Chapitre III. Étude de la structure-réactivité de l'hydrogénation de l'acide lévulinique et de ses esters correspondants

La production de GVL a été réalisée à partir de l'hydrogénation de LA ou de ses esters. Les travaux récents de Negahdar et al., [121] ont comparé les cinétiques de ML, EL et BL en utilisant le méthanol comme solvant. Cependant, ils n'ont pas pris en compte la réaction de transestérification en utilisant le méthanol, qui pourrait affecter la cinétique de réaction de chaque substrats (sauf ML). À ce stade de la thèse, outre la comparaison des cinétiques, pouvons-nous trouver une relation pour les cinétiques de LA, ML, EL et BL ? Pouvons-nous trouver un solvant approprié pour cette étude ? Ce chapitre présente les relations entre structure et réactivité pour cette réaction.

Dans ce chapitre, l'équation de Taft, basée sur la relation linéaire d'énergie libre, a été appliquée à l'hydrogénation de LA et de ses esters en GVL (Figure 10). Un modèle cinétique qui inclut le transfert de masse et l'équation de Taft a été développé et validé par des expériences de transfert de masse et de cinétique réalisées dans un réacteur à fonctionnement discontinu dans des conditions isothermes et isobares. Le coefficient de transfert de masse gaz-liquide, les constantes cinétiques et les facteurs de Taft dépendant des températures ont été estimés. En se basant sur ces valeurs, les cinétiques entre les différents substrats ont été comparées pour la réaction globale et deux étapes consécutives comprenant l'étape d'hydrogénation et l'étape de fermeture du cycle. Les effets polaires et stériques des groupes de substituants sur la cinétique ont également été examinés.

Des expériences de transfert de masse gaz-liquide et des expériences de cinétique d'hydrogénation ont été réalisées dans un réacteur discontinu dans des conditions isothermes et isobares. Le but des expériences de transfert de masse gaz-liquide est d'obtenir le coefficient de transfert de masse gaz-liquide et la constante de Henry de l'hydrogène gazeux en solution. Comme le GVL est le solvant et que la fraction massique est supérieure à 80%, nous avons considéré que cette étude peut être réalisée en utilisant du GVL pur. Ensuite, les expériences cinétiques d'hydrogénation ont été réalisées pour obtenir les données cinétiques expérimentales. L'identification et la qualification des

produits chimiques tels que les substrats, les intermédiaires et la GVL ont été réalisées en utilisant la GC-MS et la GC-FID.

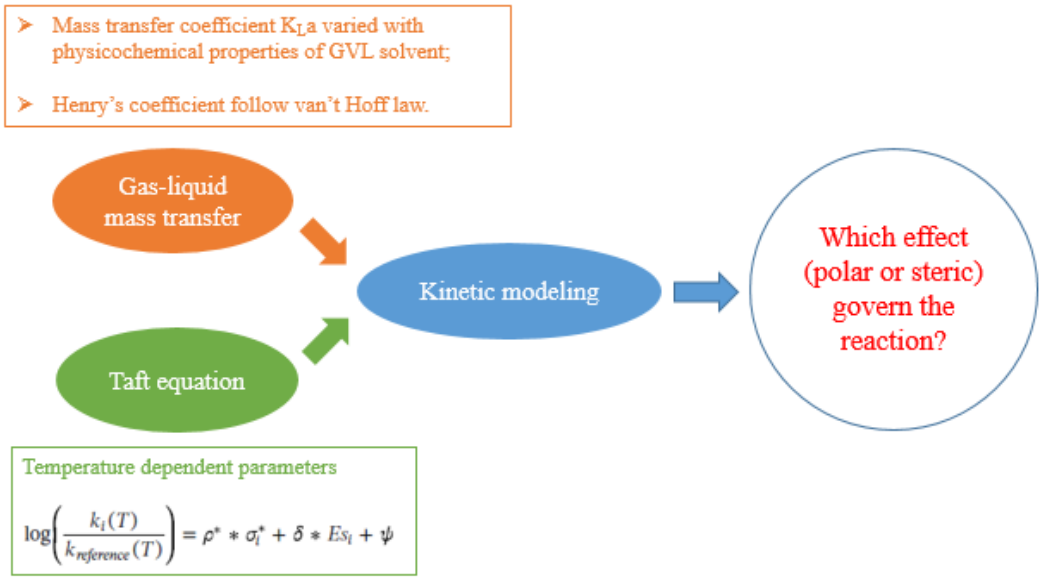

Figure 10. Schéma d'étude de la structure et de la réactivité de l'hydrogénation de LA et de ses esters.

En raison de la complexité des molécules dérivées de la biomasse par différents processus de bioraffinage, il est compliqué et long de déterminer la réactivité de toutes les molécules bio-dérivées par une étude expérimentale. En raison de cette réalité, l'utilisation du concept de structure-réactivité pourrait permettre d'accélérer ces processus pour la valorisation de la biomasse. Par exemple, l'équation de Taft, basée sur la relation linéaire d'énergie libre, peut prédire la constante de vitesse de réaction d'une série de réactions en considérant l'effet polaire, stérique et de résonance des réactifs ayant différents groupes (substituants).

Dans ce chapitre, la production de GVL à partir de LA et de ses esters catalysés par le Ru/C dans le solvant GVL a été testée par l'équation de Taft. Comme le montre la Figure 11, LA et ses esters (ML, EL et BL) ont des structures de chaîne linéaire similaires, à l'exception des groupes de substituants terminaux qui sont respectivement –H, -CH_3, -CH_2CH_3, -$CH_2CH_2CH_2CH_3$. L'équation de Taft a été initialement testée pour relier les constantes de vitesse de l'hydrogénation de LA et de ses esters avec les structures de LA et de ses esters.

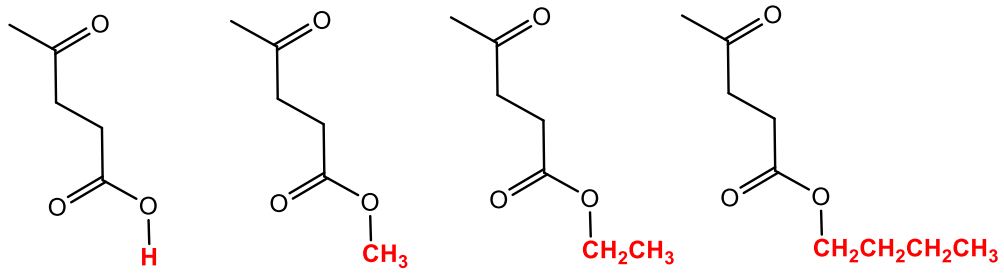

Figure 11. Structures de LA, ML, EL et BL.

Sur la base de la littérature et de nos observations expérimentales, le mécanisme de production de GVL est illustré par la Figure 12.

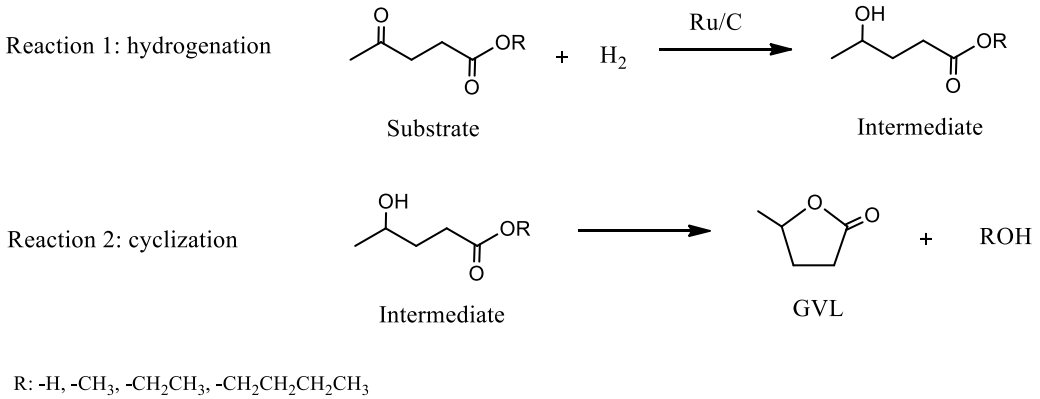

Figure 12. Mécanisme de réaction pour l'hydrogénation de LA ou de ses esters en GVL dans l'étude de la structure-réactivité.

La vitesse d'hydrogénation de LA/ML/EL/BL en intermédiaires HPA/MHP/EHP/BHP sur le catalyseur peut être écrite comme :

$$R_1 = k_1 * [H_2]_{liq} * [Substrate]_{liq} * \omega_{Cat.} \quad (1)$$

La vitesse de la deuxième réaction (fermeture du cycle) peut être exprimé comme suit :

$$R_2 = k_2 * [Intermediate]_{liq} \quad (2)$$

L'équation de Taft appliquée est exprimée comme suit :

$$\log\left(\frac{k_i(T)}{k_{reference}(T)}\right) = \rho^* * \sigma_i^* + \delta * Es_i \quad (3)$$

Il s'agit d'un système de réaction gaz-liquide-solide, le transfert de masse joue donc un rôle important. Le transfert de masse externe, le transfert de masse interne et le transfert de masse gaz-liquide sont évalués. Le transfert de masse externe et interne s'est avéré négligeable.

Le modèle du double film a été utilisé pour décrire le transfert de matière de l'hydrogène de la phase gazeuse à la phase liquide. La résistance du côté du gaz a été négligée. Afin d'avoir une description précise du transfert de matière de l'hydrogène du gaz vers le liquide, une expression du coefficient de transfert de masse volumétrique de l'hydrogène $k_L.a$ prenant en compte la température, la viscosité et la densité du système a été développée. En raison de la faible concentration des différents substrats (< 20 % en poids), l'évaluation a été faite en tenant compte du GVL pur.

Les expériences de transfert de masse ont permis de constater que $\Delta H_{Sol.H2} = 5936.8$ J.mol^{-1} et $He(T_{Ref} = 373.15K) = 1.86$ mol.m^{-3}.bar^{-1}. Comparée à l'hydrogénation de l'acide lévulinique dans l'eau, l'absorption de l'hydrogène dans les GVL est un phénomène endothermique. Ce comportement endothermique a également été observé pour d'autres solvants organiques. Cela peut être bénéfique car, à mesure que la température de la réaction augmente, la solubilité de l'hydrogène et la cinétique de l'hydrogénation augmentent. La Figure 13 montre l'ajustement du modèle aux données expérimentales. En général, on peut dire que le modèle s'adapte bien aux données expérimentales.

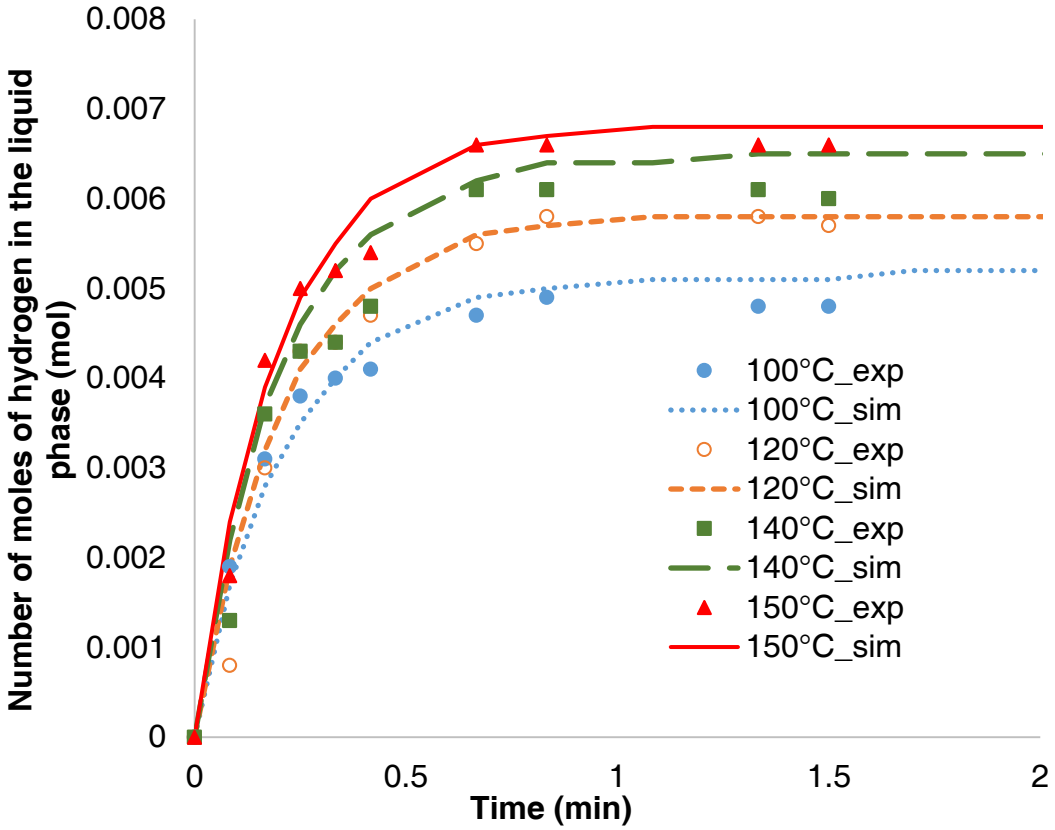

Figure 13. Ajustement du modèle aux expériences de transfert de masse sous une pression d'environ 20 bars.

La Figure 14 montre que le modèle cinétique développé correspond aux données expérimentales (LA par exemple). En général, l'ajustement est correct. On peut observer que l'ajustement du modèle à la concentration des intermédiaires est moins précis. Cela est dû à la forte réactivité de ces intermédiaires qui rend leur analyse moins précise, ce qui est particulièrement prononcé pour le HPA intermédiaire produit par l'hydrogénation de LA. L'ajustement du modèle à la concentration expérimentale de HPA est inférieur à celui des autres intermédiaires. Cela est dû au fait que cet intermédiaire est très réactif, ce qui rend son analyse difficile. Le graphique de parité (Figure 15) montre que le modèle développé est fiable.

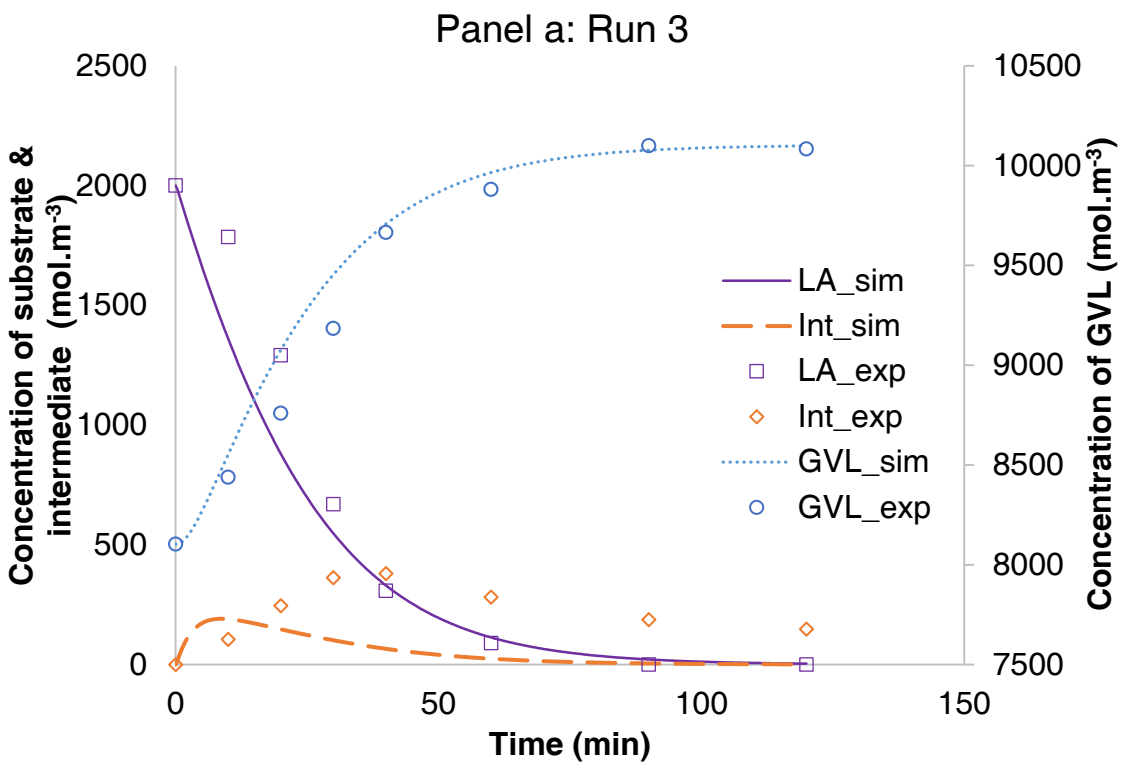

Figure 14. Ajustement du modèle aux données expérimentales pour l'hydrogénation de LA.

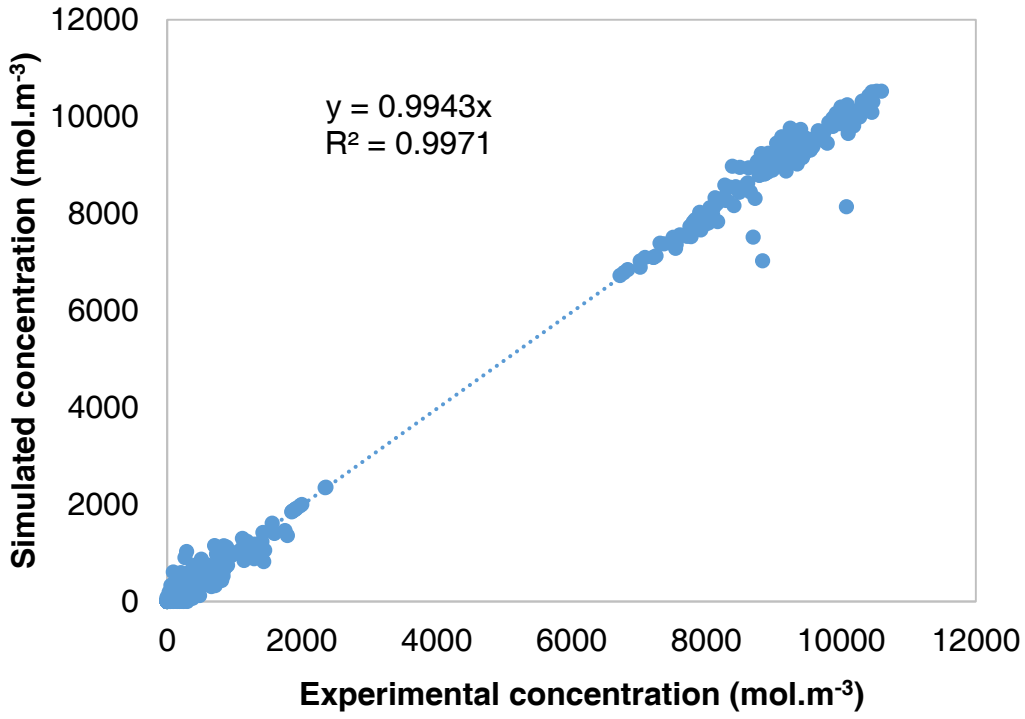

Figure 15. Tracé de la parité

A partir de ce modèle cinétique, il est possible de remarquer que les constantes de vitesse d'hydrogénation des substrats dans GVL ne sont pas proportionnelles à l'encombrement stérique des groupes alkyles substituants, en particulier pour la réaction 1. Comme l'équation de Taft a été introduite dans ce modèle avec la possibilité de quantifier l'effet polaire et stérique des différents groupes de substituants, on peut avoir une idée approfondie des relations entre la structure de la molécule et la réactivité.

La Figure 16 montre l'évolution des paramètres de Taft (ρ_1^*, ρ_2^*, δ_1 et δ_2) en fonction de la température. L'influence de l'effet polaire (ρ_1^* et ρ_2^*) sur les deux réactions est supérieure à l'effet stérique, et cette différence est plus prononcée lorsque la température de la réaction est supérieure à 110°C, car ρ_1^* et ρ_2^* sont bien supérieures à 1. L'effet stérique peut être considéré comme négligeable pour une température de réaction inférieure à 140°C pour les deux réactions, i.e., δ_1 et δ_2 sont inférieures à 1.

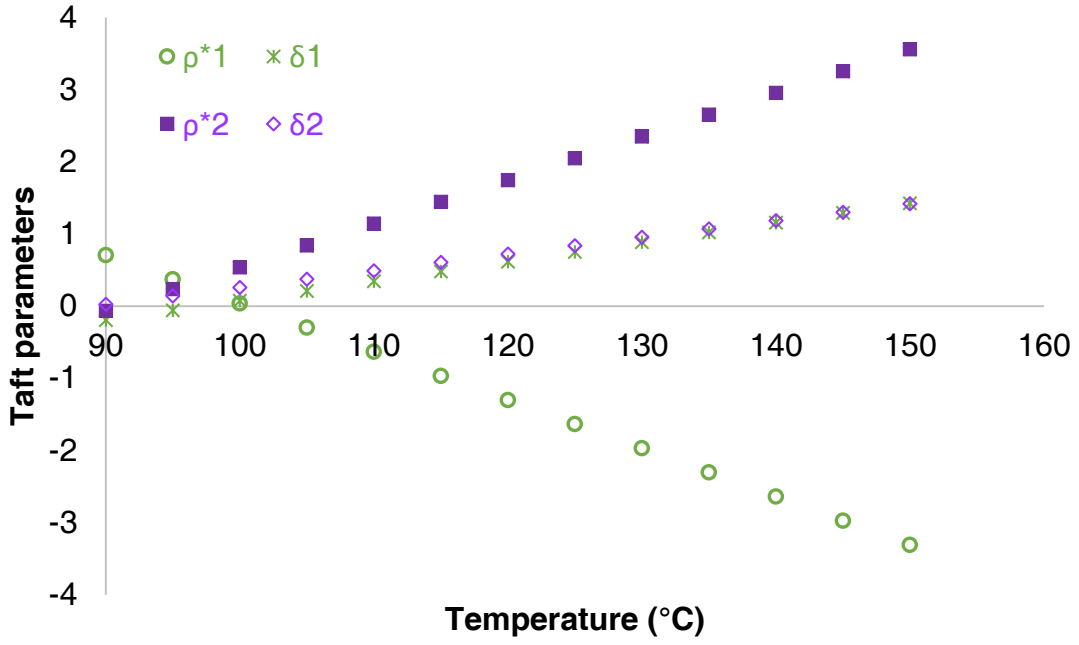

Figure 16. Influence de la température sur les paramètres de Taft.

Pour avoir une vue complète des comportements cinétiques de différents substrats, sur la base des constantes cinétiques estimées, il est possible de tracer la cinétique de la production de GVL dans les mêmes conditions opératoires pour LA, ML, EL et BL (Figure 17). Il a été constaté que la vitesse de réaction total pour la production de GVL évolue comme : $r_{GVL\ de\ LA} > r_{GVL\ de\ ML} > r_{GVL\ de\ EL} > r_{GVL\ de\ BL}$.

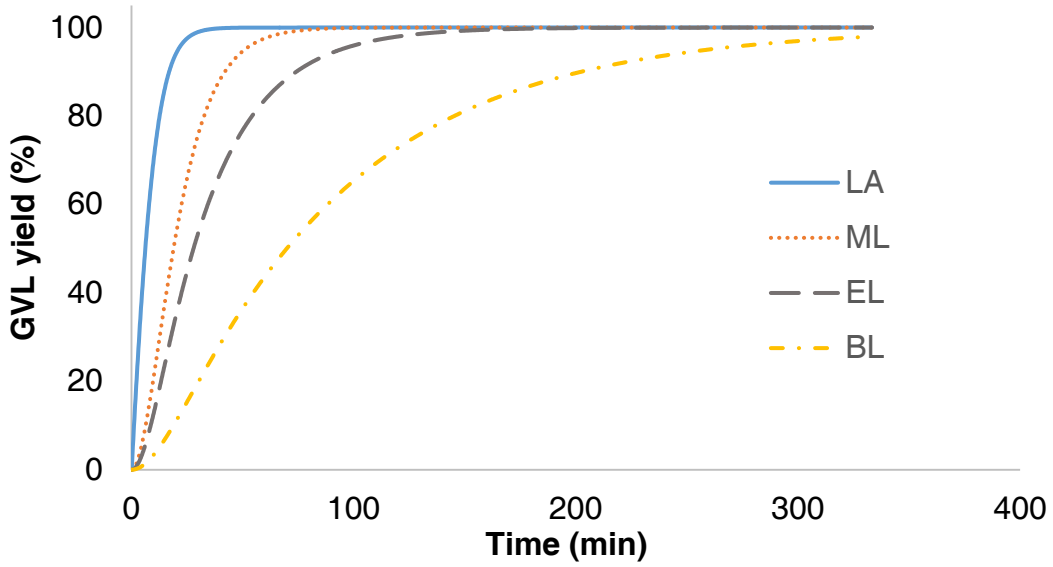

Figure 17. Cinétique de la production de GVL à partir de LA, ML, EL et BL à 140°C et 20 bar de H_2. $[Substrate]_0$ = 1000 mol.m^{-3}, $[GVL]_0$ = 7685-8250 mol.m^{-3} and $\omega_{Cat.}$ = 11.67 kg.m^{-3}.

Pour ce système de réaction, l'effet stérique s'est avéré négligeable pour les deux réactions. Néanmoins, les effets polaires se sont avérés importants pour la réaction de fermeture du cycle. La vitesse de production de GVL est plus rapide en utilisant LA, car l'effet de retrait des électrons du groupe H- augmente la cinétique de la réaction 2. La réaction 2 est plus lente pour l'hydrogénation des autres alkyles car les groupes alkyles sont des groupes donneurs d'électrons. Cette étude ouvre de nouvelles possibilités dans l'ingénierie des réactions chimiques, en connaissant les paramètres de Taft, il est possible de prédire les constantes de vitesse avec d'autres substrats.

Chapitre IV. Détermination expérimentale des enthalpies de réaction pour la production de γ-valérolactone

Les propriétés thermodynamiques comme l'enthalpie de réaction est essentielle pour prendre en compte le bilan énergétique dans les processus de réaction chimique. La réaction d'hydrogénation est normalement une réaction exothermique, qui nécessite un système de refroidissement efficace pour garantir que le processus de réaction se déroule en toute sécurité en condition isotherme. Ces informations sont aussi nécessaires pour développer un schéma de procédé (PFD) et faire une évaluation des coûts.

Ici, l'hydrogénation du lévulinate de méthyle (ML) en γ-valérolactone (GVL) a été choisie comme exemple pour la détermination de l'enthalpie de réaction dans le solvant GVL en raison de la stabilité relative de l'intermédiaire. L'enthalpie de la réaction pour ce système a été déterminée expérimentalement et de manière préliminaire par des calorimètres de réaction et l'analyse par chromatographie en phase gazeuse (GC) (Figure 18). Le calorimètre RC1 et le calorimètre Tian-Calvet C80 ont été utilisés pour mesurer le dégagement de chaleur de la réaction et l'analyse par GC a été employée pour la quantification des composés chimiques. Sur la base du mécanisme de réaction en deux étapes (Figure 19), l'enthalpie de la réaction pour chaque étape et l'enthalpie globale de la réaction ont été déterminées et résumées dans ce chapitre.

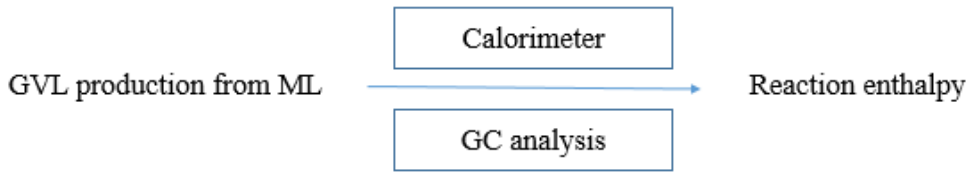

Figure 18. Détermination expérimentale de l'enthalpie de réaction pour l'hydrogénation de ML en GVL en utilisant des calorimètres et l'analyse GC.

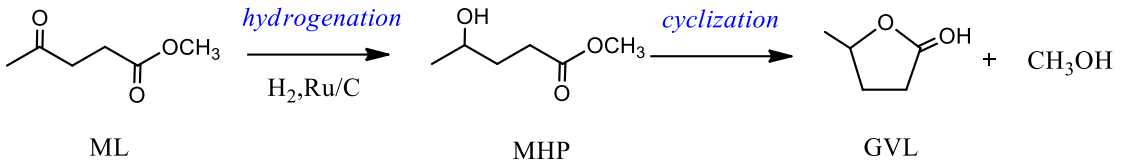

Figure 19. Mécanisme d'hydrogénation de ML en GVL.

Sur la base de ce mécanisme et de l'observation expérimentale, la détermination de l'enthalpie de réaction de chaque étape est nécessaire en raison de l'existence d'intermédiaire et une conversion incomplète. Ensuite, l'enthalpie de la réaction globale peut être calculée sur la base de l'enthalpie de réaction de ces deux étapes. Les calorimètres de réaction RC1 et C80 ont été utilisés pour mesurer le flux thermique de la réaction en combinaison avec l'analyse GC pour obtenir une valeur plus précise des enthalpies de réaction. Dans le calorimètre RC1, le ML, GVL, H_2 et Ru/C ont été mélangés pour la réaction globale, les deux étapes ont lieu. Alors qu'en C80, seule l'étape 2 a lieu, car l'expérience en C80 a utilisé le liquide final obtenu à partir de RC1 sans catalyseur Ru/C et H_2. La définition de l'enthalpie de la réaction ΔH_R, $\Delta H_{R,1}$, $\Delta H_{R,2}$ est présentée par la Figure 20.

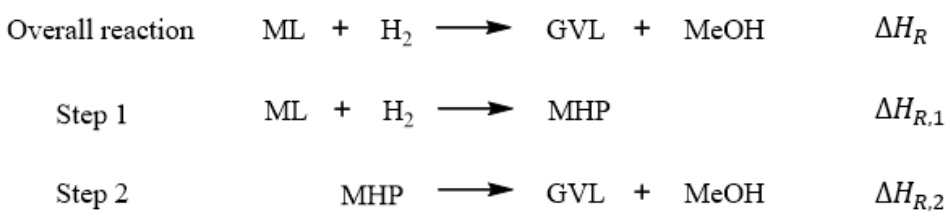

Figure 20. Définition de l'enthalpie de réaction.

Comme indiqué ci-dessus, la corrélation des enthalpies de réaction entre la réaction globale et deux étapes de réaction peut être conclue comme suit :

$$\Delta H_R = \Delta H_{R,1} + \Delta H_{R,2} \quad (1)$$

Comme dans l'expérience C80, seule l'étape 2 a lieu, l'enthalpie de réaction pour la deuxième étape ($\Delta H_{R,2}$) peut être calculée d'abord. Ensuite, en appliquant la valeur de $\Delta H_{R,2}$, l'enthalpie de réaction pour la première réaction ($\Delta H_{R,1}$) peut être obtenue. Enfin,

en utilisant l'équation (1), l'enthalpie globale de la réaction est facilement obtenue. La méthodologie de détermination de l'enthalpie de réaction en appliquant les calorimètres RC1 et C80 et l'analyse par GC est présentée par la Figure 21.

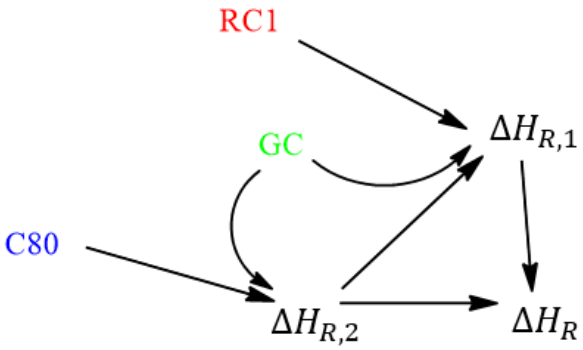

Figure 21. Schéma de détermination de l'enthalpie de réaction en utilisant RC1, C80 et l'analyse GC.

Le flux de chaleur pour la production de GVL à partir de ML dans RC1 a été mesuré toutes les 2 secondes (Figure 22). Le temps zéro a été réglé au moment du démarrage de l'agitation. Il est à noter qu'au début des 2000 seconds, le flux de chaleur a fortement augmenté puis a diminué, ce qui a entraîné un comportement exothermique extrême. Cependant, après des 2000 seconds, le flux de chaleur est resté constant jusqu'à la fin de cette expérience.

Comme le mélange liquide final du RC1 comprend du MHP, du GVL, du catalyseur Ru/C et du n-butanol, après filtration de ce mélange, le liquide a été utilisé pour la mesure du C80. L'acide sulfurique à 0,01 mol.L^{-1} dans le GVL a été utilisé comme catalyseur acide pour accélérer la réaction de la deuxième étape et le flux de chaleur pour la deuxième étape est indiqué par la Figure 23. Le phénomène endothermique a été observé dans cette mesure avec évidemment un pic significatif.

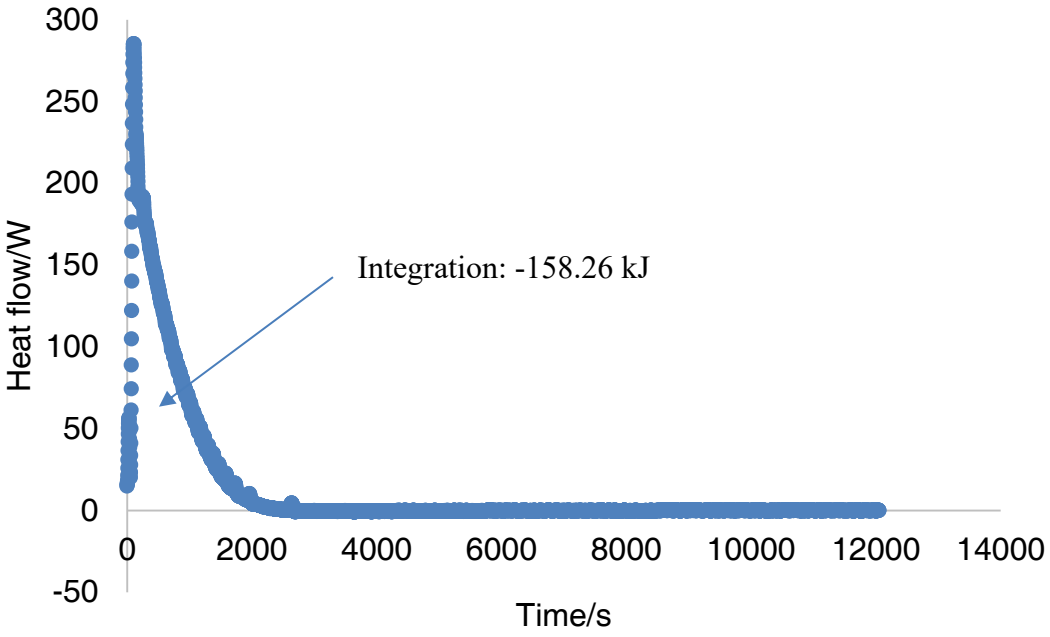

Figure 22. Flux de chaleur pour l'hydrogénation de ML en GVL dans RC1.

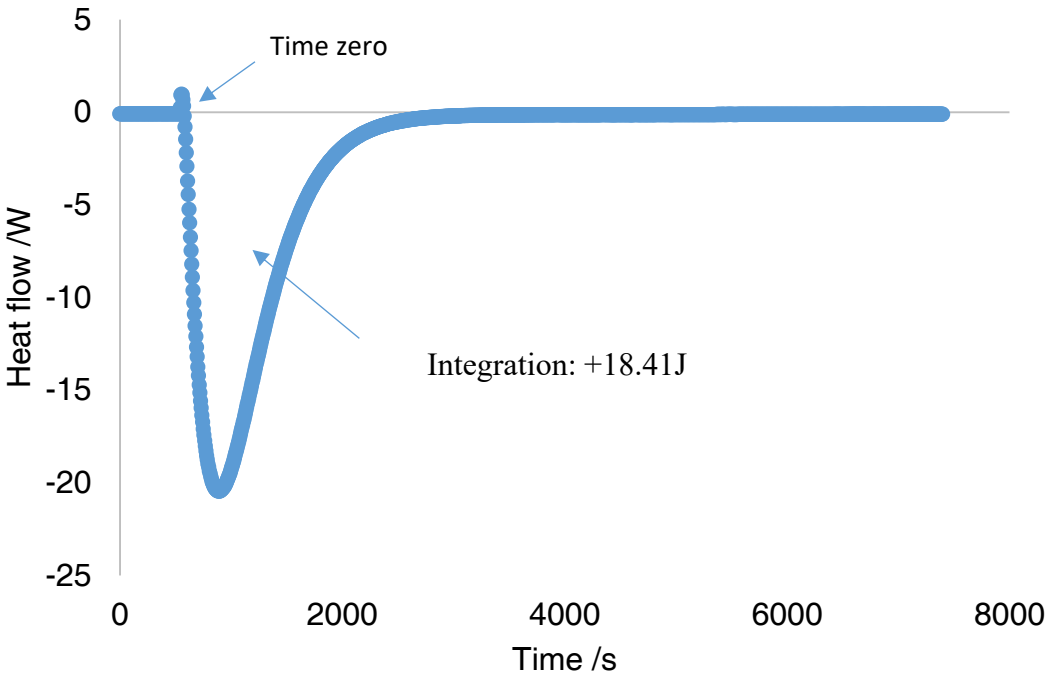

Figure 23. Flux de chaleur pour la réaction de fermeture du cycle en C80.

Il a été constaté que l'enthalpie globale de la réaction est de -51,5 kJ/mol, ce qui indique que la réaction de production de GVL à partir de ML est exothermique et qu'un certain contrôle de sécurité doit être impliqué pour ce processus (Tableau 3). Par ailleurs, le comportement thermique de chaque étape était différent selon la mesure et le calcul calorimétrique. L'enthalpie de la réaction pour la première étape d'hydrogénation était de -58,66 kJ/mol en réaction exothermique et l'enthalpie de la réaction pour la deuxième étape de fermeture du cycle était de 7,16 kJ/mol en réaction endothermique. Ces enthalpies de réaction peuvent être utilisées pour l'optimisation et la conception de procédés.

Tableau 3. Enthalpies de réaction pour chaque étape et réaction globale.

Reaction enthalpy in GVL	**Values kJ.mol^{-1}**
$\Delta H_{R,1}$	-58.66
$\Delta H_{R,2}$	+7.16
$\Delta H_{R,for\ overall\ reaction}$	-51.50

Conclusions et Perspectives

Sur la base des travaux de cette thèse, l'évaluation du risque thermique, la structure-réactivité et l'enthalpie de réaction ont été étudiées pour la production de γ-valérolactone (GVL) à partir de l'hydrogénation de l'acide lévulinique (LA) et de ses esters, notamment le lévulinate de méthyle (ML), le lévulinate d'éthyle (EL) et le lévulinate de n-butyle (BL). L'étude par couplage du bilan massique et énergétique de ce système réactionnel a été réalisée pour l'évaluation du risque thermique et la détermination de l'enthalpie de la réaction. La structure-réactivité de cette réaction a permis d'approfondir les relations entre la cinétique de la réaction et les structures. Ces trois parties peuvent être utilisées ultérieurement et guider la conception et l'optimisation du processus chimique pour cette réaction.

Dans le cadre de l'évaluation du risque thermique, la réaction d'hydrogénation de LA en GVL catalysée par le Ru/C dans l'eau a été étudiée. Un modèle cinétique dans le condition quasi-adiabatique a été construit. Des expériences dans des différentes conditions opératoires ont été réalisées dans le calorimètre ARSST (Advanced Reactive System Screening Tool). Les constantes cinétiques ont été estimées en utilisant la température de la réaction comme observable par une méthode de régression non linéaire. Une bonne concordance entre les données des expériences et le modèle a été obtenue. Sur la base du modèle, deux paramètres de risque ΔT_{ad} qui caractérise la gravité de l'emballement thermique, et TMR_{ad} qui caractérise la probabilité d'emballement thermique ont été obtenus par simulation et utilisés pour l'évaluation du risque thermique à l'aide d'une matrice de risque. Des conditions opératoires différentes telles que la concentration de LA, la température du processus, la charge du catalyseur et la pression de l'hydrogène ont été examinées. Il convient de noter que lorsque le catalyseur se trouve dans la plage de charge de 0,0014-0,014 $kg.L^{-1}$, le LA dans la plage de concentration de 0,62-6,75 $mol.L^{-1}$, la température dans la plage de 100-130°C et sous une pression d'hydrogène de 35 bars, le risque thermique est moyen dans la majorité des cas et des barrières de sécurité devraient être incluses pour empêcher un emballement thermique. L'augmentation de la pression de l'hydrogène peut également accroître le risque thermique. Cette évaluation du risque

thermique permet d'obtenir des conditions opératoires sûres pour une optimisation plus poussée du processus pour ce système de réaction.

Pour l'étude de la relation structure-réactivité pour l'hydrogénation de LA et de ses esters en GVL, LA, ML, EL et BL ont été utilisés comme substrats pour cette réaction catalysée par le catalyseur Ru/C dans le solvant GVL. Les expériences ont été réalisées dans des conditions isothermes et isobares en faisant varier les conditions de concentration du réactif, la température de la réaction, la pression d'hydrogène et la charge du catalyseur. En utilisant le GVL comme solvant, tous les substrats peuvent être solubilisés pour éviter le système de réaction liquide-liquide et faciliter le processus en aval. Le coefficient de transfert de masse (k_L.a) pour le transfert d'hydrogène de la phase gazeuse à la phase liquide a été évalué en tenant compte de l'influence de la température du processus, de la viscosité et de la densité du solvant. Il a été constaté que la constante de Henry pour l'absorption d'hydrogène dans la GVL suit la loi de van't Hoff. Cette absorption s'est avérée être endothermique, ce qui signifie que l'augmentation de la température entraîne une augmentation de la quantité d'hydrogène absorbée. Un modèle cinétique a été développé en incluant des paramètres de transfert de masse et en intégrant l'équation de Taft, les effets stériques et polaires des substituants (H-, CH_3-, CH_3-CH_2-, CH_3-CH_2-CH_2-CH_2-) sur la réaction en deux étapes, l'étape d'hydrogénation et l'étape de fermeture du cycle, ont été étudiés par une étude cinétique. Pour ce système de réaction, l'effet stérique s'est avéré négligeable pour les deux étapes de réaction. Néanmoins, les effets polaires se sont avérés importants pour l'étape de fermeture du cycle. La vitesse de production de GVL est plus rapide en utilisant LA car l'effet de retrait des électrons du groupe H- augmente la cinétique de la réaction 2. La réaction 2 est plus lente pour les autres lévulinates d'alkyle car les groupes alkyles sont des groupes donneurs d'électrons. La vitesse globale de la réaction suit l'ordre suivant : $r_{GVL\ de\ LA} > r_{GVL\ de\ ML} > r_{GVL\ de\ EL} > r_{GVL\ de\ BL}$. En connaissant les paramètres de Taft, il est possible de prédire les constantes de vitesse avec d'autres substrats.

Ensuite, comme l'enthalpie de réaction est une propriété thermodynamique importante pour la conception et l'optimisation des procédés, une détermination expérimentale de l'enthalpie de réaction à partir de l'hydrogénation de ML catalysée par Ru/C dans le solvant

GVL a été réalisée. Une méthode originale de détermination de l'enthalpie de réaction pour cette réaction a été proposée. Les enthalpies de réaction pour la réaction globale et les réactions en deux étapes, y compris l'hydrogénation et la cyclisation, ont été déterminées à l'aide des calorimètres RC1 et Tian-Calvet C80. L'analyse GC a été utilisée pour quantifier la concentration des substrats, des intermédiaires et du produit GVL. Par calcul, il a été constaté que l'enthalpie globale de la réaction était de -51,5 $kJ.mol^{-1}$ de GVL produit, ce qui indique que la réaction globale pour la production de GVL à partir de ML est exothermique. Certaines opérations de contrôle de sécurité doivent être conçues pour ce procédé. L'enthalpie de la réaction pour la première étape d'hydrogénation a été calculée à -58,66 $kJ.mol^{-1}$, et l'enthalpie de la réaction pour la deuxième étape de fermeture du cycle a été calculée à +7,16 $kJ.mol^{-1}$. Le comportement thermique de ces deux étapes est différent et l'étape exothermique est beaucoup plus prononcée que l'étape endothermique.

Les perspectives de ce travail de thèse pourraient être axées sur :

- Développement d'un modèle cinétique intrinsèque prenant en compte le transfert de masse interne et externe en mode adiabatique et l'influence des principaux paramètres d'entrée tels que la distribution granulométrique du catalyseur et la vitesse de rotation sur le risque thermique.
- Tester l'équation de Taft sur d'autres substrats alkyles et mieux comprendre l'évolution des paramètres de Taft en fonction de la température.
- Détermination de l'enthalpie pour d'autres substrats alkyles, tels que EL et BL et comparaison du risque thermique pour substrats différents.
- Mesure des propriétés physico-chimiques de ce système de réaction pour l'élaboration d'un diagramme de processus et l'évaluation des coûts.
- Discrimination de modèles pour la cinétique de la production de GVL.

Table of contents

Chapter I. Context of the study

1.1 Introduction

Energy valorization is one of the most important issues all over the world as the energy supports the development of all aspects of our human society. As geographical location of oil reserves, regarded as the "blood" of the modern industry, is not balanced worldwide and its storage is decreasing due to the increase of energy consumption. So the petroleum has greatly affected the development of economy and society for each country. Although the petroleum industry provides a facile and efficient way for energy supply, it is necessary to look for the alternative way to substitute the petroleum due to its unsustainable and unrenewable characteristics. Meanwhile, the utilization of petroleum also causes the emission of greenhouse gas which has been considered as the main reason for climate change [1].

As a renewable carbon source, biomass valorization has attracted great interests from all over the world with attractive characteristics as it is abundant, sustainable and renewable. Second generation biomass lignocellulose has no competition with alimentary sector and has been paid more attention in recent decades. Huge amounts of products can be obtained from lignocellulose valorization. Thus, biorefinery based on this biomass has appeared and expanded steadily. Among these products derived from biomass, levulinic acid (LA) and its esters have shown great potential as a platform to synthesize and replace the corresponding petroleum-based products. For example, one can upgrade these molecules, by hydrogenation, to another platform molecule γ-valerolactone (GVL).

In this chapter, the second generation biomass valorization is reviewed in section 1.2. The tendency of renewable energy, composition and structures of biomass, biorefinery process are introduced in detail in this section. Then, focused on the reaction studied in this doctoral thesis, application and production of LA and its esters are summarized in section 1.3. Wide application of LA and its esters is shown in section 1.3.1. Production of LA and its esters from different carbohydrates are introduced in Section 1.3.2.

Application and production of GVL are presented in the following section 1.4. The wide and potential application of GVL is introduced in section 1.4.1. The production of GVL from LA and its esters are reviewed in section 1.4.2 depending on different sources of hydrogen donor. More detail about advantages, mechanisms and advancements are discussed in section 1.4.2.1 by using formic acid as hydrogen donor, in section 1.4.2.2 by using alcohols as hydrogen donor, in section 1.4.2.3 by using hydrogen gas as hydrogen donor, respectively. Kinetic study for production of GVL is summarized in section 1.4.3. At the end, objectives of this doctoral thesis is briefly given in section 1.5.

1.2 Second generation biomass valorization

To build eco-friendly and sustainable processes it is necessary to steadily employ cleaner, greener, sustainable and renewable energy [2, 3]. As predicted in BP energy outlook (Figure 1.1) [4], although fossil energy including oil, gas and coal will account for more than 75% energy supply in 2035, the use of renewables in primary energy supply will increase. Additionally, renewable energy is predicted to be the fastest growing source of energy (7.1% p.a.), with its share in primary energy increasing to 10% by 2035. Biomass is a sustainable and renewable carbon source for substituting petroleum-based chemicals and materials [5, 6], which makes it attractive not only for its renewability but also for its added-value [7]. As each year over 150 billion tons of biomass can be produced by photosynthesis, only 3-4% is used by humans for food and non-food purpose [6]. Although the markets prefer cheaper petroleum-based products, transformation of biomass to value chemicals and biofuels has presented great potential to account for portions of market due to its significance characteristics.

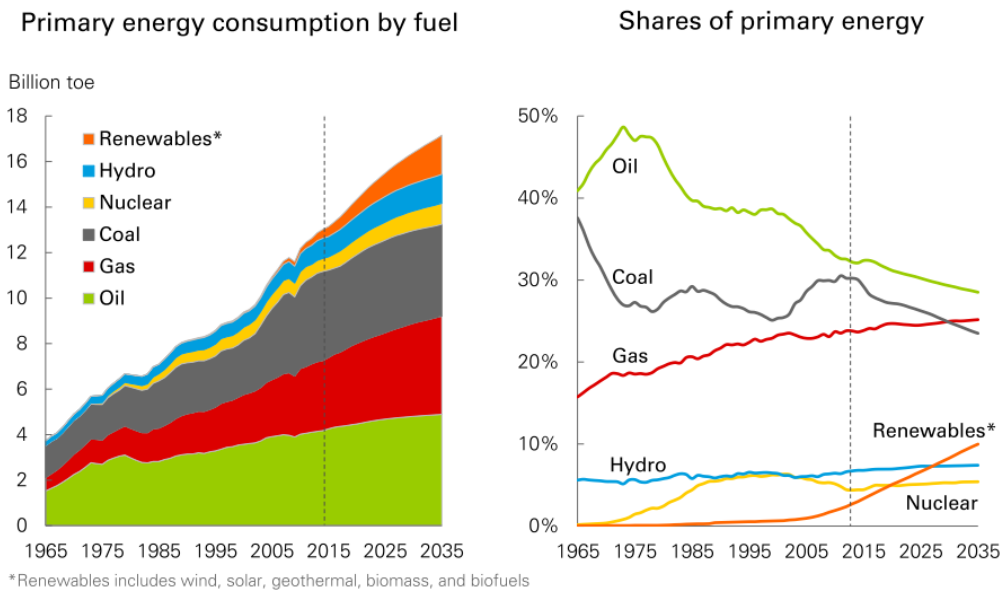

Figure 1.1. Primary energy outlook in the next 20 years [4].

Biomass is defined as "any organic matter that is available on a renewable basis, including dedicated energy crops and trees, agricultural food and feed crop residues, aquatic plants, wood and wood residues, animal wastes and other waste materials" [8]. It is mainly composed of three components: cellulose, hemicellulose and lignin (Figure 1.2). The content of these three parts vary with different resources (Table 1.1). Cellulose is a well-structural and high crystaline polymer of glucose units linked via β-1,4-glycosidic linkage, which makes it hard to be hydrolyzed. Hemicellulose is an amorphous oligomer of mixed C5- and C6-sugars (mainly including glucose and xylose). As an amorphous polymer composed of methoxylated phenylpropane structures, lignin provides plants with structural rigidity and a hydrophobic vascular system for the transportation of water and solutes [9].

Due to its abundance and renewability, conversion of biomass to commodity chemicals and biofuels has attracted great attentions from all over the world based on the issues from environmental pollution and sustainable development [1, 10, 11]. Considered as the only sustainable organic carbon source, biomass has positive potential to replace petroleum-based product, which could provide a more sustainable and renewable way to meet the needs of economic and social development. For example, bioethanol, derived from fermentation of starch or sugar crops, has already been applied in transportation industries

according to CO_2 reduction emission plan [12]. Compared to the first generation starchy feedstock, development of transformation technologies from inedible biomass such as lignocellulosic biomass to avoid competition with food has become a hot pot in green chemistry [13]. Lignocellulosic biomass as the second generation biomass can be supplied as raw materials for production of platform chemicals with wide applications through biorefinery process, which can also provide a more comprehensive way for waste recycle-use [14, 15].

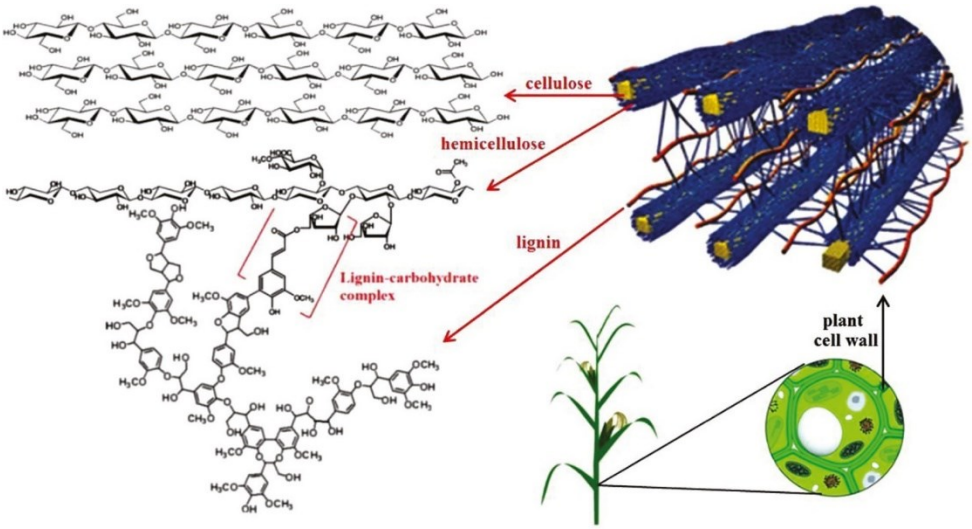

Figure 1.2. Structure and interaction of cellulose, hemicellulose and lignin in biomass.

Table 1.1. Composition analysis of selected lignocellulosic sources [16].

Type	Cellulose/wt%	Hemicellulose/wt%	Lignin/wt%
Agricultural residues	35-55	25-35	15-30
Energy crops	30-50	20-40	10-20
Forestry residues	40-50	25-35	20-30

Biorefinery is the concept of using biomass to obtain multiple products through complex processing methods [17]. Similar to petrorefinery, a biorefinery system integrates biomass production, conversion processes, end use to produce transportation biofuels, power and chemicals from biomass [11], providing a sustainable and carbon cycle scenario for development (Figure 1.3). The aim of biorefinery is to maximize the added value from

biomass, taking into account the issues from environment, economy and society [1]. However, differ from petroleum, the biomass feedstock varies by different type of raw materials and content of C, H, O in biomass is also different from crude oil, which makes the biorefinery system more complex to operate but more easier to get various chemicals and materials [18]. Due to a larger range of processing technologies is needed, most of them are still studied at laboratory scale.

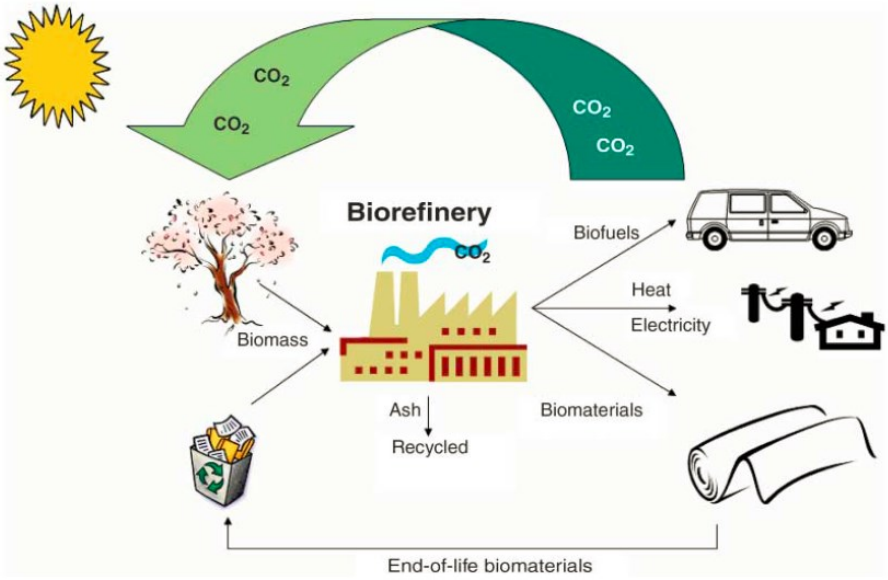

Figure 1.3. The fully integrated agro-biofuel-biomaterial-biopower cycle for sustainable technologies [11].

Depending on the feedstock and the desired product, the biorefinery process can be classified into four main pathways: thermochemical, biochemical, mechanical and chemical processes [1]. These different pathways can be employed for energy supply and producing various bioproducts such as biogas, biofuels, sugars, chemicals. By changing the chemical structure of the molecules, chemical processes can create desired products in two main methods: hydrolysis and transesterification. In particular, an important platform molecule levulinic acid (LA) can be mainly obtained by acid-hydrolysis of cellulose with several intermediates (hexoses, 5-hydoxymethylfurfural (HMF)) and steps (dehydration and rehydration). Meanwhile, LA can be also synthesized by acid-hydrolysis of hemicellulose to furfural, hydrogenation of furfural to furfural alcohol followed by ring-

opening step. Further catalytic hydrogenation of LA with H_2, formic acid or alcohol as hydrogen donors can produce stable C-5 ring molecule γ-valerolactone (GVL) [19]. These two platforms can be widely used in industries and provide an alternative way for substituting petroleum-based materials. More details of production of LA and its derivative esters and GVL are illustrated in the following sections.

1.3 Applications and production of levulinic acid (LA) and its esters

As discussed in section 1.2 about second generation biomass, LA and its esters, which can be produced from both cellulose and hemicellulose of lignocellulosic biomass, can be used as platforms for biofuels and synthesis of value-added chemicals which can substitute the petroleum-based chemicals through biorefinery processes. Due to the commodity solvents used to produce LA and its esters, such as water, methanol, ethanol and n-butanol, the LA and its esters studied by researchers in general are LA, methyl levulinate (ML), ethyl levulinate (EL), n-butyl levulinate (BL), etc. The information of these molecules were depicted in Table 1.2.

LA and its esters are mainly produced from C6 sugar such as glucose and fructose derived from cellulose in biomass (Figure 1.4). Firstly, cellulose is obtained by pretreatment of biomass raw materials. Secondly, cellulose converts to C6 sugar glucose and fructose through hydrolysis process or alkyl-glucoside and alkyl-fructoside catalyzed by acid catalyst. Thirdly, C6 sugar or its alkyl derivatives are dehydrated to 5-hydroxyl-methylfurfural (HMF) or its alkyl ether, which is also identified as one of important platforms. At last, by rehydration with water or alcohols, HMF or its alkyl ether further decomposes to LA and formic acid or LA esters and formate esters. Though LA and its esters are mainly produced from C6 compounds, it is also possible for C5 compounds such as xylose, furfural and furfural alcohol to be converted to LA and its esters by reasonable process design [20, 21].

Table 1.2. Properties of LA and its esters.

Product	CAS	Formula	MW.	Structure
LA	123-76-2	$C_5H_8O_3$	116.11	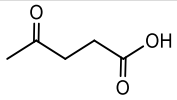
ML	624-45-3	$C_6H_{10}O_3$	130.14	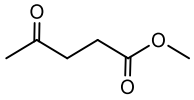
EL	539-88-8	$C_7H_{12}O_3$	144.17	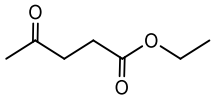
BL	2052-15-5	$C_9H_{16}O_3$	172.22	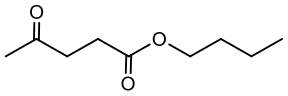

As production of LA and its esters from either cellulose or hemicellulose needs several steps, it is necessary to analyze different systems for a better integration of each step in view of economy, technology and safety. Herein, recent advances of production of LA and its esters are reviewed based on different materials or molecules with complex components and structures for a better comprehension of technologies for conversion of biomass to LA and its esters.

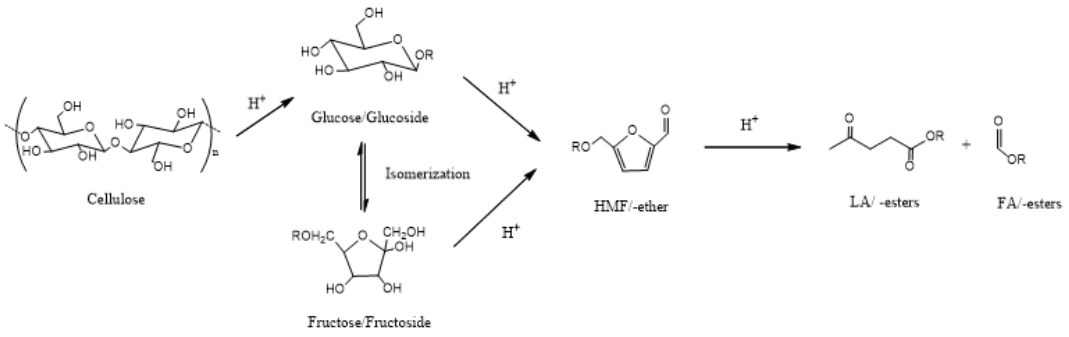

Figure 1.4. Proposed mechanism of hydrolysis of cellulose to LA and its esters.

In this section, applications of LA and its esters are introduced at first to show their wide use and great potential as bio-based platform. Then, production of LA and its esters are discussed briefly from different reactants such as raw materials, poly-, oligo-, disaccharides,

monosaccharides and furfural alcohol. These biomass derived-carbohydrates can be converted to LA and its esters selectively.

1.3.1 Applications of LA and its esters

Levulinic acid (LA), which is considered as one of the top 12 biobased platform chemicals by department of energy in US in 2004 [22], can be obtained by acid-catalysis hydrolysis from lignocellulosic biomass. With two active groups hydroxyl- and carboxyl- group in the molecule, LA can be a versatile platform and easily soluble in water, ethanol, acetone, diethyl ether and other organic solvents. Furthermore, it has great potential of conversion to lots of outstanding molecules such as diphenolic acid (DPA), succinic acid, methyltetrahydrofuran (THF) [23], γ-valerolactone (GVL) [24-26], succinic acid, pyrrolidones [27], etc. by different types of reactions (Figure 1.5). These series of chemicals can be widely used as polymers, herbicides, pharmaceuticals, biofuels, plasticizers, solvents, etc. by replacing petroleum-based chemicals due to its biocompatible and biodegradable characteristics. LA esters that can be obtained from solvolysis of biomass carbohydrates in alcohol solvents or by esterification of LA [28-35], were regarded as an alternative molecule of LA to produce the value-added products and also used as fuel-blending additive components and bio-lubricants [36].

In commercial view of LA production, the market size of LA in 2000 was 450 tons and 2600 tons in 2013 and will reach 3800 tons in 2020 as predicted [37, 38]. While for LA esters, the industrial scale-up and potential applications are still in the primary research stage but are expected to be expanded in the future [39].

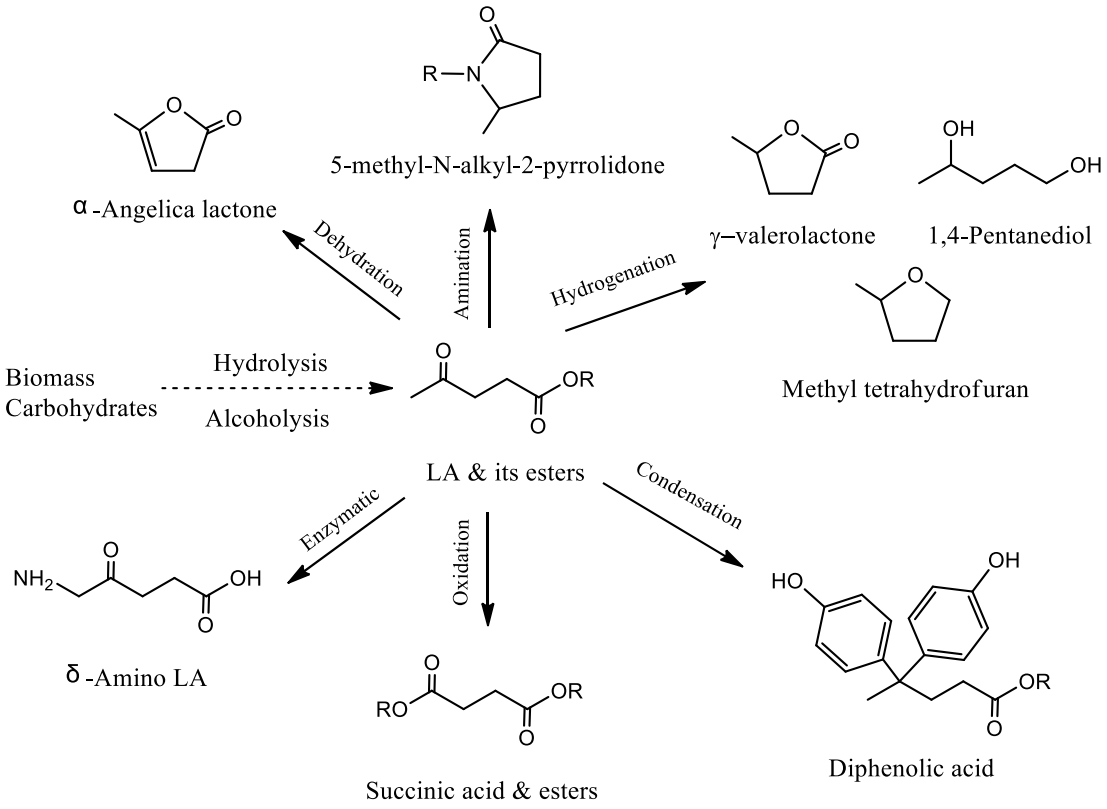

Figure 1.5. Products from LA and its esters by different reactions.

1.3.2 Production of LA and its esters

Due to easy-available and few pretreatment, biomass raw materials like sorghum grain, wheat straw, bagasse, sawdust were tested for LA and its esters production. As cellulose content is around 30-50 wt% in biomass resource, acid-catalysis conversion of raw materials to the final stable product LA has attracted interests. Because they have shown potential in upgrading of chemicals and valorization of the residue from industry and municipal waste in the viewpoint of source-recycle and social sustainable development [40].

Maximum yield of LA was 32.6 wt% from sorghum grain [41]. However, it is noting that there is 73.8 wt% starch in sorghum grain, resulting in comparatively higher yield of LA than other raw materials. By adding a pre-hydrolysis process, the yield of LA increased from 21.3wt% to 29.3wt% under the same condition, which indicates the significance of pretreatment before hydrolysis for easier access of acid into the interior structure of raw

materials [42]. The same phenomenon was also observed for ethyl levulinate production from wood chips by using sulfuric acid and heterogeneous catalyst H-USY [43].

One important reason for low yield of LA and its esters is the formation of huge amount of byproduct humins. Humins can cause the clogging and fouling of the reactor, separators and filters in the downstream process. Furthermore, deposition of humins on reactor walls makes it difficult to control the thermal exchange and the process temperature, resulting in further decrease of yield and selectivity.

As the main portion of lignocellulosic biomass, cellulose (~50wt%) is the primary source for hexoses and its downstream value products like HMF and LA [44]. Due to its high degree of crystalline and immiscible with water and alcohols, generally, it needs relatively harsh conditions for depolymerization of cellulose, for example, high temperature and high acid concentration. Nevertheless, these harsh conditions also accelerate the side reactions and cause formation of humins and deactivate the catalysts. Thus, suitable catalyst should be designed for an easier access to acid site and β-1,4-glycosidic linkage of cellulose [28]. Compare to high stable structure of cellulose (Figure 1.6), starch consisting of glucose connected by α-1,4-glycosidic linkage is easier to be hydrolyzed or alcoholyzed by acid with moderate conditions [45, 46]. However, production of LA from starch is in competition with human foods, which makes cellulose from lignocellulosic biomass more feasible and available for commercial-scale production of LA.

Besides cellulose and starch, oligosaccharides and disaccharides such as β-cyclodextrins [47], sucrose [48, 49], inulin [44, 50], cellobiose [51], maltose [47] can be converted to LA and its esters. The components of these poly-, oligo- and disaccharides were listed in Table 1.3, which indicates their components of monosaccharides and somehow gives an explanation for the different yield of product under the same conditions.

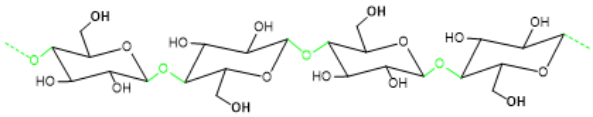

Cellulose (β-1,4-glycosidic linkages)

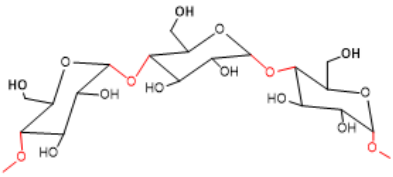

Starch (α-1,4-glycosidic linkages)

Figure 1.6. Structure comparison of cellulose and starch.

Table 1.3. Components of polysaccharides, oligosaccharides and disaccharides

Type	Components
Cellulose (polymer)	Glucose
Starch (polymer)	Glucose
Inulin (polymer)	Fructose
Sucrose (disaccharide)	Glucose+Fructose (mole ratio=1:1)
Cellobiose (disaccharide)	Glucose
Maltose (disaccharide)	Glucose
β-cyclodextrins (oligosaccharides)	Glucose

Although homogeneous acid catalysts like HCl and H_2SO_4 have shown good yield in conversion of cellulose, new systems need to be developed to improve the catalyst performance, costs and recycle use. Alonso et al. [52] have demonstrated that the following system composed by 90wt% GVL and 10wt% H_2O and Amberlyst 70 as the solid catalyst for direct conversion of cellulose to LA and GVL, works well. GVL could efficiently convert cellulose into soluble products and can significantly solubilize humins, which can reduce the purification step. High LA yield (49wt%) was achieved under 160ºC after 16h of reaction. Catalyst regeneration is easy and stable yield of product was obtained from this novel system.

As C6 sugars mainly include glucose and fructose as the single precursor molecule for synthesis of LA and its esters, the reaction of dehydration of C6 sugar to HMF and further rehydration and ring-opening of HMF to LA and its esters has attracted lots of research in reaction mechanism and system design to gain insight into this process. In fact, glucose is more preferred than fructose because glucose is the unique product from cellulose by acid hydrolysis. Nevertheless, conversion of fructose gives higher yield of LA than glucose as glucose needs to transfer to fructose by isomerization and then further dehydrated to HMF and rehydration to LA (Figure 1.7). The mechanism for production of LA esters were proposed in the similar way like LA. The difference of the mechanisms between production of LA and LA esters is the formation of alkylated intermediates, such as alkyl glucoside etc. As the process for production of LA and LA esters leads to co-product formic acid (FA) or formate esters, the yield of product in mass weight and molar ratio is different. For example, one should notice that the maximum theoretical mass yield of LA from hexoses is 64.5wt%, while the mole yield of LA and esters from hexoses is 100 mol%.

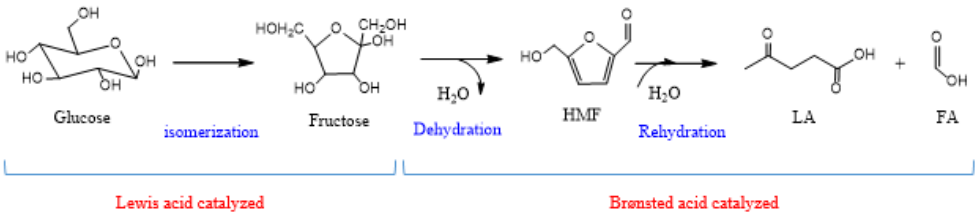

Figure 1.7. Mechanism of conversion of glucose to LA.

Both homogeneous and heterogeneous catalysts were used for LA and its esters production from C6 sugar. For instance, heterogeneous graphene oxide (GO)-based catalysts modified with sulfonic acid (SO_3H) functional groups was developed for conversion of C6 sugars to LA [53]. A 50wt% yield of LA was obtained in 2h under 200°C and SO_3H functional groups have shown good thermal stability for reuse. Transition metal chlorides especially for $CrCl_3$ has shown significance positive effect on conversion of glucose to LA due to its key role in isomerization of glucose to fructose [54, 55]. However, this Lewis acid catalyst also promoted the overall rate of conversion of glucose when combining with Brønsted acid

HCl for further rehydration of HMF, resulting in side reactions and byproducts. Optimization of both concentrations of Lewis acid and Brønsted acid in this cascade reaction should be done to maximize the desired product yield [55]. By developing a hybrid catalyst ($CrCl_3$/HY) and applying central composite design (CCD) under the response surface methodology (RSM) for LA production, 47 wt% yield of LA based on hexoses content was obtained at 145.2°C and 147min. Biphasic continuous flow process [56] has been employed for different products including 5-(chloromethyl)-furfural (CMF), HMF and LA from carbohydrates such as sucrose, glucose and fructose. A mixture with 2M HCl aqueous-methanol (v:v=1:2) was inserted into continuous flow reactor and gave 46wt% yield of LA under 140°C and 80min after filtering insoluble byproducts.

One of advantage by alcoholysis of glucose was reported by Hu et al. [57] that the alkylated intermediate formed in alcohol can suppress the formation of humins polymers. The alkyl group can protect the reactive intermediate and enhance the production of LA esters. This advantage of using alcohol was also identified by their group on the study of one-pot synthesis of LA esters from xylose [58]. Despite this advantage, it is worth noticing that intermolecular dehydration of alcohols to ethers was significant in the alcoholysis reactions, which can hinder the scale-up of this process [59]. A maximum 86% mole yield of ethyl levulinate was obtained under 120°C for 24h through different sulfonic acid-functionalized carbon nanotubes catalyzing fructose dehydration to ethyl levulinate [60]. A linear relationship between catalytic activity and acid density of the catalyst was found and this catalyst shown the facile separation, high thermal stability and ease of recovery.

Until now, there are few articles [20, 58, 61] in production of LA from C-5 compounds such as hemicellulose, xylose, furfural, etc. However, some articles on production of LA esters from furfuryl alcohol have been published in recent years [21, 62-68]. The reason may be because LA cannot be directly produced by hydrolysis from these C-5 compounds. After hydrolysis of hemicellulose to stable molecular furfural, it needs additional hydrogenation step for transformation of furfural to furfuryl alcohol, which has been regarded as the precursor for target production of levulinate ester by alcoholysis reaction. However, as the acid-catalyzed conversion of furfural alcohol to LA in aqueous solution

resulted in different intermediate or final products, side reactions such as polymerization and rearrangement can occur, reducing yield and selectivity of LA [69, 70].

To improve the yield of LA from xylose, a novel strategy employing biphasic systems was developed by using alkylphenol solvents as the organic layer for direct conversion of hemicellulose in three steps [20] (Figure 1.8). Firstly, low concentration of xylose was obtained from dilute acid treatment of real biomass feedstock (corn stover). Then, organic solvent 2-sec-butylphenol (SBP) was added to give a biphasic system for dehydration of xylose and extraction of furfural from aqueous layer saturated with NaCl. Then by hydrogenation of furfural in the second step, furfural alcohol was slowly fed into another biphasic reactor, where conversion of furfural alcohol to LA occurs in aqueous layer. It is worth noting that most of furfural alcohol still remains in SBP, which decreases its concentration in the aqueous layer and the rates of side reactions as well. Adding NaCl into the system can significantly improve partition coefficient of furfural from 50% to 90%, which allows high yield of furfural in organic phase. 70% yield of LA was obtained in this system at 398K. Due to high boiling point, 4-n-hexylphenol (NHP) and 4-propylguaiacol [71] were selectively used as solvents for removal of LA to organic phase and further distillation of LA from top column. This strategy was proved to be efficient for conversion of hemicellulose to LA with alkylphenol solvents in a biphasic reactor system.

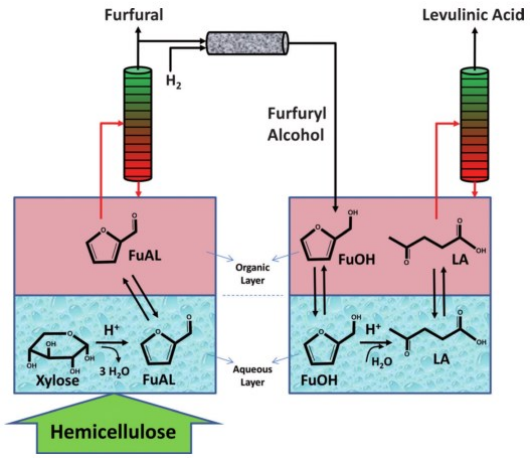

Figure 1.8. Biphasic systems applied for extraction of furfural from aqueous phase where dehydration of xylose occurs and extraction of LA from aqueous phase where conversion of furfural alcohol occurs [20].

Alcoholysis of furfuryl alcohol to LA esters in alcohol medium such as methanol, ethanol, n-propanol, n-butanol, etc. has been studied in different reactors including batch, semi-batch and continuous reactors. High yield of product was obtained in majority of studies by employing both homogeneous and heterogeneous catalysts. Wang et al. developed the double SO_3H-functionalized ionic liquids for alkyl levulinate production. In this system, remarkably, the side reaction of the dehydration of alcohols is negligible. The Hammett method was used to determine the acidity of different ionic liquids and this method indicate the significant effect of molecular structure on acidity of ionic liquids [67]. In different alcohol medium, the H-ZSM-5-50 [21] shown the decrease of yield by increasing the alcohol molecule. On the contrary, by using α-Fe_2O_3 as catalyst, the opposite phenomenon was observed [68]. As conversion of furfuryl alcohol to LA esters needs several steps, the mechanism for this reaction is not clear and it needs more study on this part.

1.4 Applications and production of γ-valerolactone (GVL)

1.4.1 Applications of GVL

γ-valerolactone (GVL), further hydrogenated from LA or levulinate esters, can be mainly used as fuel additives and solvents and has great potential for further upgrading to valuable chemicals, biodiesel and jet fuels [72] as an important platform (Figure 1.9). For example, 2-MTHF, hydrogenated from GVL, can be used as a component of non-petroleum P-series fuel that can be substituted for or blended with gasoline with a potential market of 10,000-100,000 million lb/year [5, 37]. 5-nonanone, synthesized from GVL derived pentanoic acid, can be also used as diesel fuel [73]. Enantiomeric pure GVL can be employed as a chiral building block for the synthesis of pharmaceutically active molecules [74]. Additionally, as GVL also has a sweet and herbaceous odor, it can be suitable for the production of perfumes and food additives [75]. Recently, numerous research and reviews have been reported for GVL synthesis in different systems [19, 25, 26, 76, 77]. However, scale-up of GVL production has not been established yet.

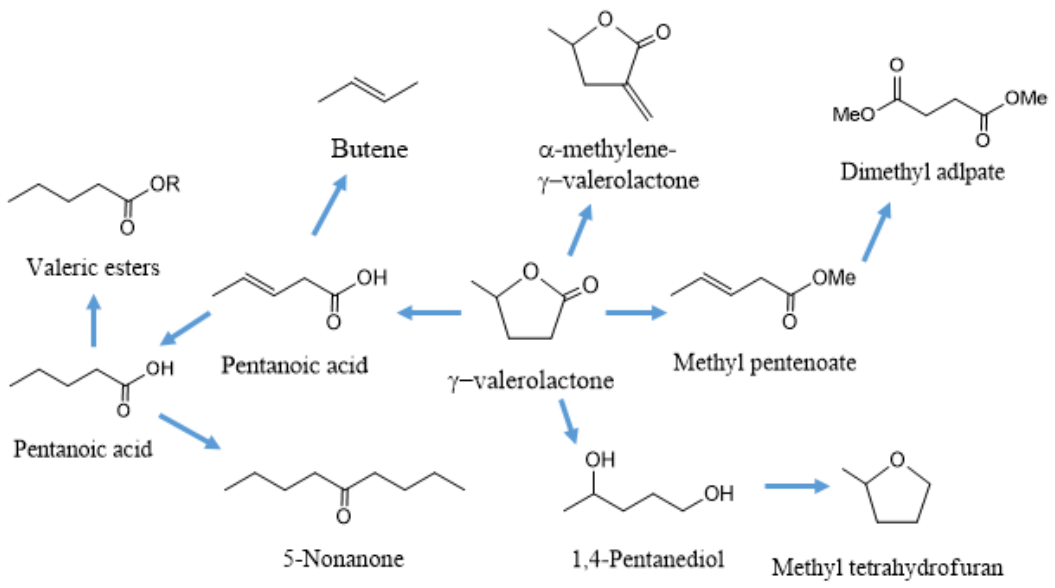

Figure 1.9. Upgrading of GVL to biofuels and chemicals.

GVL is mainly used as: green solvent for biomass conversion, such as pretreatment of depolymerization of lignocelluloses, synthesis of furans, etc.; biofuel precursor and additives, such as upgrading of GVL to MTHF, valerates, liquid hydrocarbon fuels, etc.; chemical raw materials, such as monomers to synthesize polymers.

In particular, GVL has shown great potential and excellent performance as a green solvent for biomass conversion [78-83]. For example, to relieve from solid humins accumulation, recently, Alonso et al [84] have reported a new system by using GVL/H_2O as solvent for direct conversion of corn stover to LA and furfural (Figure 1.10). GVL has shown efficient solubility of cellulose, hemicellulose, lignin and its derivative humins, which provides a feasible process by eliminating pretreatment and separation steps caused by solids accumulation problems. A yield of 66 mol% of LA was obtained based on C6 fraction in corn stover by using a mixture of GVL 80wt%/H_2O 20wt% as solvent over 19h at 170ºC. Due to different hydrolysis conditions, integrated conversion of cellulose and hemicellulose, the two highest content of biomass, needs to be adjust for improving the yield of furfural and LA. With short time (<3h) and lower sulfuric acid concentration (<0.1M), it was beneficial for production of furfural because hemicellulose is amorphous and easy-hydrolyzed by acid. While by prolonging the reaction time and increasing acid

concentration, LA yield increased and C5 fraction turned to degrade to humins. The mixture of LA and furfural after neutralization can be further upgraded to the target product GVL.

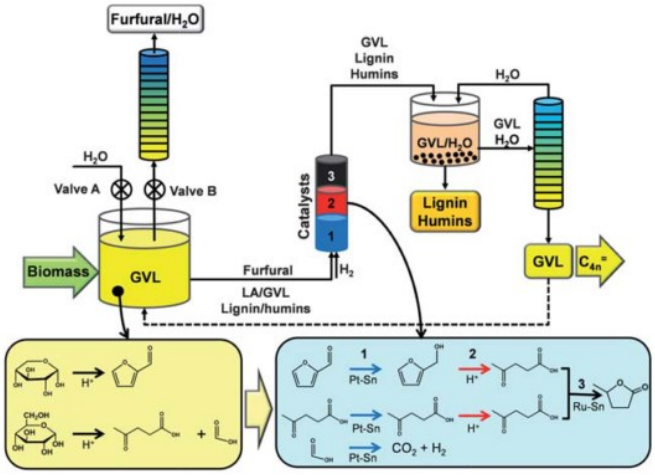

Figure 1.10. Integrated conversion of hemicellulose and cellulose portions to GVL and its C4 hydrocarbon derivatives by using GVL as solvent [84].

1.4.2 Hydrogen donor for production of GVL

As building block and additive for diesel, fine chemical and solvent which has been demonstrated in previous section about GVL, production of GVL has attracted great interests from all over the world [85]. Properties of GVL are shown in Table 1.4. Employing different homogeneous or heterogeneous catalytic systems, LA or its esters derived from biomass can be efficiently hydrogenated to produce GVL in good yield. Though LA esters such as methyl levulinate, ethyl levulinate and n-butyl levulinate are also regraded as important fuel additives [45, 86], it provides an alternative way to produce GVL in full utilization of both cellulose and hemicellulose.

Depending on different hydrogen donor, there are three pathways for conversion of LA or its esters to GVL: using H_2 directly for hydrogenation; using formic acid for decomposing to H_2 and further hydrogenation; using alcohols for catalytic transfer hydrogenation by Meerwein-Ponndorf-Verley (MPV) reaction (Figure 1.11). Using H_2 can directly hydrogenate LA and its ester, resulting easy, fast and efficient reaction. As produced with LA at molar ratio of 1:1 in theoretical yield by hydrolysis of cellulose, formic acid can be

further used as hydrogen donor without separation and external H_2 in the principal of atom economy. In the recent years, by using MPV reductive reaction, aldehydes and ketones can be reduced to corresponding alcohols, which can be applied for hydrogenation of carbonyl group in LA and its ester to GVL. Herein, recent advances of technologies in production of GVL from biomass derivatives, especially from LA and its esters are reviewed depending on different hydrogen donor and catalysts.

Table 1.4. Properties of γ-valerolactone (GVL).

Property	Value
CAS-No.	108-29-2
Formula	$C_5H_8O_2$
MW	100.112
Refractive index (20°C)	1.432
Density (g/ml)	1.05
Melting point (°C)	-31
Boiling point (°C)	207-208
Solubility in water	Soluble

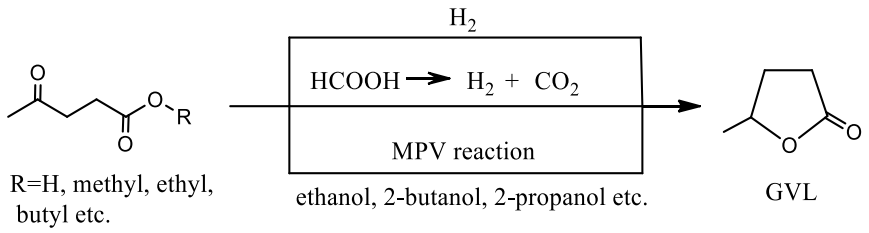

Figure 1.11. Hydrogenation of LA and its ester to GVL with different hydrogen donors.

1.4.2.1 Using formic acid as hydrogen donor

Hydrogenation of LA with formic acid (FA) as hydrogen donor has attracted interests because hydrolysis of cellulose can produce equivalent mole of LA and FA in theory. As FA has been reported as one of important hydrogen source [87], direct in-situ decomposition of FA to hydrogen for hydrogenation of LA to GVL makes this reaction feasible from an atom-economic viewpoint. As results, various heterogeneous or

homogeneous catalysts have been exploited to apply for hydrogenation of LA with FA (Table 1.5). Proposed mechanism of LA hydrogenation with FA undergoes in three steps: firstly, formic acid decomposes to H_2 and CO_2; secondly, LA hydrogenation with in-situ formed H_2 to intermediate 4-hydroxypentanoic acid (HPA); thirdly, HPA transforms to GVL by intra-molecule cyclization (Figure 1.12).

Table 1.5. Hydrogenation of LA to GVL by using formic acid as hydrogen donor[a]

Feedstock n_{LA}/n_{FA}	Catalyst	Temperature /°C	Time /h	Yield mol%	Ref.
1:36.9[b]	$[(\eta^6\text{-}C^6Me_6)R\text{-}u(bpy)(H_2O)][SO_4]$	70	8	25	[88]
1:1[c]	$RuCl_3$,PPh_3, pyridine	150	12	93	[89]
1:6.6[d]	TFA, Ru/C	180	16	52	[90]
1:1	Ru-P/SiO_2	150	12	96	[91]
1:1	Cu/ZrO_2	200	5	100	[92]
1:5.4	$[Ru_3(CO)_{12}]$	130	24	100	[93]
1:3	Au/ZrO_2	150	5	97	[94]
1:6.2	Ru/C (Cl) HR	190	5	57	[95]
1:1	Ag-Ni/ZrO_2	220	5	99	[96]
1:1	Au/ZrO_2-VS	150	6	99	[97]
1:1.5	Shvo catalyst	100	8	99.9	[98]

[a] water as solvent except noted; [b] Sodium formate as hydrogen donor; [c] without solvent; d n(fructose):n(FA)

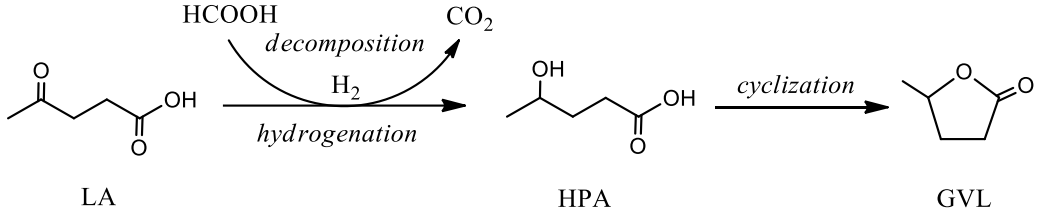

Figure 1.12. Mechanism of hydrogenation of LA with FA as hydrogen donor.

For example, a new route to convert cellulose, starch, glucose into GVL catalyzed by $RuCl_3/PPh_3$ catalyst without external H_2 was reported [89] (Figure 1.13). LA can be selectively reduced to GVL instead of 1, 4-pentanediol by tuning the base and ligand in Ru-based catalytic systems. More importantly, this route avoids the energy-cost separation step of LA from the mixture of LA and FA in aqueous solution. Neat 1:1 LA and FA by adding $RuCl_3$, PPh_3 and pyridine without water under 150°C for 12h resulted in 93% yield of GVL. By further applying this catalyst for LA from hydrolysis of cellulose, 48% yield of GVL can be obtained from glucose.

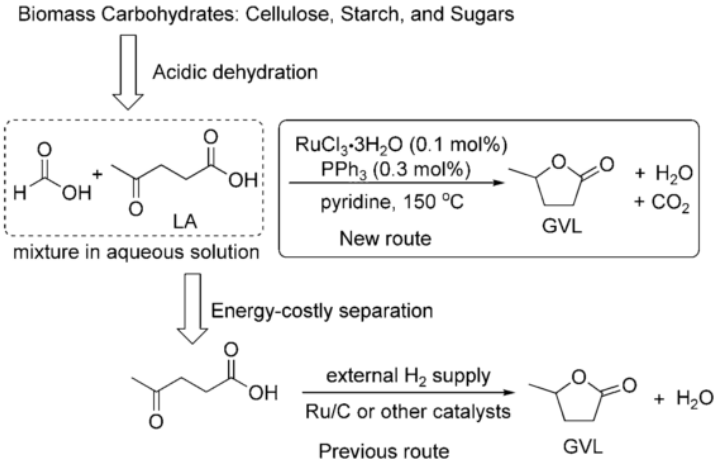

Figure 1.13. Direct hydrogenation of LA without external H_2 supply [89].

Hans Heeres et al. [90] has employed trifluoroacetic acid (TFA) as acid catalyst and Ru/C as hydrogenation catalyst for catalytic hydrolysis and hydrogenation of monomeric C6 sugar (D-glucose and D-fructose) as well as sucrose and cellulose in water with either H_2 or FA as the hydrogen donors. Because sulfuric acid is likely poorly compatible with Ru catalysts due to the presence of sulfur [99, 100], TFA was attempted to be used as organic acid for hydrolysis and it showed no effect on hydrogenation of LA. However, when acid and hydrogenation catalysts are added together for GVL production, hydrogenation of fructose or glucose to sorbitol needs to be considered. In addition, although Ru/C is valuable in hydrogenation of LA, it will be deactivated when formic acid exists in the system, which limits utilization of Ru catalyst for the direct conversion of biomass to GVL [91, 94, 95]. In consequence, developing new robust catalyst is necessary for integration

of hydrolysis of biomass and further hydrogenation of LA with FA.

Recently, new non-noble, earth-abundant and robust metal catalyst Cu/ZrO_2 was developed to catalyze the hydrogenation of LA with equimolar FA in the absence of external added hydrogen [92]. Remarkably, 100% yield of GVL can be achieved under 200°C after 5h and the Cu/ZrO_2 prepared from the oxalate-gel co-precipitation method can lead to good FA conversion with consistently low CO content (<20ppm). It also appears that both the initial FA decomposition and the subsequent LA hydrogenation reactions are the kinetically relevant steps in the present Cu/ZrO_2–OG-catalyzed system.

1.4.2.2 Using alcohols as hydrogen donor

By mainly employing non-noble heterogeneous catalysts and due to special chemo-selectivity for the reduction of carbonyl groups, Meerwein-Ponndorf-Verley (MPV) reaction has been used for hydrogenation of LA to GVL (Table 1.6). In this reaction, secondary alcohols are mainly used as hydrogen donors for catalytic transfer hydrogenation (CTH) process and corresponding ketones which could also be sold as commodity chemicals are produced (Figure 1.14).

Chia and Dumesic [101] firstly reported ZrO_2 was the most active oxide for CTH of LA esters. It is worthy noticing that LA undergoes CTH process to GVL synthesis less efficient compared with its esters because of the strong binding of acid functional group in LA to basic sites on ZrO_2. Main byproducts were formed through self-condensation of the formed aldehyde from alcohols or reaction between the aldehydes and levulinate esters.

Table 1.6. Hydrogenation of LA and its esters to GVL by using alcohols as hydrogen donors

Subs.	Solvent	Catalyst	Temperature /°C	Time /h	Yield mol%	Ref.
BL[a]	2-butanol	ZrO_2	150	16	85	[101]
LA	2-butanol	ZrO_2	150	16	22	[101]
EL[b]	Ethanol	Amorphous ZrO_2	250	1	63	[102]
EL	Ethanol	m-ZrO_2	250	1	29	[102]
EL	2-propnanol	Al_2O_3- ZrO_2	220	4	83	[103]
EL	2-propnanol	Zr-HBA	150	4	94	[104]
EL	2-butanol	Zr-HBA	150	4	96	[104]
LA	2-propnanol	HCl/$ZrO(OH)_2$	240	1	83	[105]
EL	2-propnanol	Zr-PhyA	130	8	95	[106]
ML[c]	2-propnanol	ZrO_2/SBA-15	150	3	91	[107]
LA	2-propnanol	ZrO_2/SBA-15	250	--[d]	93	[108]
EL	2-propnanol	ZrFeO	230	0.5	87	[109]
EL	2-propnanol	Ni_5Zr_5	200	3	94	[110]

[a] Butyl levulinate; [b] Ethyl levulinate; [c] Methyl levulinate; [d] continuous reactor;

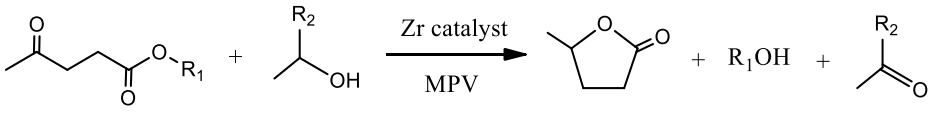

LA or its ester

R_1=H, C_xH_{2x+1}

GVL

Figure 1.14. Catalytic transfer hydrogenation of LA or its esters with secondary alcohols by MPV reaction.

By preparing Zr catalysts with different methods and structure, several catalysts such as Zr-HBA, Zr-PhyA, ZrO_2/SBA-15, ZrFeO, Ni_5Zr_5 etc. were reported to give a good performance in CTH of LA to GVL by MPV reaction. And mechanism depending on Zr catalyst was reviewed by Amin Osatiashtiani et al [26]. Tang et al [105] has developed an in-situ generated catalyst system for CTH of LA to GVL (Figure 1.15). A 83% yield of

GVL was obtained at 240ºC, 1h in 2-propanol solvent. Significantly, 82% high yield of GVL can be obtained from biomass derived LA by extracting LA with 2-BuOH and further CTH of LA to GVL even in the presence of humins.

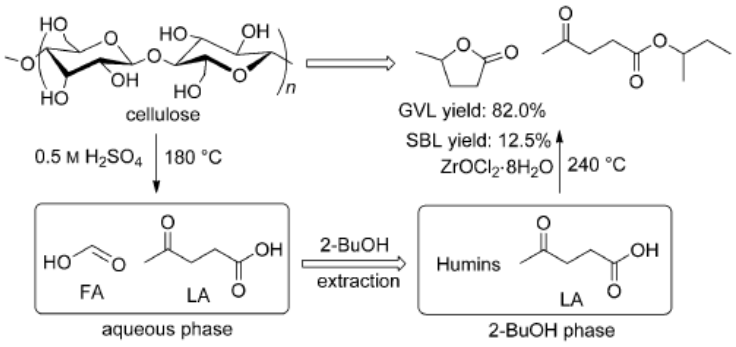

Figure 1.15. GVL production from cellulose by integrating acid hydrolysis, extraction of LA and CTH process catalyzed by in-situ generated $ZrO(OH)_2$ and HCl [105].

1.4.2.3 Using hydrogen gas

So far, using hydrogen gas for hydrogenation of LA is the most direct and efficient way. Huge amount of homogeneous and heterogeneous catalysts based on non-noble, noble metals and miscellaneous metals have been developed for this reaction with H_2 and some results are listed below in Table 1.7.

Iridium nanoparticles supported on carbon nanotubes (Ir/CNT) was reported to give good performance for hydrogenation of LA even in the presence of FA [111]. They obtained 91% yield of GVL at 50ºC in 1h under 20bar H_2. The catalyst can be used in the presence of FA due to the mild reaction conditions avoiding the decomposition of FA. Ru catalyst has been screened as one of most active and selective for GVL synthesis [112]. Therefore, extensive research in Ru catalyst with different support such as carbon, TiO_2, zeolites, etc is done. For example, Ru supported on hydroxyapatite catalyst [113] demonstrated higher activity and selectivity than Pt, Pd and Ni for hydrogenation of LA in low pressure and temperature. However, supports of Ru-catalysts and solvents also have significance effects on hydrogenation of LA [114], non-acidic catalysts selectively attribute to GVL synthesis as main product, while the zeolite-supported acidic catalysts can directly convert LA to

pentanoic acid in dioxane under mild conditions. Besides, deactivation of catalyst due to loss of acid sites by dealumination limits the reuse of catalyst. Possible mechanism of hydrogenation of LA to GVL catalyzed by Ru/C is illustrated in Figure 1.16. In the first step, hydrogenation of LA or its esters with H_2 to intermediate is catalyzed by Ru/C. In the second step, intra-cyclization of intermediate occurs to form GVL.

Table 1.7. Hydrogenation of LA and its esters to GVL by using H_2 in batch reactor

Catalyst	**Solvent**	**Temperature /ºC**	**P(H_2) /bar**	**Time /h**	**Yield mol%**	**Ref.**
$Ru(acac)_3$+TPPTS	H_2O	140	69	12	95	[88]
Ni/HAP	H_2O	70	5	4	65	[113]
Pt/HAP	H_2O	70	5	4	88	[113]
Cu/ZrO_2	H_2O	200	34.5	5	100	[115]
Fe/C	H_2O	170	5	3	99	[116]
Ni-MoO_x/C	--	140	8	5	97	[117]
Ni-MoO_x/C	H_2O	140	8	5	2	[117]
Pd/HMS	H_2O	160	150	6	89	[118]
Ir/CNT	$CHCl_3$	50	20	1	91	[111]
Ru/C	Methanol	130	12	2.67	84	[119]
Ru/C	H_2O	130	12	2.67	86	[119]
Ru/HAP	H_2O	70	5	4	99	[113]
Ru/TiO_2	Dioxane	130	12	4	92	[114]
Ru/ZSM-5	Dioxane	200	40	4	50	[114]

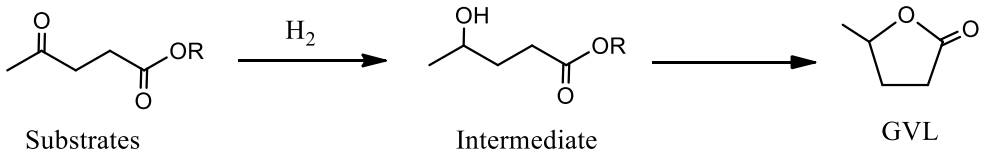

Figure 1.16. Possible mechanism of hydrogenation of LA and its esters with H_2 to GVL.

Non-noble metals including Ni, Cu, Fe can also be used for the development of hydrogenation catalysts. For instance, Amol M. Hengne et al. [115] developed non-noble catalysts Cu/ZrO_2 for hydrogenation of LA and its ester to GVL. Among different support for preparation of catalysts, Cu/ZrO_2 has afforded 100% selectivity of GVL and metal leaching was avoided when experiment was performed with this catalyst in methanol. To avoid leaching of active metal during the reaction, Ja Young Park [116] has developed a carbon-encapsulated Fe catalyst which can be reused for 5 times with negligible loss of catalytic activity.

1.4.3 Kinetic study

Piskun et al. [120] reported a study on the hydrogenation of LA to GVL in water by using Ru/C (3 wt% Ru) as the catalyst in batch reactor. They demonstrated that there are two steps for production of GVL: the first step is the hydrogenation of the ketone group of LA leading to the formation of 4-hydroxypentanoic acid (HPA). The second step is the reversible ring-closure reaction of HPA to GVL. The mechanism of this reaction is illustrated in Figure 1.17.

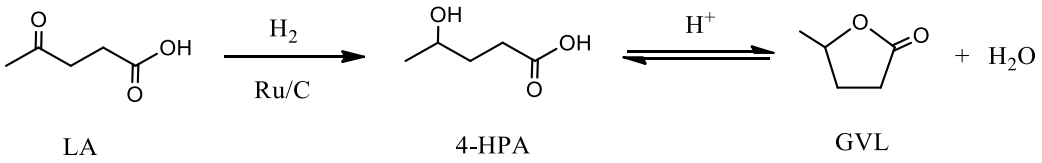

Figure 1.17. Reaction mechanism for the hydrogenation of LA to GVL catalyzed by Ru/C in water in the study of Piskun et al.

Hydrogenation of LA to HPA was modelled using Langmuir-Hinshelwood type expression with competitive adsorption of LA and GVL on the metal site of catalyst. The cyclization of HPA to GVL was modelled as an equilibrium reaction that occurs in the bulk liquid catalyzed by protons from dissociation of carboxylic acid LA and HPA. Two models including heterogeneous model by taking into account the mass transfer and homogeneous model in absence of mass transfer were developed and compared. Both models give good fit with the experimental data and heterogeneous model shows better performance due to

the catalyst used for this study. The homogeneous model shows the general Langmuir-Hinshelwood equations without simplification, the hydrogenation rate can be shown as:

$$R_1 = -\frac{k_1.P_{H_2}.K_{LA}.[LA]}{(1 + K_{LA}.[LA] + K_{GVL}.[GVL] + K_{HPA}.[HPA])^2} \times \frac{m_{cat}}{V} \quad (1)$$

The cyclization rate is shown as:

$$R_2 = k_{HPA}C_{H+}C_{HPA} - k_{GVL}C_{H+}C_{GVL} \quad (2)$$

The activation energy for the first hydrogenation is 34.1 ± 0.1 kJ.mol^{-1}. For the cyclization reaction, the activation for the forward reaction is 66.9 ± 3.3 kJ.mol^{-1}, for the backward reaction is 70.6 ± 5.6 kJ.mol^{-1}. The activation energy for the cyclization reaction is larger than the hydrogenation reaction. Thus, higher temperature favors the GVL production while lower temperature favors the production of intermediate HPA.

Negahdar et al. [121] has reported the kinetic analysis for hydrogenation of alkyl levulinate such as ML, EL and BL to GVL catalyzed by Ru/C (5 wt%) in methanol as the solvent. The reaction also contains two steps: the first hydrogenation of alkyl levulinate to the intermediates and the second cyclization step of intermediates to GVL. The mechanism of this kinetic study was shown in Figure 1.18. The difference of the mechanisms with Piskun et al. is the second step is assumed to be irreversible in methanol. On this study, mass transfer limitations is neglected and the reaction is carried out in the intrinsic regime. Langmuir-Hinshelwood model was developed for the first hydrogenation step and further simplified.

The first hydrogenation reaction rate and the second cyclization rate are listed below:

$$R_1 = -\rho_{cat}k_1C_{H2}C_{AL} \quad (3)$$

$$R_2 = k_2C_{AHV} \quad (4)$$

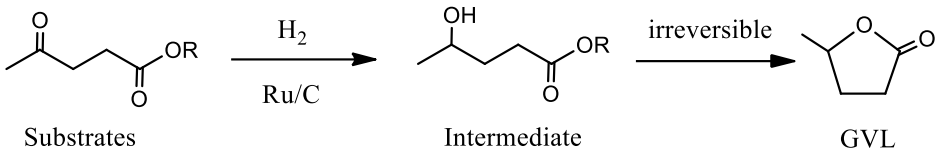

R = methyl, ethyl, n-butyl

Figure 1.18. Reaction mechanism for the hydrogenation of alkyl levulinate to GVL catalyzed by Ru/C in methanol.

The authors elucidated that the cyclization reaction is the rate determination step and controls the overall reaction rate. Substrates with shorter alkyl substituent exhibit a lower energy barrier for their transformation. The activation energy for the two step reactions are shown in Table 1.8. However, the relationships between the structures and the kinetics are not defined by the authors. It is worth noticing that using methanol as solvent can cause side transesterification reaction when experiments performed with EL and BL.

Table 1.8. Activation Energy for production of GVL from alkyl levulinate.

Substrate	Activation energy kJ.mol^{-1}	
	Hydrogenation	Cyclization
ML	41	50
EL	45	58
BL	58	63

1.5 Objectives of this doctoral thesis

Based on the literature review of γ-valerolactone production, a lot of effort has been done on the catalyst issue, but there are still some needs to fill. Indeed, to scale up this process, the following questions should be answered: How safe is this hydrogenation reaction? What are the reaction enthalpies at stake for this system? Which reactants among levulinic acid and its ester are better?

The objective of this doctoral thesis is to study the kinetics and thermodynamics of hydrogenation of levulinic acid (LA) and its esters to GVL. This doctoral thesis is divided

into three parts:

- Thermal risk assessment for hydrogenation of levulinic acid to γ-valerolactone;
- Structure-reactivity study on hydrogenation of levulinic acid and its esters;
- Experimental determination of reaction enthalpies for γ-valerolactone production.

In chapter II, thermal risk assessment for hydrogenation of LA to GVL catalyzed by Ru/C in water was performed. A kinetic model including energy balance under near-adiabatic condition was built. Experiments were performed in ARSST (Advanced Reactive System Screening Tool) under different conditions to estimate the kinetic constants of the reaction system. Two thermal risk parameters TMR_{ad} (the Time to reach the Maximum temperature Rate under adiabatic condition), which characterizes the probability of thermal runaway, and ΔT_{ad} (the difference between the maximum and initial reaction temperature), which characterizes the severity of thermal runaway, were used to assess the thermal risk of this reaction system. Based on the model, these two risk parameters were determined at different operating conditions. Finally, with help of a risk matrix, the thermal risk was assessed, which can provide the safe operation conditions for this reaction system.

In chapter III, application of Taft equation, derived from the concept of Linear Free Energy Relationships to hydrogenation of LA and its esters to GVL catalyzed by Ru/C for structure-reactivity study of this reaction system was performed. A kinetic model including gas-liquid mass transfer effect and Taft equation was developed. Experiments were performed in autoclave under isothermal and isobaric conditions to estimate the kinetic constants and find a relationship between reactant structure and reactivities. The kinetics of hydrogenation of LA, methyl levulinate (ML), ethyl levulinate (EL) and n-butyl levulinate (BL) to GVL catalyzed by Ru/C were compared and the polar and steric effect of the substitute groups were studied. From this study, it is possible to predict the kinetics by knowing the structure of one series molecules.

In chapter IV, experimental determination of reaction enthalpy for production of GVL was performed. Methyl levulinate was selected for this study. A method which links calorimetry

measurement with composition analysis was developed to determine the reaction enthalpy of this hydrogenation reaction. The calorimeter RC1 and Tian-Calvet calorimeter C80 were used to measure the heat release from the reaction system. Combined with Gas-Chromatography analysis, it is possible to determine the reaction enthalpy for the overall reaction and two consecutive steps, which can be further used for process flow diagram and cost-evaluation study of this reaction system.

At the end, a conclusion and perspective are summarized to conclude this thesis work and propose the continuation study based on this work.

Chapter II. Thermal risk assessment for hydrogenation of levulinic acid to γ-valerolactone

Part of this chapter is adapted from the post print of the following articles:
Y. Wang, L. Vernières-Hassimi, V. Casson-Moreno, J.-P. Hébert, S.b. Leveneur, Thermal risk assessment of levulinic acid hydrogenation to γ-valerolactone, Org. Process Res. Dev. 22 (2018) 1092-1100.
Link: https://doi.org/10.1021/acs.oprd.8b00122

2.1 Introduction

To develop a safe process for production of GVL, thermal risk assessment of GVL production from levulinic acid hydrogenation must be performed. As highlighted in the introduction, some kinetic models were developed for this synthesis but none of them studied its thermal behavior. As hydrogenation of unsaturated molecules is known to be exothermic reactions, the thermal runaway risk cannot be neglected. The thermal runaway could occur when there is cooling failure during the process. The reaction will run under adiabatic condition and temperature increases rapidly to cause accidents if no safety operation is performed. This study will allow determining the safe operation conditions for further industry application. This study is especially important for batch reactor in which thermal accumulation can be higher than semi-batch or continuous reactor system.

In this chapter, thermal risk assessment for hydrogenation of LA to GVL catalyzed by Ru/C in water was performed. To assess the thermal risk, a kinetic model under near-adiabatic condition was developed and two thermal risk parameters ΔT_{ad} and TMR_{ad} were determined. The thermal risk parameter TMR_{ad} defines the time to reach the maximum temperature rate and characterizes the probability of thermal runaway. The thermal risk parameter ΔT_{ad} is the difference between the maximum and initial reaction temperature and characterizes the severity of thermal runaway. When there is cooling failure, the reaction will run under

adiabatic condition, so it is important to know the TMR_{ad} and ΔT_{ad} to assess the thermal risk of reaction system. The definition of TMR_{ad} and ΔT_{ad} is shown in Figure 2.1. The experiments under adiabatic mode were performed in ARSST (Advanced Reactive System Screening Tool).

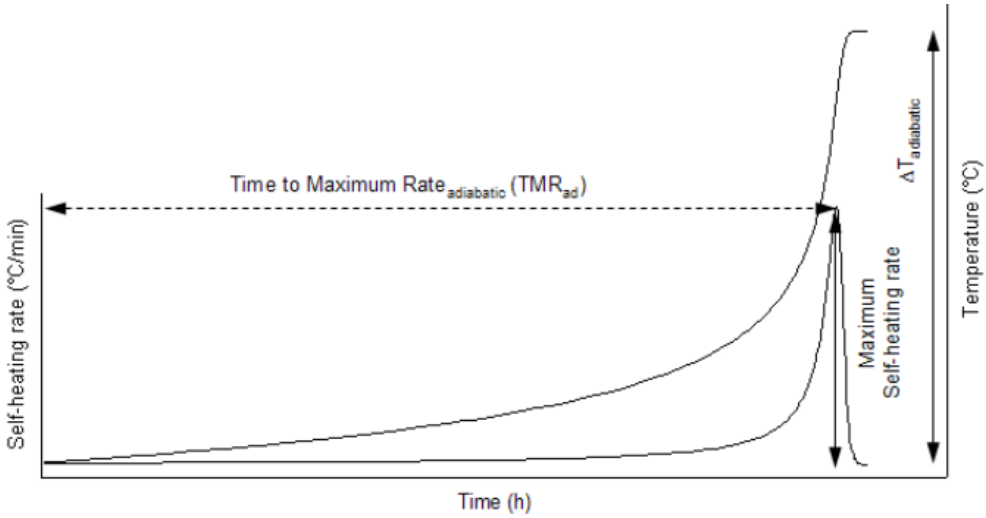

Figure 2.1. The definition of TMR_{ad} and ΔT_{ad}.

Usually, to estimate these parameters, the zero-order approach is used because it represents the worst senario [122]. In this study, we took into account both of step reactions to derive the rate expression. Finally, we developed a thermal risk matrix by multiplying severity and probability of risk in order to make the thermal risk assessment of this reaction. The methodology of this thermal risk assessment is depicted in Figure 2.2.

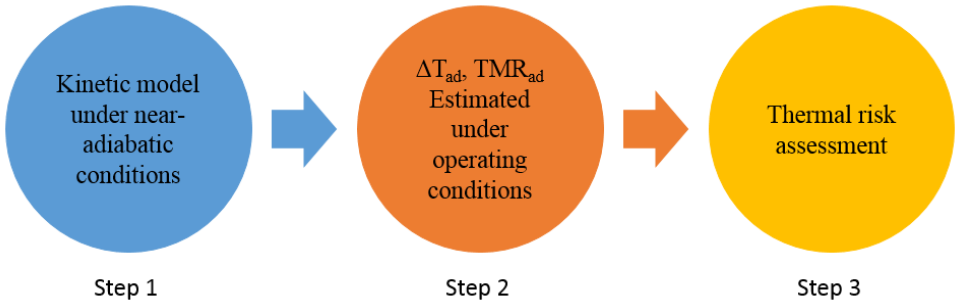

Figure 2.2. Methodology of thermal risk assessment for hydrogenation of LA to GVL.

The experimental section is shown in Section 2.2. Details about the kinetic model which took into account the mass and energy balances are shown in Section 2.3.1 and 2.3.2. The validation of kinetic model with experimental temperature observation from ARSST is summarized in Section 2.3.3. Then, thermal risk assessment for this reaction system is shown in Section 2.3.4. Section 2.4 gives the conclusion of this chapter.

2.2 Experimental section

2.2.1 Chemicals

Levulinic acid was obtained from Sigma-Aldrich. The γ-valerolactone (98 wt%) was purchased from MERCK. The catalyst Ru/C (5%wt ruthenium on activated carbon powder, reduced and 50% water wet) was provided by Alfa Aesar. H_2 (>99.999%) and N_2 (>99.9%) were supplied from Linde. Distilled water was used as the solvent. All the chemicals were used without further treatment.

2.2.2 Experiments performed in ARSST

The calorimeter ARSST (Advanced Reactive System Screening Tool) works under near-adiabatic conditions under the heat loss compensation principle [123, 124]. Several research groups have used this calorimeter to study exothermic chemical system in liquid phase [123-130]. The advantages of this calorimeter are the use of small amount of chemicals, i.e., ca. 10 grams, possibility to work under high pressure to neglect evaporation and fast screening of exothermic reactions in a safe way [131, 132].

This calorimeter used for our experiments consists of two main parts, as shown in Figure 2.3. One part is an open 10 mL glass cell with low phi factor. Inside the 10 mL glass cell there are the reaction mixture and a magnetic stirring bar. The cell is surrounded by a thin heater belt which could provide electrical heating, and insulated by aluminum paper and isolated by glass fiber in a small containment. It is possible to adjust the electrical heating to obtain the desired background heating rates. A thermocouple T1 (T1 in Figure 2.3) is put inside the glass cell to contact with the reaction mixture.

The other part is a 450 mL stainless steel containment which could stand high pressure (maximum pressure 100 bar) and is supported by magnetic plate which could ensure efficient stirring in the glass cell. It is linked with hydrogen gas supply system, pressure and temperature monitor which are controlled by a computer. A thermocouple T2 (T2 in Figure 2.3) is put in the headspace of the stainless steel containment to record the evolution of temperature in the gas phase.

In our experiments, the ARSST was used to record the variation of pressure and temperature for the hydrogenation of LA to GVL catalyzed by Ru/C in water under near-adiabatic conditions.

Before starting the experiment, the 10 mL glass cell was filled with desired amount of LA, distilled water and Ru/C catalyst. The sealed system was purged with pure nitrogen and hydrogen. Then, ca. 35 bar of H_2 was supplied into the system as reactant and to minimize the evaporation of the liquid mixture as well. The experiment was started without magnetic stirring until the temperature of the reaction mixture reached ca. 60°C by electrical heating. The aim of this step is to heat the mixture and avoid the start of chemical reaction. Time zero was set when the stirring started. When the temperature of the mixture reached the maximum temperature, the process was stopped and cooled down. As the variation of recorded pressure was quite low (<1.4%), the system can be considered under isobaric conditions.

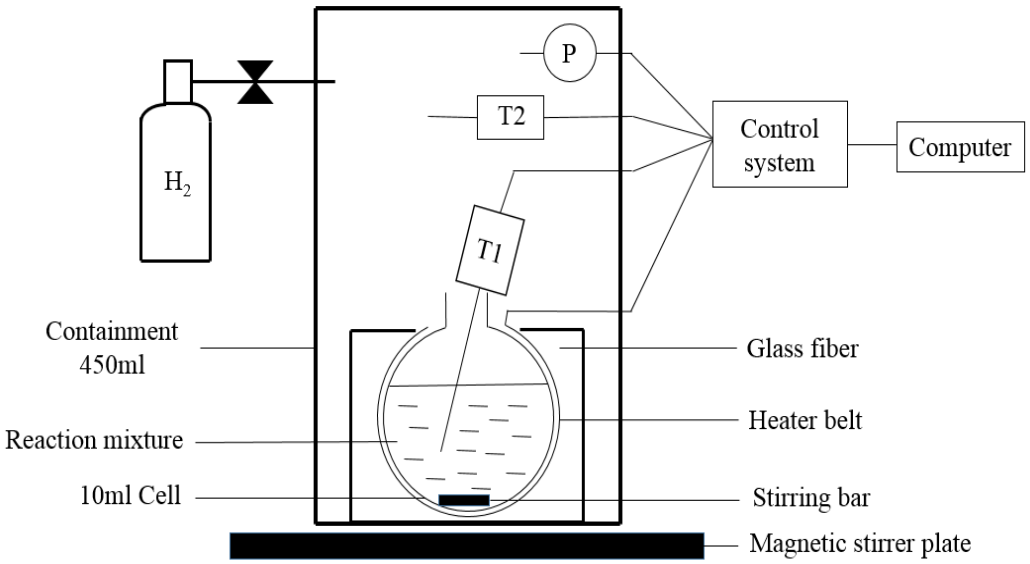

Figure 2.3. Advanced Reactive System Screening Tool (ARSST).

2.3 Results and discussion

2.3.1 Kinetic model under adiabatic condition

Hydrogenation of levulinic acid to γ-valerolactone includes two steps: the first step is the hydrogenation of the ketone group of LA leading to the formation of 4-hydroxypentanoic acid (HPA). The second step is the reversible ring-closure reaction of HPA to GVL [120, 133]. The mechanism of hydrogenation of levulinic acid is illustrated in Figure 2.4.

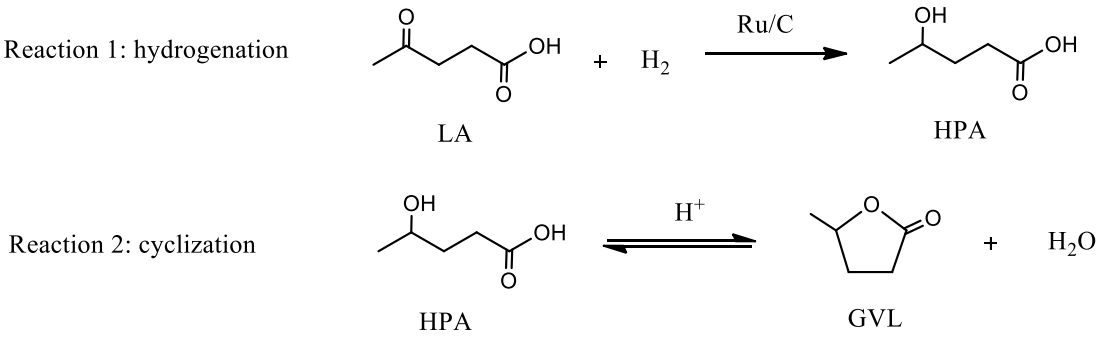

Figure 2.4. Reaction mechanism for the hydrogenation of LA to GVL catalyzed by Ru/C in water.

Piskun et al.[120] have developed homogeneous model based on a Langmuir-Hinshelwood type mechanism and by assuming an equilibrium reaction for the ring-closure reaction. One of the objectives of this work was to develop a kinetic model under near-adiabatic conditions, which takes into account the concentration of LA, proton, H_2 pressure and catalyst loading. For simplicity, this kinetic model of Piskun et al.[120] without considering mass transfer and diffusion limitations was used in this study.

The hydrogenation of LA to HPA on the catalyst surface is described by a Langmuir-Hinshelwood model (eq. 1):

$$R_1 = \frac{k_1 . P_{H_2} . K_{LA} . [LA]}{(1 + K_{LA} . [LA] + K_{GVL} . [GVL] + K_{HPA} . [HPA])^2} \quad (1)$$

where, K_{LA}, K_{GVL} and K_{HPA} are the adsorption coefficients for LA, GVL and HPA, respectively. These thermodynamic constants (K_{LA}, K_{GVL} and K_{HPA}), which do not depend on reactor characteristic, were assumed to be the same than the ones estimated by Piskun et al.

As the first reaction depends on the heterogeneous catalyst and on the gas-liquid, liquid-solid mass transfers, thus this reaction is sensitive to the stirring system. For that reason, the kinetic constants for the first reaction, $k_1(T_{Ref})$ and Ea_1, were estimated in this work and compared to the ones obtained from the work of Piskun et al. [120].

For the second reaction, reversible transformation of HPA to GVL occurs in the bulk phase and is catalyzed by Brönsted acid LA and HPA. As the second reaction occurs in the bulk aqueous phase and does not involve the heterogeneous catalyst. Thus, this reaction can be considered to have the same kinetics in our system as the one of Piskun et al. [120]. Hence, in this work, the kinetic constants of the second reaction estimated by Piskun et al. [120] were used.

Originally, Piskun et al. [120] have described the reversible transformation of HPA to GVL

as 2 reactions (direct and indirect reactions) occurring in the bulk phase and catalyzed by Brönsted acid. These two reactions can be summarized into one reaction and expressed as:

$$R_2 = k_2.[H^+]\left([HPA] - \frac{1}{K_2}[GVL]\right) \quad (2)$$

where, K_2 is the equilibrium constant of the second reversible reaction and can be expressed as $K_2 = \frac{k_2}{k_{-2}}$. According to Piskun et al. [120], the concentration of protons can be expressed as:

$$[H^+] = \sqrt{K_{LA}^{diss}.[LA] + K_{HPA}^{diss}.[HPA]} \quad (3)$$

where, K_{LA}^{diss} and K_{HPA}^{diss} are the dissociation constants of LA and HPA and equal to $10^{-4.6}$ and $10^{-5.7}$, respectively [134].

From the kinetic data of Piskun et al. [120], it was possible to estimate K_2 by a van't Hoff law:

$$K_2(T) = K_2(T = 90°C).exp\left(\frac{-\Delta H_{R,2}}{R}.\left(\frac{1}{T} - \frac{1}{90°C}\right)\right) \quad (4)$$

It was found that at 90°C, the value of $K_2(T = 90°C)$ was equal to 10 and the reaction enthalpy $\Delta H_{R,2}$ was found to be -3.2 kJ.mol^{-1}.

2.3.2 Mass and energy balances for the system

2.3.2.1 Mass balance

Mass balance in the gas phase

Due to the high gas volume (ca. 450 mL) compared to the liquid volume (ca. 10 mL) and

quite low variation of recorded pressure (<1.4%), the variation of pressure in the ARSST was negligible. Thus, the system was considered to be under isobaric condition.

Mass balance in the liquid phase

Pressure of the gas phase was ca. 35 bar, thus the evaporation of the liquid had a minor effect on the mass balance in the liquid. Mass balance for the different compounds present in the liquid phase can be expressed as:

$$\frac{dC_{LA}}{dt} = -\frac{m_{cat}}{V}R_1 \quad (5)$$

$$\frac{dC_{W}}{dt} = R_2 \quad (6)$$

$$\frac{dC_{GVL}}{dt} = R_2 \quad (7)$$

$$\frac{dC_{HPA}}{dt} = \frac{m_{cat}}{V}R_1 - R_2 \quad (8)$$

2.3.2.2 Energy balance in the liquid phase

Energy balance in the liquid phase is expressed as:

$$\frac{dT}{dt} = \frac{q_{rx}+q_{el}}{m_{LA}(t).C_{P_{LA}}(T)+m_W(t).C_{P_W}(T)+m_{GVL}(t).C_{P_{GVL}}(T)+m_{HPA}(t).C_{P_{HPA}}(T)+m_{cat}.C_{P_{cat}}(T)+m_{insert}.C_{P_{insert}}(T)}$$
$$= \frac{q_{rx}}{m_{LA}(t).C_{P_{LA}}(T)+m_W(t).C_{P_W}(T)+m_{GVL}(t).C_{P_{GVL}}(T)+m_{HPA}(t).C_{P_{HPA}}(T)+m_{cat}.C_{P_{cat}}(T)+m_{insert}.C_{P_{insert}}(T)} + \beta \quad (9)$$

The heat balance in the ARSST system includes the energy release from the exothermic reactions q_{rx} and the energy provided by the electrical heating q_{el}. The temperature ramp depends on the total energy of q_{rx} and q_{el}, mass and specific heat capacities of all related composition including reaction mixture and inserts. The determination of β, which is the background electrical heating rate, estimated from initial temperature ramp stage by electrical heating without reaction [125, 130]. This parameter was fixed for each experiments (Table 2.3 in section 2.3.3).

Evolution of specific heat capacities with temperature for water, LA and GVL were determined by using Aspen Plus software v9.0 (Aspen Technology, Inc.), using the Peng-Robinson with modified Huron-Vidal mixing rules thermodynamic model (Figure 2.5). This thermodynamic model was used based on the recommendation of Carlson [135]. Due to the instability of HPA, it is difficult to measure its heat capacity. Thus, heat capacity of HPA was assumed to be the same as the one of LA, because the chemical structure of LA is similar to GVL. Heat capacity of catalyst was found to be equal to 1000 J.(kg.K)$^{-1}$ [136]. Heat capacity of the inserts is equal to 837.36 J.(kg.K)$^{-1}$ according to the manufacturer. In our model, we have taken into account the evolution of the different heat capacities with temperature and the variation of chemical molecules.

The energy q_{rx} due to the chemical exothermic reactions can be expressed as:

$$q_{rx} = \left(-R_1 . \Delta H_{R,1} . \frac{m_{cat}}{V_{liq}} - R_2 . \Delta H_{R,2} \right) . V_{liq} \quad (10)$$

The reaction enthalpy value of $\Delta H_{R,2}$ was found to be -3.2 kJ.mol^{-1}. The enthalpies of formation for LA and GVL in liquid phase are -678.64 kJ.mol^{-1} and -469.86 kJ.mol^{-1}, respectively [137]. The enthalpy of formation of water in liquid is -285.3 kJ.mol^{-1} [138]. Thus, by knowing the second reaction enthalpy $\Delta H_{R,2}$ and the enthalpies of formation of water and GVL, one can determine the enthalpy of formation of HPA, which is -751.96 kJ.mol^{-1}. Thus, the first reaction enthalpy value $\Delta H_{R,1}$ is -73.318 kJ.mol^{-1}. Enthalpies of formation and of reaction are listed in Table 2.1.

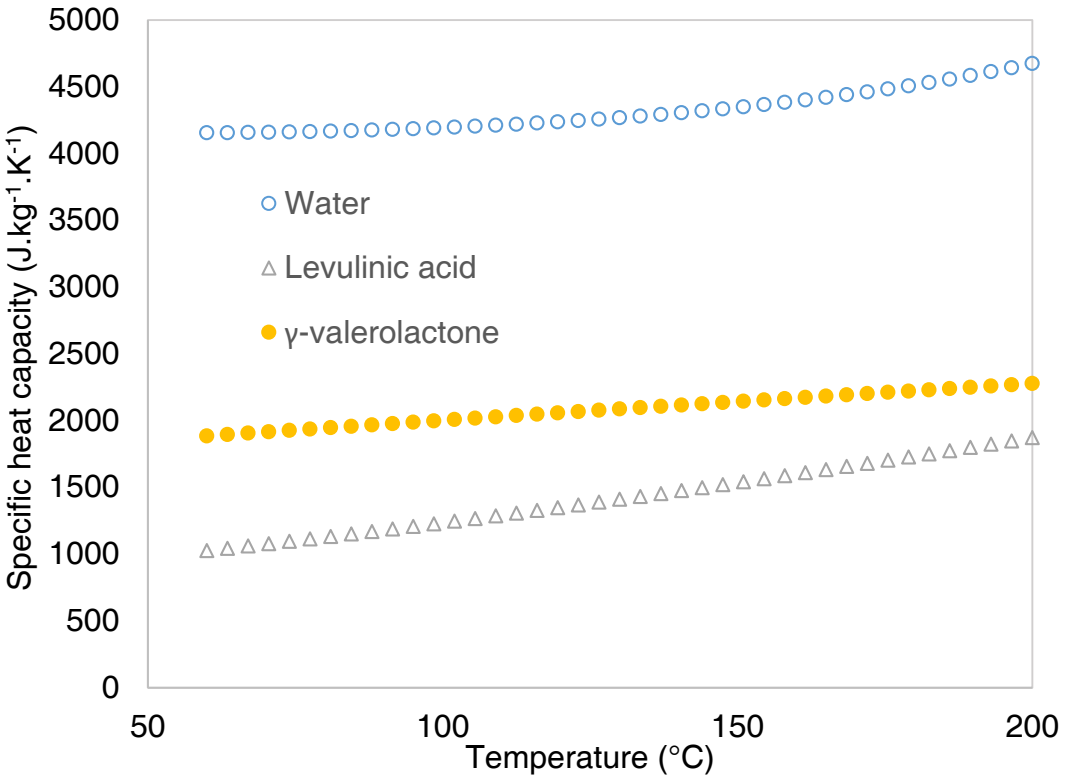

Figure 2.5. Evolution of heat capacity of water, LA and GVL at different temperature.

Table 2.1. Enthalpies of formation and of reaction [137, 139].

Compound	**Enthalpy of formation (kJ.mol^{-1})**
Levulinic acid (LA)	-678.64
γ-valerolactone (GVL)	-469.86
4-hydroxypentanoic acid (HPA)	-751.96
Water (H_2O)	-285.3
Reaction	**ΔH_R kJ.mol^{-1}**
Reaction 1	-73.318
Reaction 2	-3.2

2.3.3 Validation of kinetic model

Eqs. (5)-(9) were solved out by using ODESSA algorithm [140] through ModEst software

[141]. A modified Arrhenius equation was used to express the rate constants:

$$k_i(T_R) = k_i(T_{Ref}).exp\left(\frac{-Ea_i}{R}\left(\frac{1}{T_R} - \frac{1}{T_{Ref}}\right)\right) \quad (11)$$

The objective function $\omega = \left(T_{R,exp} - T_{R,model}\right)^2$ was minimized by using Simplex and Levenberg-Marquardt algorithms. The terms $T_{R,exp}$ and $T_{R,model}$ are the experimental and the simulated values of the observable. Reaction temperature was used as an observable value for the non-linear regression stage. The following parameters were estimated: $k_1(T_{Ref})$ and Ea_1. Table 2.2 shows the values of the estimated parameters with their standard deviations.

Table 2.2. Estimated and statistical data at T_{Ref} = 66.85°C.

Constant	Unit	Estimated parameters	Standard error (%)
$k_1(T_{Ref})$	[mol.(kg.s.bar)$^{-1}$]	6.16×10^{-4}	7.0
Ea_1	[kJ.mol^{-1}]	45.0	3.6
		Kinetic constants from Piskun et al. [120]	
$k_2(T_{Ref})$	[L.(mol.s)$^{-1}$]	9.85×10^{-2}	
Ea_2	[kJ.mol^{-1}]	62.5	

The high value of the coefficient of determination, i.e., 95% and low values of standard deviation (Table 2.2) show that the model is reliable. Piskun et al. [120] have found that the kinetic constant of reaction 1 was 1.24×10^{-2} mol.(kg.s.bar)$^{-1}$ at 66.85°C, and the associated activation energy Ea_1 was found to be 34.1 kJ.mol^{-1}. Within the temperature range 66.85-106.85°C, the ratio $\frac{(k_1)_{from\ Piskun\ et\ al.[32]}}{(k_1)_{from\ this\ work}}$ is ca. 20.

Three factors can explain this difference:

a. Difference of heterogeneous catalyst: Ru/C catalyst (3 wt.% Ru) from Evonik for the study performed by Piskun et al. [120] and Ru/C catalyst (5 wt.% Ru) from Alfa Aesar company for this study;
b. Stirring system of Piskun et al. [120] was more efficient (Ruschton type impeller);
c. Thermal mode was different. Piskun et al. [120] have performed their experiments under isothermal mode, whereas in this study experiments were performed under near-adiabatic conditions. Furthermore, for this reaction system, by increasing the reaction temperature, the hydrogen solubility decreases. Hence, the kinetics of HPA production is slower leading to lower the heat-flow rate due to chemical reactions.

Different experiments with different initial operating conditions, listed in Table 2.3, were performed to estimate the kinetic constants. Fitting of the model to the experimental data provided by ARSST are shown in Figures 2.6A-C. Generally, the model fits well with the experimental data and can be considered to predict correctly the temperature trend.

Table 2.3. Experimental matrix for ARSST experiments under 35 bar of hydrogen.

Run	LA ($mol.L^{-1}$)	Water ($mol.L^{-1}$)	Catalyst ($kg.L^{-1}$)	Volume (L)	Initial temperature T1 (°C)	β ($°C.min^{-1}$)
1	6.50	18.79	0.015	0.0074	61.46	0.48
2	5.46	24.66	0.02	0.0076	62.53	0.65
3	5.43	24.85	0.027	0.0076	68.45	0.88
4	5.50	24.42	0.013	0.0075	63.32	0.43
5	2.67	40.47	0.006	0.0078	68.30	0.68
6	3.86	33.58	0.029	0.0078	71.35	1.11

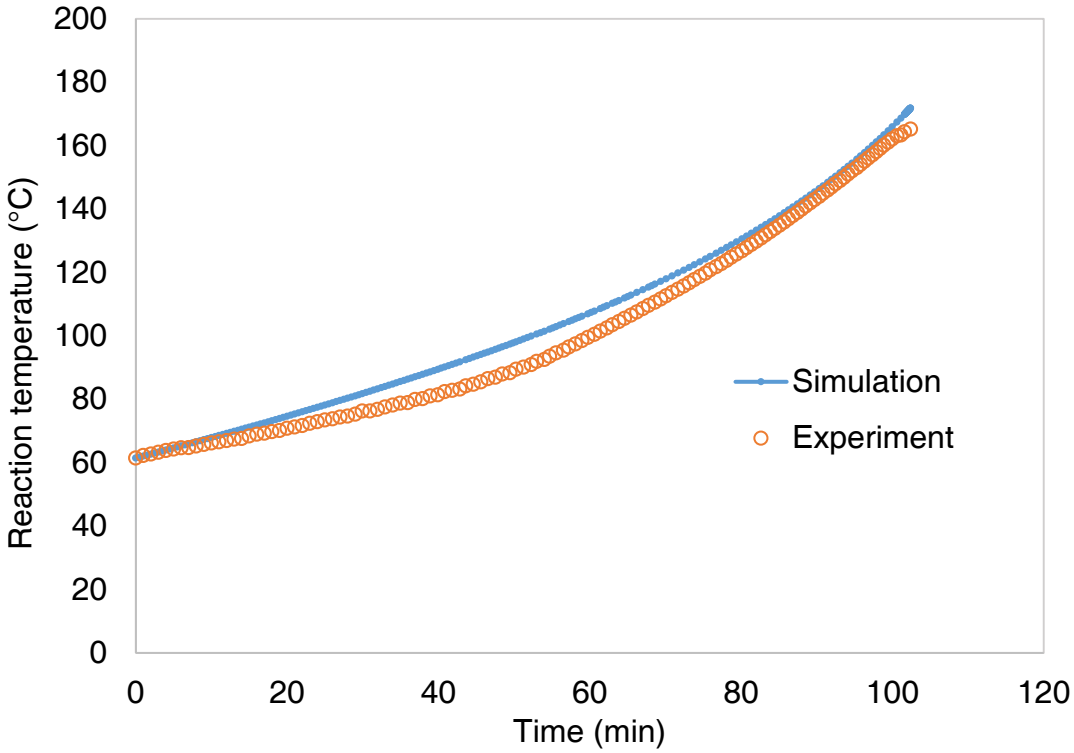

Figure 2.6A. Fit of the model to the experimental data for Run 1.

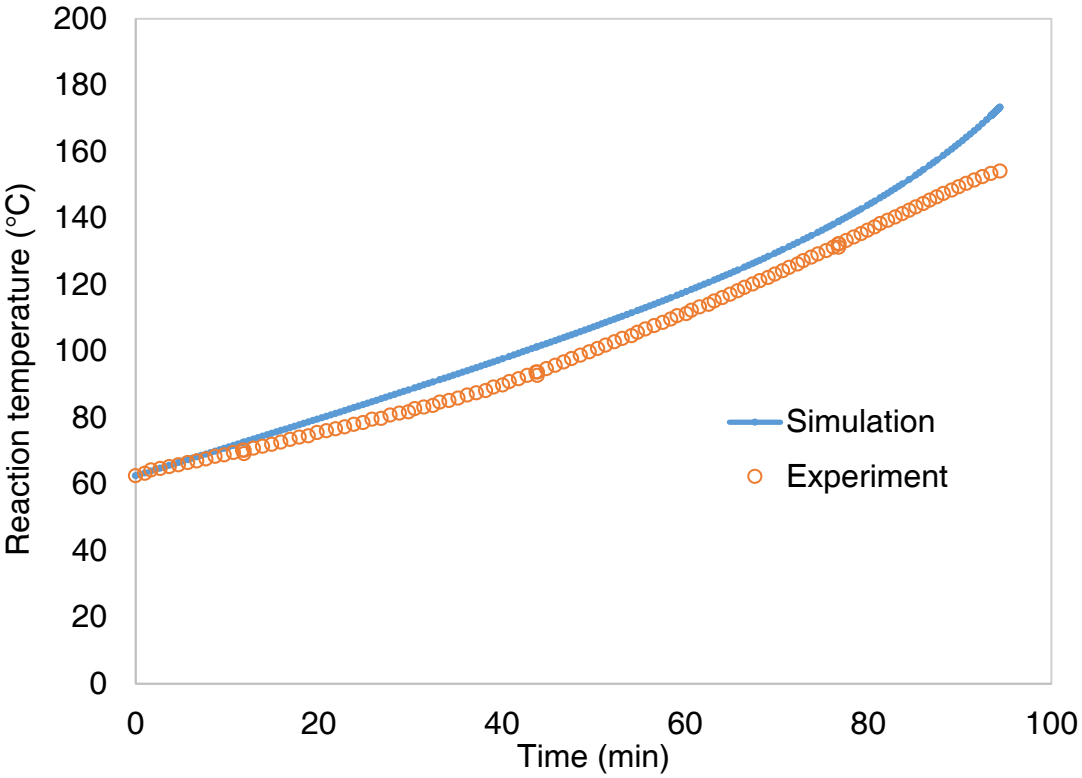

Figure 2.6B. Fit of the model to the experimental data for Run 2.

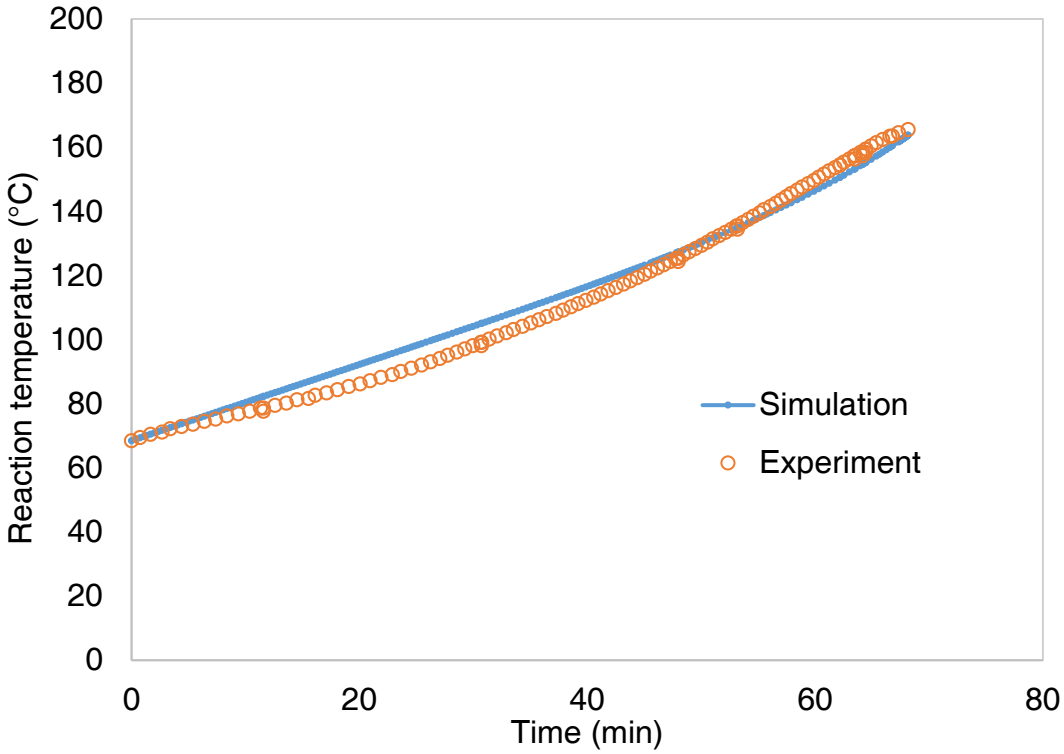

Figure 2.6C. Fit of the model to the experimental data for Run 3.

2.3.4 Thermal risk assessment

Thermal risk assessment is based on the determination of probability and severity of a thermal runaway. For that, it is important to determine the value of TMR_{ad} at the process temperature which characterizes the probability of thermal runaway and the value of the adiabatic temperature rise ΔT_{ad} which characterizes the severity of thermal runaway.

For the definition of these two thermal risk parameters, TMR_{ad} at a process temperature T_p was measured as the time difference between the time when the temperature increasing rate reached the maximum $\left(\frac{dT}{dt}\right)_{max.}$ and the initial time. The parameter ΔT_{ad} was calculated as the temperature difference between the maximum temperature reached during the reaction process and the initial temperature, i.e., the process temperature T_p.

Stoessel [142] has established some criteria for the values of ΔT_{ad} (Table 2.4) and TMR_{ad} (Table 2.5). For instance, when the TMR_{ad} value for a chemical process is lower than one

hour, thus the probability of thermal runaway is frequent. When this value is higher than one hundred hours the probability can be considered as impossible. When the adiabatic temperature rise ΔT_{ad} is found to be higher than 400°C, then the severity of the thermal runaway can be assumed to be catastrophic, and when this value is lower than 50°C, then the severity can be assumed to be negligible because the reactor structure can stand this temperature increase.

Table 2.4. Assessment criteria for ΔT_{ad} [142].

Severity	ΔT_{ad} (°C)	Factor
Catastrophic	>400°C	4
Critical	200-400°C	3
Medium	50-200	2
Negligible	50 and no pressure	1

Table 2.5. Assessment criteria for TMR_{ad} [142].

Probability	TMR_{ad} (hrs)	Factor
Frequent	<1	6
Probable	1 to 8	5
Occasional	8 to 24	4
Seldom	24 to 50	3
Remote	50 to 100	2
Impossible	>100	1

To assess the thermal risk of a chemical process at a defined operating conditions, one needs to estimate the products of severity and probability [143]. For that reason, a factor was attributed to each situation. When the severity and probability of thermal risk was negligible or impossible then a factor one was attributed (Tables 2.4 and 2.5).

By using the factors (Tables 2.4 and 2.5), it is possible to create a risk matrix for thermal runaway presented in Table 2.6 according to guidelines for designing risk matrices [143]. When the value obtained from TMR_{ad} factor multiplied by ΔT_{ad} factor is higher than 12,

then the risk can be assumed to be non-acceptable (red zone in Table 2.6). In that case, the manager should modify this installation or implement risk reduction measure. When the value is between 6 and 12, the thermal risk can be assumed to be medium (green zone in Table 2.6), which also needs risk management and safety control. When the value is lower than 6, the thermal risk can be assumed to be negligible (white zone in Table 2.6).

Table 2.6. Risk matrix for a thermal runaway.

	Severity	Negligible	Medium	Critical	Catastrophic
Probability	Factor	*1*	*2*	*3*	*4*
Frequent	*6*	6	12	18	24
Probable	*5*	5	10	15	20
Occasional	*4*	4	8	12	16
Seldom	*3*	3	6	9	12
Remote	*2*	2	4	6	8
Impossible	*1*	1	2	3	4

Non-acceptable Medium Negligible

To study thermal risk assessment for this reaction system, effects of LA concentration, temperature, catalyst loading and hydrogen pressure were investigated. The two risk parameters TMR_{ad} and ΔT_{ad} were determined by using the developed kinetic model under near-adiabatic condition in this chapter by simulation with varying the catalyst loading from 0.0001 to 0.14 $kg.L^{-1}$, the process temperature from 100 to 130°C, the initial LA concentration from 0.62 to 6.75 $mol.L^{-1}$ and hydrogen pressure from 15 to 50 bar.

Tables 2.7A-D show the variation of the thermal risk for this reaction system under 35 bar at different catalyst loadings: 0.0001, 0.0014, 0.014 and 0.14 $kg.L^{-1}$, respectively and in the LA initial concentration range and temperature range described above. One can notice that when the catalyst loading is lower than 0.0001 $kg.L^{-1}$, the thermal risk is almost negligible (Table 2.7A). The thermal risk is medium when the concentration is of 0.62 $mol.L^{-1}$, because the kinetic is faster due to a higher amount of active sites (from the catalyst) compared to the concentration of LA. Nevertheless, the estimated adiabatic temperature

rise was found to be negligible, i.e., lower than 12°C.

When the catalyst loading is in the range of 0.0014-0.014 $kg.L^{-1}$, the thermal risk is medium in the majority of cases according to the risk matrix (Tables 2.7B-D). Generally, by increasing the catalyst loading, temperature and LA concentration, the thermal risk increases, which makes this process less safe.

For example, when LA concentration is 6.75 $mol.L^{-1}$, in the temperature range of 100-130°C, by increasing the catalyst loading from 0.0014 to 0.14 $kg.L^{-1}$, the thermal risk value of this process increases from 8 to 12. When LA concentration is of 3.22 $mol.L^{-1}$ and catalyst loading is 0.0014 $kg.L^{-1}$, by increasing the temperature from 100 to 130°C, the thermal risk value increases from 8 to 10 (Table 2.7B).

Some safety barriers should be included to prevent such medium risk, specifically if one cannot use different operating conditions for productivity reasons. When the risk is defined as medium and it is not possible to modify the operating conditions, the following safety barriers could be used: rupture disk to avoid the explosion of the reactor structure, install additional heat carrier pump to avoid any cooling failure and/or to implement an emergency cooling system to slow down the reaction temperature increase. However, by adjusting LA concentration between 1.25 and 1.90 $mol.L^{-1}$, the thermal risk is negligible as TMR_{ad} is more than 1hr and ΔT_{ad} is lower than 50°C.

Table 2.7A. Evolution of thermal risk in function of process temperature and LA concentration at a catalyst loading of 0.0001 kg.L^{-1} under 35 bar H_2 (**Medium** **Negligible**)

RISK	*[LA] mol.L^{-1}*									
Tp °C	*0.62*	*1.25*	*1.90*	*2.55*	*3.22*	*3.90*	*4.59*	*5.30*	*6.02*	*6.75*
100	**6**	**3**	**2**	**2**	**2**	**2**	**2**	**2**	**2**	**2**
110	**6**	**3**	**2**	**4**	**2**	**2**	**2**	**2**	**2**	**2**
115	**6**	**4**	**2**	**4**	**4**	**2**	**2**	**2**	**2**	**2**
120	**6**	**4**	**3**	**4**	**4**	**2**	**2**	**2**	**2**	**2**
125	**6**	**4**	**3**	**4**	**4**	**4**	**4**	**2**	**2**	**2**
126	**6**	**4**	**3**	**4**	**4**	**4**	**4**	**2**	**2**	**2**
127	**6**	**4**	**3**	**6**	**4**	**4**	**4**	**2**	**2**	**2**
128	**6**	**4**	**3**	**6**	**4**	**4**	**4**	**2**	**2**	**2**
129	**6**	**4**	**3**	**6**	**4**	**4**	**4**	**4**	**2**	**2**
130	**6**	**4**	**3**	**6**	**4**	**4**	**4**	**4**	**2**	**2**

Table 2.7B. Evolution of thermal risk in function of process temperature and LA concentration at a catalyst loading of 0.0014 kg.L^{-1} under 35 bar H_2 (**Medium** **Negligible**)

RISK	*[LA] mol.L^{-1}*									
Tp °C	*0.62*	*1.25*	*1.90*	*2.55*	*3.22*	*3.90*	*4.59*	*5.30*	*6.02*	*6.75*
100	**6**	**5**	**4**	**8**	**8**	**8**	**8**	**8**	**6**	**6**
110	**6**	**5**	**5**	**8**	**8**	**8**	**8**	**8**	**8**	**8**
115	**6**	**5**	**5**	**10**	**8**	**8**	**8**	**8**	**8**	**8**
120	**6**	**5**	**5**	**10**	**8**	**8**	**8**	**8**	**8**	**8**
125	**6**	**5**	**5**	**10**	**10**	**8**	**8**	**8**	**8**	**8**
126	**6**	**5**	**5**	**10**	**10**	**8**	**8**	**8**	**8**	**8**
127	**6**	**5**	**5**	**10**	**10**	**8**	**8**	**8**	**8**	**8**
128	**6**	**5**	**5**	**10**	**10**	**8**	**8**	**8**	**8**	**8**
129	**6**	**5**	**5**	**10**	**10**	**10**	**8**	**8**	**8**	**8**
130	**6**	**5**	**5**	**10**	**10**	**10**	**8**	**8**	**8**	**8**

Table 2.7C. Evolution of thermal risk in function of process temperature and LA concentration at a catalyst loading of 0.014 kg.L^{-1} under 35 bar H_2 (**Medium** **Negligible**)

RISK	*[LA] mol.L^{-1}*									
Tp °C	*0.62*	*1.25*	*1.90*	*2.55*	*3.22*	*3.90*	*4.59*	*5.30*	*6.02*	*6.75*
100	**6**	**6**	**6**	**10**	**10**	**10**	**10**	**10**	**10**	**10**
110	**6**	**6**	**6**	**12**	**10**	**10**	**10**	**10**	**10**	**10**
115	**6**	**6**	**6**	**12**	**10**	**10**	**10**	**10**	**10**	**10**
120	**6**	**6**	**6**	**12**	**12**	**12**	**10**	**10**	**10**	**10**
125	**6**	**6**	**6**	**12**	**12**	**12**	**10**	**10**	**10**	**10**
126	**6**	**6**	**6**	**12**	**12**	**12**	**12**	**10**	**10**	**10**
127	**6**	**6**	**6**	**12**	**12**	**12**	**12**	**10**	**10**	**10**
128	**6**	**6**	**6**	**12**	**12**	**12**	**12**	**10**	**10**	**10**
129	**6**	**6**	**6**	**12**	**12**	**12**	**12**	**12**	**10**	**10**
130	**6**	**6**	**6**	**12**	**12**	**12**	**12**	**12**	**10**	**10**

Table 2.7D. Evolution of thermal risk in function of process temperature and LA concentration at a catalyst loading of 0.14 kg.L^{-1} under 35 bar H_2 (**Medium** **Negligible**)

RISK	*[LA] mol.L^{-1}*									
Tp °C	*0.62*	*1.25*	*1.90*	*2.55*	*3.22*	*3.90*	*4.59*	*5.30*	*6.02*	*6.75*
100	**6**	**6**	**6**	**12**	**12**	**12**	**12**	**12**	**12**	**12**
110	**6**	**6**	**6**	**6**	**12**	**12**	**12**	**12**	**12**	**12**
115	**6**	**6**	**6**	**6**	**12**	**12**	**12**	**12**	**12**	**12**
120	**6**	**6**	**6**	**6**	**12**	**12**	**12**	**12**	**12**	**12**
125	**6**	**6**	**6**	**6**	**12**	**12**	**12**	**12**	**12**	**12**
126	**6**	**6**	**6**	**6**	**12**	**12**	**12**	**12**	**12**	**12**
127	**6**	**6**	**6**	**6**	**12**	**12**	**12**	**12**	**12**	**12**
128	**6**	**6**	**6**	**6**	**12**	**12**	**12**	**12**	**12**	**12**
129	**6**	**6**	**6**	**6**	**12**	**12**	**12**	**12**	**12**	**12**
130	**6**	**6**	**6**	**6**	**12**	**12**	**12**	**12**	**12**	**12**

Effect of hydrogen pressure were also investigated for thermal risk assessment of this reaction system. At a catalyst loading of 0.014 kg/L, by elevating the pressure from 15 to 50 bar, thermal risk is medium in the majority of cases (Tables 2.8A-B). Compared with Table 2.7C, which shown the same catalyst loading under 35 bar, the thermal risk kept the same value in most cases in the LA concentration range of 0.62 -1.90 mol/L due to lower

ΔT_{ad}. However, when LA concentration is higher than 1.90 mol/L, by elevating the hydrogen pressure from 15 to 50 bar, the thermal risk increases from 10 to 12 gradually because of higher hydrogen solubility which can accelerate the reactions.

Table 2.8A. Evolution of thermal risk in function of process temperature and LA concentration at a catalyst loading of 0.014 $kg.L^{-1}$ under 15 bar H2 (**Medium** **Negligible**)

RISK	*[LA] mol.L^{-1}*									
Tp °C	*0.62*	*1.25*	*1.90*	*2.55*	*3.22*	*3.90*	*4.59*	*5.30*	*6.02*	*6.75*
100	**6**	**6**	**5**	**10**	**10**	**10**	**10**	**10**	**10**	**10**
110	**6**	**6**	**5**	**10**	**10**	**10**	**10**	**10**	**10**	**10**
115	**6**	**6**	**5**	**10**	**10**	**10**	**10**	**10**	**10**	**10**
120	**6**	**6**	**5**	**10**	**10**	**10**	**10**	**10**	**10**	**10**
125	**6**	**6**	**6**	**10**	**10**	**10**	**10**	**10**	**10**	**10**
126	**6**	**6**	**6**	**10**	**10**	**10**	**10**	**10**	**10**	**10**
127	**6**	**6**	**6**	**10**	**10**	**10**	**10**	**10**	**10**	**10**
128	**6**	**6**	**6**	**10**	**10**	**10**	**10**	**10**	**10**	**10**
129	**6**	**6**	**6**	**10**	**10**	**10**	**10**	**10**	**10**	**10**
130	**6**	**6**	**6**	**10**	**10**	**10**	**10**	**10**	**10**	**10**

Table 2.8B. Evolution of thermal risk in function of process temperature and LA concentration at a catalyst loading of 0.014 $kg.L^{-1}$ under 50 bar H_2 (**Medium** **Negligible**)

RISK	*[LA] mol.L^{-1}*									
Tp °C	*0.62*	*1.25*	*1.90*	*2.55*	*3.22*	*3.90*	*4.59*	*5.30*	*6.02*	*6.75*
100	**6**	**6**	**6**	**12**	**10**	**10**	**10**	**10**	**10**	**10**
110	**6**	**6**	**6**	**12**	**12**	**10**	**10**	**10**	**10**	**10**
115	**6**	**6**	**6**	**12**	**12**	**12**	**12**	**10**	**10**	**10**
120	**6**	**6**	**6**	**12**	**12**	**12**	**12**	**12**	**12**	**10**
125	**6**	**6**	**6**	**12**	**12**	**12**	**12**	**12**	**12**	**12**
126	**6**	**6**	**6**	**12**	**12**	**12**	**12**	**12**	**12**	**12**
127	**6**	**6**	**6**	**12**	**12**	**12**	**12**	**12**	**12**	**12**
128	**6**	**6**	**6**	**12**	**12**	**12**	**12**	**12**	**12**	**12**
129	**6**	**6**	**6**	**12**	**12**	**12**	**12**	**12**	**12**	**12**
130	**6**	**6**	**6**	**12**	**12**	**12**	**12**	**12**	**12**	**12**

2.4 Conclusion

In this chapter, thermal risk assessment of levulinic acid (LA) hydrogenation to γ-valerolactone (GVL) catalyzed by Ru/C in water was performed.

To evaluate the thermal risk of this process, a kinetic model under near-adiabatic condition was developed. Experiments at different operating conditions were performed in a near-adiabatic reactor, i.e., ARSST (advanced reactive system screening tool). A non-linear regression method was used to estimate the kinetic constants using the reaction temperature as an observable. Good agreement between experimental data and the model was obtained.

Based on this model, adiabatic temperature rise (ΔT_{ad}), which characterizes the severity of thermal runaway and Time-to-Maximum Rate under adiabatic conditions (TMR_{ad}), which characterizes the probability of thermal runaway, were obtained by simulation and used for thermal risk assessment. Different operating conditions including levulinic acid concentration, temperature, catalyst loading and hydrogen pressure were tested for the thermal risk assessment of this process.

It should be noticed that when the catalyst is within the loading range of 0.0014-0.014 $kg.L^{-1}$, LA within the concentration in range of 0.62-6.75 $mol.L^{-1}$, temperature in the range of 100-130°C and under 35 bar hydrogen pressure, the thermal risk is medium in the majority of cases and safety barriers should be included to prevent a thermal runaway situation. Elevating hydrogen pressure can also increase the thermal risk.

Form the thermal risk assessment of this reaction system, a safe operation condition range could be identified which could be further applied for optimization of this process operating conditions based on mass and energy balance and chemical reactor design. According to the guide of thermal risk assessment, a further structure-reactivity study on hydrogenation of LA and its esters to GVL was performed and shown in chapter III.

Chapter III. Structure-reactivity study on the hydrogenation of levulinic acid and its corresponding esters

Part of this chapter is adapted from the post print of the following article:
Y. Wang, M. Cipolletta, L. Vernières-Hassimi, V. Casson-Moreno, S. Leveneur, Application of the concept of Linear Free Energy Relationships to the Hydrogenation of Levulinic acid and its corresponding esters, Chem. Eng. J. 374(2019) 822-831.
Link: https://doi.org/10.1016/j.cej.2019.05.218

3.1 Introduction

The production of GVL was carried from hydrogenation of LA or its esters. The recent work of Negahdar et al. [121] shows the comparison of kinetics from ML, EL and BL by using methanol as solvent. However, there exists transesterification reaction by using methanol, which could affect the reaction kinetics of each substrate (except ML). At this moment of the doctoral thesis, besides comparison of kinetics, can we find a relationship for the kinetics of LA, ML, EL and BL? Can we find a proper solvent for this study? This chapter presents the relationships between structure and reactivity for this reaction.

In this chapter, Taft equation, based on the linear free energy relationship, has been applied to hydrogenation of LA and its esters to GVL (Figure 3.1). A kinetic model which includes mass transfer and Taft equation was developed and validated by mass transfer and kinetic experiments performed in a batch reactor under isothermal and isobaric conditions. Gas-liquid mass transfer coefficient, kinetic constants and sensitivity factors dependent on temperatures were estimated. Owning to these values, kinetics between different substrates were compared for the overall reaction and two consecutive steps including hydrogenation step and ring-closure step. Polar and steric effects of the substituent groups on the kinetics

were also discussed.

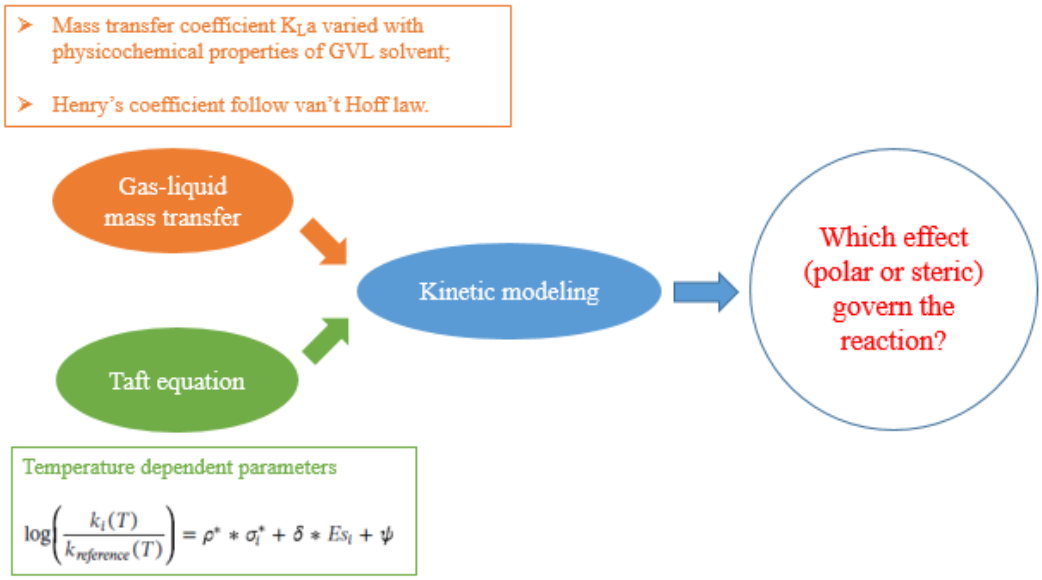

Figure 3.1. Scheme of structure-reactivity study on hydrogenation of LA and its esters.

Section 3.2 details the experimental and analytical part. Mass transfer experiments aimed to obtain the gas-liquid mass transfer coefficient that varied by physicochemical properties of GVL solvent with temperatures and the Henry's constant of hydrogen in GVL solvent. Hydrogenation kinetic experiments aimed to obtain the experimental kinetic matrix. The solvent screening, including corrosion issue, is described in section 3.3. For the sake of clarity, Section 3.4 shows the introduction and application of linear free energy relationships, especially Taft equation, for the structure-reactivity study and its possibility to be employed for hydrogenation of LA and its esters.

In section 3.5.1, mechanism of this reaction is depicted and kinetic model, including Taft equation, is developed. Mass balance of this reaction system is described in section 3.5.2. Section 3.5.3 focuses on mass transfer study and includes two sub-sections. Section 3.5.3.1 studies the mass transfer of this gas-liquid-solid reaction system and gas-liquid mass transfer model was developed by taking the density and viscosity of the solvent GVL into account. Section 3.5.3.2 shows the evolution of density and viscosity of GVL with temperature. Validation of models including gas-liquid mass transfer model and kinetic

model is summarized in section 3.5.4. Section 3.5.5 gives a further comparison of kinetics between different substrates and discussed with Taft equation parameters dependent on temperatures. This section discusses the polar and steric effect on the two steps of the reaction respectively. At the end, section 3.6 concludes this chapter.

3.2 Experimental and analytical section

3.2.1 Chemicals

Levulinic acid (wt% ≥ 97%), γ-valerolactone (wt% ≥ 99%) and methyl levulinate (wt% ≥ 98%) were purchased from Sigma-Aldrich. Ethyl levulinate (wt% ≥ 98%) and furfural (wt% ≥ 99%) were obtained from Acros Organics. Ru/C (5 wt % ruthenium on activated carbon powder, reduced and 50% water wet) and n-Butyl levulinate (wt% ≥ 98%) were provided by the Alfa Aesar. H_2 (>99.999%) was supplied by Linde. Acetone (Analytical grade) was bought from VWR. All the chemicals were used without further treatment.

3.2.2 Experimental section

Gas-liquid mass transfer experiments and hydrogenation kinetic experiments were performed in a batch reactor under isothermal and isobaric conditions. The aim of gas-liquid mass transfer experiments is to obtain gas-liquid mass transfer coefficient and Henry's constant of hydrogen gas in solution. As GVL is the solvent and mass fraction is more than 80%, we considered that this study can be done by using pure GVL. Then, the hydrogenation kinetic experiments were performed to obtain the experimental kinetic data.

A 300ml reactor equipped with efficient gas entrainment impeller, gas reservoir and recording system was used for these experiments (Figure 3.2). For the gas-liquid mass transfer experiments, firstly, valve V1 was opened and a desired amount of hydrogen gas was purged into the reservoir from the gas storage bottle through the pressure regulator R1. Secondly, valve V1 was closed and GVL solvent was poured into the reactor and vacuumed to make sure there is no air in the reactor. Thirdly, the reactor was heated to the desired temperature and kept under isothermal condition. Fourthly, valve V2 was opened and the

outlet pressure was set to 20 bar by adjusting the pressure regulator R2. Fifthly, the valve V3 was opened and the reactor was purged with hydrogen. Then, the stirring was set at 1000 rpm and valves V2, V3 and regulator R2 were kept open until the end of the experiment to make sure the experiment was performed under isobaric conditions. The experiment lasted for 30 min (to reach the equilibrium), then all the valves were closed and the reactor was cooled down. The pressure and temperature of the gas reservoir and reactor were recorded online during the experiment. To evaluate the value of gas-liquid mass transfer coefficients, four experiments in pure GVL were carried out at 20 bars and at four temperatures: 373.15K, 393.15K, 413.15 K and 423.15 K. This pressure and these temperatures were the ones used during the kinetic experiments.

For the kinetic experiments of hydrogenation of LA and its esters, the same procedure described above was employed. The desired amount of GVL, substrates and Ru/C catalyst were introduced into the reactor. During the reaction, the samples were obtained from valve Vs at different times and reserved for further treatment and analysis. Experimental matrix for the hydrogenation is shown in Table 3.1. The time zero was set when the stirring started.

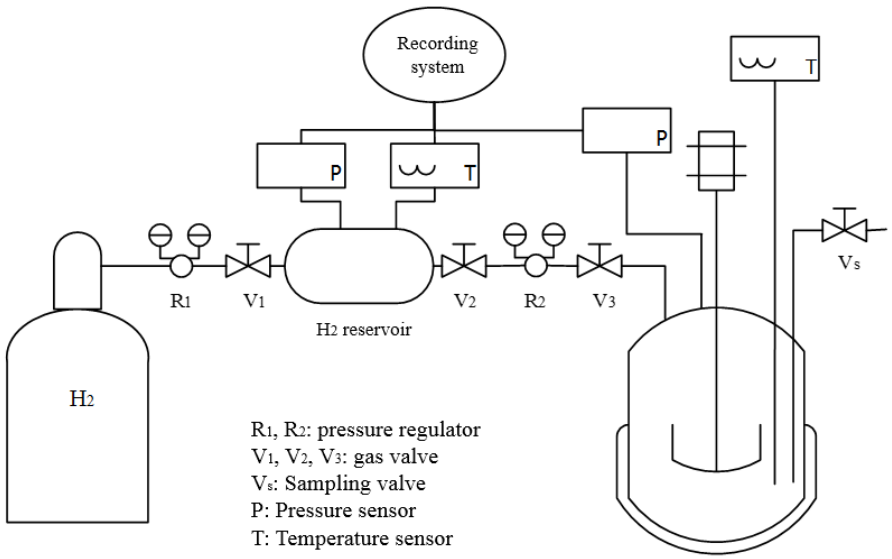

Figure 3.2. Scheme of batch reactor, gas reservoir and recording system.

3.2.3 Analytical section

The evolution of density and viscosity with temperature for GVL at atmospheric pressure were obtained by using DMA 4100 M and LOVIS 2000 ME microviscometer (Anton Paar, Austria). Temperature range from 283K-363K with 10K step was employed for the measurement with temperature accuracy of 0.02°C, density accuracy of 0.05 $kg.m^{-3}$, viscosity accuracy of <0.5%.

To identify and quantify the chemical compounds from the hydrogenation kinetic experiments, at first, samples obtained from the batch reactor were immediately filtered to separate the Ru/C catalyst in the solution. Then, the colorless samples were diluted in acetone by using furfural as internal standard. Later the diluted solutions were prepared in vials for the further qualification and quantification analysis.

The identification of intermediate products from hydrogenation of LA and its esters, such as HPA (4-hydroxypentanoic acid), MHP (methyl 4-hydroxypentanoate), EHP (ethyl 4-hydroxypentanoate), BHP (n-butyl 4-hydroxypentanoate), was performed by using GC-MS analysis. Gas chromatography Varian 3900 with Varian Saturn 2000 were applied with a capillary column (ZB-5ms, 30 m × 0.32 mm internal diameter × 0.25 μm film thickness). Helium (99.99%) was used as carrier gas at a constant flow rate of 1.0 $mL.min^{-1}$. The temperature of the injector and the detector was set at 270 °C. The oven temperature was programmed as 35 °C (3 min)-15 $°C.min^{-1}$-300°C. The injection volume was 5 μL, and the split ratio was 30:1.

The concentration of LA and its esters, GVL and intermediates was obtained from GC-FID analysis. Bruker Scion GC436 gas chromatography (GC) equipped with FID detector (flame ionization detector), an autosampler and capillary column (Rxi-5ms, 30 m × 0.32 mm internal diameter × 0.25 μm film thickness) were used. Helium (99.99%) was used as carrier gas at a constant flow rate of 1.2 $mL.min^{-1}$. Other configurations of GC methods were the same with the GC-MS analysis. The standard deviation of analytical measurement was found to be lower than 0.70% showing the high repeatability of the analysis.

Table 3.1. Experimental matrix for the kinetic study.

Substrate	Run	Initial concentration mol.m^{-3}	Initial liquid mass kg	Temperature °C	Catalyst amount (dry) kg	H_2 pressure bar
LA	1	984.7	0.1267	100	0.0014	20
	2	893.3	0.1267	130	0.0014	20
	3	1818.2	0.1279	110	0.0007	20
	4	1921.3	0.1279	140	0.0007	20
ML	5	929.5	0.1256	100	0.0014	20
	6	953.4	0.1256	120	0.0014	20
	7	1908.3	0.1257	100	0.0007	20
	8	1875.0	0.1257	140	0.0007	20
	9	2346.3	0.1257	110	0.0016	15
	10	2357.4	0.1257	150	0.0016	15
EL	11	942.2	0.1251	100	0.0014	20
	12	921.7	0.1251	130	0.0014	20
	13	1971.2	0.1245	110	0.0007	20
	14	1859.6	0.1245	140	0.0007	20
BL	15	953.1	0.1240	100	0.0014	20
	16	897.9	0.1240	130	0.0014	20
	17	1422.8	0.1231	110	0.00105	15
	18	1895.0	0.1225	130	0.0007	20
	19	1849.3	0.1225	140	0.0007	20

3.3 Solvent screening

At the initial stage for systematic experiments on hydrogenation of LA catalyzed by Ru/C in water solvent in the Parr stainless reactor, corrosion phenomenon was observed. The reaction solution color changed to green and later to yellow due to the dissociation of LA and existence of the ions Fe^{2+} and Fe^{3+}. The metal ions Fe^{2+} and Fe^{3+} were identified by dropping 1mol/L NaOH solution into the experimental mixture and there were some of green or yellow precipitation formed. The possible corrosion process was shown in Figure 3.3 and Figure 3.4 shown the solution obtained immediately after the experiments. The corrosive behavior of LA can lead to increase the investment cost due to the use of expensive resistant-materials towards corrosion.

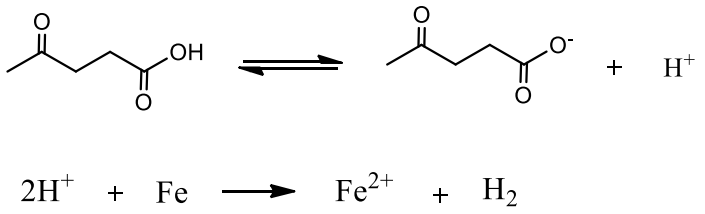

Figure 3.3. Possible corrosion reaction by dissociation of LA and redox reaction.

Figure 3.4. Green solution after experiments due to the existence of ion Fe^{2+}.

Then, limited by the reactor materials, neutral substrates for GVL production, LA esters such as ML, EL and BL were chosen for further kinetic study as these esters can be directly obtained from alcoholysis of cellulose in corresponding alcohol solvent like methanol, ethanol and butanol (more detail in Chapter I section 1.3.2). To compare the kinetics under the same condition, the same solvent should be used to avoid solvent effect on the reaction or mass transfer. Different solvents such as DMSO, water, methanol, binary mixture GVL/water were tested for the solubilization of the four

substrates. Remarkably, despite the solubility of the solvents, other characteristics of solvents also need to be considered, such as safe, non-toxic, green, inert in the reaction system, low vapor pressure etc.

DMSO has shown potential to solubilize all the substrates but the hydrogenation experiment with DMSO shown there is no GVL produced. Based on the decreasing polarity of ML, EL and BL as the carbon atom in molecule increases from C6 to C9, water is not a suitable solvent because of low solubility of BL and EL, which can cause two liquid phase and more complex mass transfer process. Methanol is also not suitable as it is toxic and the side transesterification reaction can occur between the solvent and reactants like LA, EL and BL and consequently affect the kinetics. The binary mixture GVL/water was tested with BL and demonstrated better solubilization of substrates than pure water. By increasing the fraction of GVL, the maximum concentration of BL solubilized in the mixture also increased (Table 3.2).

Table 3.2. Solubility test of BL in binary mixture GVL/water.

w/w% of GVL in water	Max conc. of BL mol.L^{-1}
50	0.40
60	0.65
70	0.88
80	1.76
90	>4

Finally, to make sure the solubilization of all substrates, pure GVL, the product itself was chosen as the aprotic solvent with its high capacity of solubility of ML, EL and BL by experimental test at room temperature. As aprotic solvent, GVL can also inhibit LA dissociation and decrease pH of the solution, which can limit the corrosion. Importantly, it is worth noticing that GVL as solvent has shown great potential in biomass valorization in recent years and shown better performance than other common solvent, by feedback, this advantage stimulates the production of GVL as well. In addition, GVL as solvent for GVL production can also simplify the layout of the plant and minimize the downstream process.

Through the preliminary study, corrosion problem was solved out and screening of

solvent was done, which can benefit for the following study including structure-reactivity study and calorimetry investigation on GVL production based on the laboratory experiments.

3.4 Application of Taft equation for structure-reactivity study

Due to complexity of molecules derived from biomass through different bio-refinery processes, it is cumbersome and time-consuming to determine the reactivity for all of the bio-derived molecules by experimental study. Because of this reality, the use of concept structure-reactivity could provide a way to accelerate these processes for biomass valorization.

Free-energy relationship or Gibbs energy relation relates the logarithm of a reaction rate constant or equilibrium constant for one series of reactions with the logarithm of the reaction rate constant or equilibrium constant for a related series of reactions. The most common form of free-energy relationship is linear free energy relationship (LFER).

Furthermore, Daoutidis et al. [144] have demonstrated the importance of LFER for determination of kinetic and thermodynamic constants in biomass transformation. LFER can be used for congeneric series of compounds which share the same reaction center like –SH, -CO, etc. and vary with the substituents/radicals R related to these compounds. For example, the Taft equation predicts the reaction rate constant of one series of reactions by considering the polar, steric and resonance effect from the reactants with different substituent groups [145-151]. Meanwhile, it could help us to have a better understanding of the mechanism of reaction. The Taft equation is expressed as follows:

$$\log\left(\frac{k}{k_{ref}}\right) = \rho^* * \sigma^* + \delta * Es + \psi \quad (1)$$

where,

k is the rate constant of one compound at the same temperature with k_{ref},

k_{ref} is the rate constant of reference compound,

ρ^* is the sensitivity factor of the reaction to polar effect,

σ^* is the polar substituent constant on functional groups or reaction center,

δ is the sensitivity factor of the reaction to steric effect,

Es is the steric substituent constant on functional groups or reaction center,

ψ is the resonance effect between the substituent and the reaction center, in this project there is no resonance effect between the substituents and functional groups or reaction center.

Normally, polar substituent constant σ_i^* and steric substituent constant Es_i are independent of the reaction and based on the nature property of the substituents. For Taft equation, the substituent group $–CH_3$ is chosen as reference substituent and the polar and steric substituent constant are both set at 0.

According to Taft equation, for the polar effect on the reaction kinetics, if $\rho^*>1$, the reaction accumulates the negative charge in the transition state and is accelerated by electron withdrawing groups. By contrast, if $\rho^*<-1$, the reaction accumulates the positive charge in the transition state and is accelerated by electron donating groups. If $1>\rho^*>-1$, the reaction is mildly to polar effects and there is no polar effect if $\rho^*=0$.

Based on the same logic, for the steric effect on the reaction kinetics, if $\delta>1$, increasing steric bulk decreases the reaction rate and steric effects are greater in the transition state. if $\delta<-1$, increasing steric bulk increases the reaction rate and steric effects are lessened in the transition state. If $1>\delta>-1$, the reaction is mildly to steric effects and there is no steric effect if $\delta=0$.

The Taft equation mainly involves polar, steric and resonance effect in aliphatic systems, which could be distinguished from Hammett equation involving these effects in aromatic systems [152]. From the early research with Taft equation, esterification reaction with aliphatic carboxylic acid and alcohols were widely studied, which focus on a homogeneous and heterogeneous system and unique reaction center [145, 149-151].

In the previous study of our group, perhydrolysis of different carboxylic acids over homogeneous and heterogeneous catalysts was studied to follow Taft equation and

steric hindrance was demonstrated to be the major effect for the mechanism [150]. Taft equation was extended to a multiphase system of epoxidation of vegetable oils and free fatty acids with several reactions and reaction centers [125]. Thermal risk parameters, TMR_{ad}, stands for time-to-maximum-rate under adiabatic conditions, was tested to follow Taft equation which was confirmed by experiments performed in ARSST. The results elucidated that the polar effect governs this reaction from the viewpoint of safety parameter TMR_{ad}.

In this chapter, production of GVL from LA and its esters catalyzed by Ru/C in GVL solvent were tested by Taft equation. As shown in Figure 3.5, LA and its esters (ML, EL and BL) have similar linear chain structures except of the end substituent groups which are –H, $-CH_3$, $-CH_2CH_3$, $-CH_2CH_2CH_2CH_3$, respectively. Taft equation was initially tested to link the rate constants of the hydrogenation of LA and its esters with the structures of LA and its esters, from which the kinetics of LA esters with other substituents can be predicted.

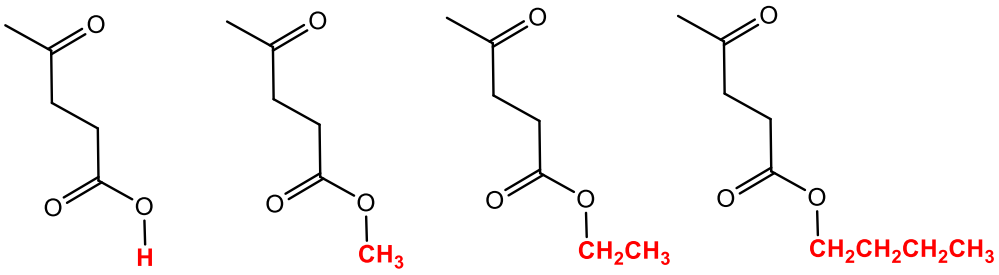

Levulinic acid Methyl levulinate Ethyl levulinate n-Butyl levulinate

Figure 3.5. Structures of LA, ML, EL and BL.

3.5 Results and discussion

3.5.1 Kinetic model

As described in several articles [120, 139, 153], hydrogenation of LA or its corresponding esters occurs in two reaction steps. The first step is the hydrogenation of the ketone group producing the following intermediates: 4-hydroxypentanoic acid (HPA) for LA, methyl 4-hydroxypentanoate (MHP) for ML, ethyl 4-hydroxypentanoate (EHP) for EL or butyl 4-hydroxypentanoate (BHP) for BL. The second step is the ring closure reaction of the intermediate to GVL. The mechanism of GVL production is

illustrated in Figure 3.6.

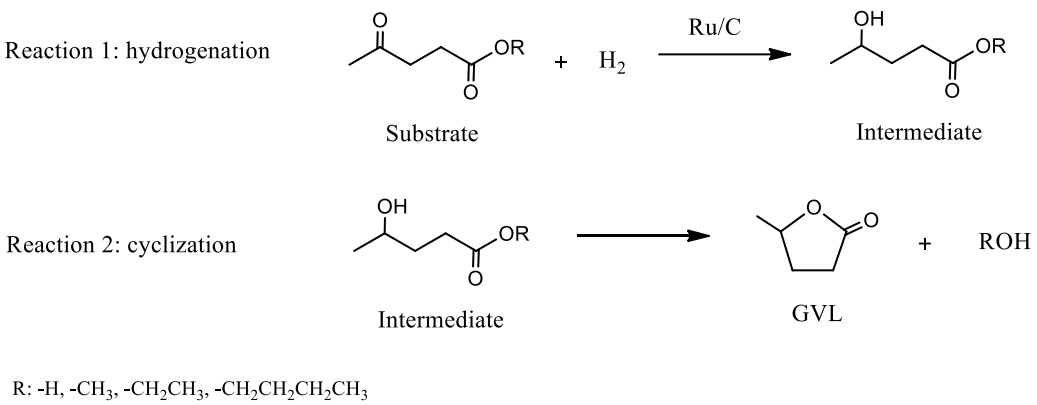

Figure 3.6. Reaction mechanism for the hydrogenation of LA or its esters to GVL.

The second reaction is often described as reversible for the case of hydrogenation in aqueous solvent [120, 139]. Based on our experimental observation, the reaction was found to be irreversible when using GVL as a solvent. As the work of Piskun et al. [120] and Negahdar et al. [121], the second reaction was assumed to occur in the bulk liquid phase, implying that the catalyst does not interfere on this second reaction.

The rate of hydrogenation of LA/ML/EL/BL to HPA/MHP/EHP/BHP on the catalyst can be described as:

$$R_1 = k_1 * [H_2]_{liq} * [Substrate]_{liq} * \omega_{Cat.} \quad (1)$$

where, $\omega_{Cat.}$ is the catalyst loading ($kg.m^{-3}$).

The rate of the second reaction (ring-closure) can be expressed as:

$$R_2 = k_2 * [Intermediate]_{liq} \quad (2)$$

The first reaction can be described by a more complex reaction mechanism such as Langmuir-Hinshelwood. Nevertheless, the description of such mechanism needs the adsorption coefficients that are cumbersome to estimate. In this study, we have deemed that the use of equations (1) and (2) can perfectly describe the kinetic rates.

The Taft equation applied for this study is expressed as follows:

$$\log\left(\frac{k_i(T)}{k_{reference}(T)}\right) = \rho^* * \ \sigma_i^* + \delta * Es_i \tag{3}$$

The Taft equation uses the substrate with the substituent methyl as the reference. So the rate constant for the hydrogenation of methyl levulinate (ML) for the first reaction ($k_{1,ML}(T)$) and the rate constant of methyl 4-hydroxypentanoate (MHP) ring closure for the second reaction ($k_{2,MHP}(T)$) were used as references. The term (T) was added to highlight the fact that these rate constants depend on the reaction temperature.

By introducing Taft equation (3) in equations (1) and (2), we obtain:

$$R_{1,Subst.} = k_{1,ML}(T) * 10^{\rho_1^*(T)*\sigma_{Subst.}^* + \delta_1(T)*Es_{Subst.}} * [H_2]_{liq} * [Substrate]_{liq} * \omega_{Cat.} \tag{4}$$

$$R_{2,Int.} = k_{2,MHP}(T) * 10^{\rho_2^*(T)*\sigma_{Int.}^* + \delta_2(T)*Es_{Int.}} * [Intermediate]_{liq} \tag{5}$$

where, Subst. and Int. are the suffix for substrate and intermediate, respectively.

The values of σ_i^* and Es_i are available from literature [125] for each substituent as summarized in Table 3.3. The substrate and the corresponding intermediate have the same substituent, thus the same values of Taft substituent parameters, i.e., σ_i^* and Es_i.

Table 3.3. Taft parameters for the reference (ML) and substituents (BL, EL, LA) [125].

Substrates & Intermediates	σ_i^*	Es_i
BL & BHP	-0.13	-0.39
EL & EHP	-0.1	-0.07
LA & HPA	0.49	1.24
ML & MHP	0	0

From a previous study of our group [125], we have noticed that Taft parameters $\rho^*(T)$ and $\delta(T)$ are temperature dependent. For that reason, the term T was added for these parameters. In this study, a linear relationship between $\rho^*(T)$ and $\delta(T)$ and the reaction temperature was assumed. Therefore, one can describe them by the following

equations:

$$\rho_1^*(T) = A_1 + B_1 * T(K) \quad (6)$$

$$\delta_1(T) = C_1 + D_1 * T(K) \quad (7)$$

$$\rho_2^*(T) = A_2 + B_2 * T(K) \quad (8)$$

$$\delta_2(T) = C_2 + D_2 * T(K) \quad (9)$$

During the modeling stage in section 3.5.4, the rate constants $k_{1,ML}(T)$ and $k_{2,MHP}(T)$, and the parameters A_1, B_1, C_1, D_1, A_2, B_2, C_2 and D_2 were estimated.

3.5.2 Mass balance

As experiments were performed under isothermal and isobaric conditions, hydrogen pressure was kept constant during the reaction.

Mass balance in the liquid phase

Mass balance for the different compounds present in the liquid phase can be expressed as:

$$\frac{dC_{Substrate}}{dt} = -R_1 \quad (10)$$

$$\frac{d[H_2]_{liq}}{dt} = k_L.a * \left([H_2]^*_{liq} - [H_2]_{liq}\right) - R_1 \quad (11)$$

$$\frac{dC_{Intermediate}}{dt} = R_1 - R_2 \quad (12)$$

$$\frac{dC_{ROH}}{dt} = R_2 \quad (13)$$

$$\frac{dC_{GVL}}{dt} = R_2 \quad (14)$$

where, $[H_2]^*_{liq}$ is the concentration of hydrogen at the gas-liquid interface, that was determined using Henry's constant $He(T) = \frac{[H_2]^*_{liq}}{P_{H_2,Reactor}}$ (mol.m^{-3}.bar^{-1}), $k_L.a$ is the volumetric gas to liquid mass transfer coefficient for hydrogen (s^{-1}). The detailed description of the mass transfer study is given in the following section 3.5.3.

3.5.3 Mass transfer study

3.5.3.1 Mass transfer model

This is a gas-liquid-solid reaction system, thus, mass transfer plays an important role. Herein, the external mass transfer, internal mass transfer and gas-liquid mass transfer are discussed below.

The effect of external mass transfer (from the bulk of the liquid phase to the surface of the solid catalyst) was experimentally verified for levulinic acid and butyl levulinate hydrogenation by varying the stirring rate. It was found that the external mass transfer resistance can be neglected at 1000 rpm (Figure 3.7). If the rotating speed was higher than 1200 rpm, the kinetics were slower maybe due to the vortex which can decrease the turbulence.

The effect of internal mass transfer (diffusion in the pores of the solid catalyst) was evaluated by using the Weisz-Prater criterion as used in Piskun et al. [120]. It was found that internal mass transfer can be assumed to be negligible.

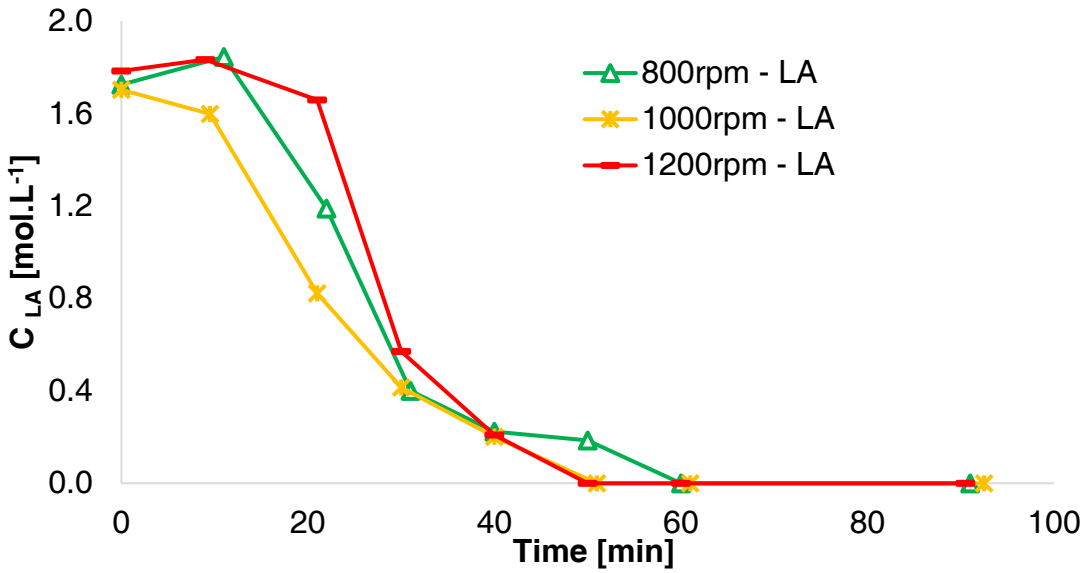

Figure 3.7. Effect of stirring rate on the rate of LA consumption with an initial concentration of 2 mol.L^{-1} in GVL as solvent, at 130°C, hydrogen pressure of 20 bars and catalyst loading of 11 kg.m^{-3}.

A two-film theory was used to describe the mass transfer of hydrogen from the gas to the liquid phase [154-157]. The resistance from the gas side was neglected. In order to have an accurate description of gas to liquid mass transfer for hydrogen, an expression for the volumetric mass transfer coefficient for hydrogen k_L.a taking into account the temperature, viscosity and density of the system was developed [157, 158]. Due to the low concentration of the different substrates (< 20 % by weight), the evaluation was done considering pure GVL.

Kawase and Moo-Yong [159] have demonstrated that the mass transfer coefficient in an aerated tank reactor can be expressed as:

$$k_L = \frac{2}{\sqrt{\pi}} * \sqrt{D_{H_{2/Liq}}} * \xi^{0.25} * \left(\frac{\rho_{Liq}}{\mu_{Liq}}\right)^{0.25} \quad (15)$$

where $D_{H_{2/Liq}}$ is the coefficient for the diffusion of hydrogen in the liquid phase ($m^2.s^{-1}$), k_L is the gas-liquid mass transfer coefficient of hydrogen from liquid side ($m^{-2}.s^{-1}$), ξ is the energy dissipation rate per unit mass ($W.kg^{-1}$), ρ_{Liq} is the density of the liquid ($kg.m^{-3}$) and μ_{Liq} is the dynamic viscosity (Pa.s).

The diffusion coefficient $D_{H_{2/Liq}}$can be expressed by the correlation of Wilke-Chang [160]:

$$D_{H_{2/Liq}} = \frac{7.4 * 10^{-8} * (\phi * M_{Liq})^{\frac{1}{2}} * T_{Liq}}{\mu_{Liq} * V_{H_2}^{0.6}} \quad (16)$$

where, ϕ is the association factor (-), M_{Liq} is the molar mass of the solvent ($g.mol^{-1}$), T_{Liq} is the temperature of the liquid phase (K), μ_{Liq} is the viscosity (cP) and V_{H_2} is the normal molar volume of hydrogen equal to 14.3 ($cm^3.mol^{-1}$).

By combining equations (15) and (16) and assuming the surface area of gas-liquid phase a constant, we obtain:

$$k_L.\mathrm{a} = (k_L.\mathrm{a})_{modified} * \left(\frac{T_{Liq}}{\mu_{Liq}}\right)^{0.5} * \left(\frac{\rho_{Liq}}{\mu_{Liq}}\right)^{0.25} \quad (17)$$

where $(k_L.\mathrm{a})_{modified} = \frac{2}{\sqrt{\pi}} * \sqrt{\frac{7.4*10^{-8}*(\phi*M_{Liq})^{0.5}}{V_{H2}^{0.6}}} * \xi^{0.25}$ was assumed constant for all the experiments, considering GVL as the main chemical compound. The temperature dependence of the density and kinematic viscosity of GVL was measured, and the results are shown in the following section 2.3.5.2.

To estimate the mass transfer coefficient $(k_L.\mathrm{a})_{modified}$, different experiments with only GVL solution were performed in the absence of chemical reactions. It was assumed that the number of moles disappearing in the reservoir corresponds to the number of moles of hydrogen in the liquid phase. Ideal gas law was used to determine the number of moles based on the pressure. Finally, in order to determine Henry's constant as a function of temperature, mass transfer experiments were carried out at four different temperatures for a long period, in order to reach the thermodynamic equilibrium. Van't Hoff equation was used to express Henry's temperature's dependence:

$$He(T_R) = He\left(T_{Ref} = 373.15K\right) * exp\left(\frac{-\Delta H_{Sol.}}{R} * \left(\frac{1}{T_R} - \frac{1}{373.15}\right)\right) \quad (18)$$

3.5.3.2 Physicochemical properties of solvent

The same methodology developed by our group [161] was used to measure the evolution of density and kinematic viscosity of GVL with temperature.

Density (kg.m^{-3}) varies with temperature T (K) as:

$$\rho = \mathrm{a}' + \mathrm{b}' * T \quad (19)$$

Viscosity follows an Arrhenius law:

$$\mu = \mathrm{A} \times e^{\frac{-E_a}{R*T}} \quad (20)$$

where, μ is the dynamic viscosity (Pa.s), A is the pre-exponential factor, *Ea* is the activation energy (J.mol^{-1}), *R* is the universal gas constant (J.K^{-1}.mol^{-1}) and *T* is temperature (K).

Figure 3.8 shows the evolution of the measured density versus temperature, as for Equation (19). Figure 3.9 shows that viscosity follows Equation (20).

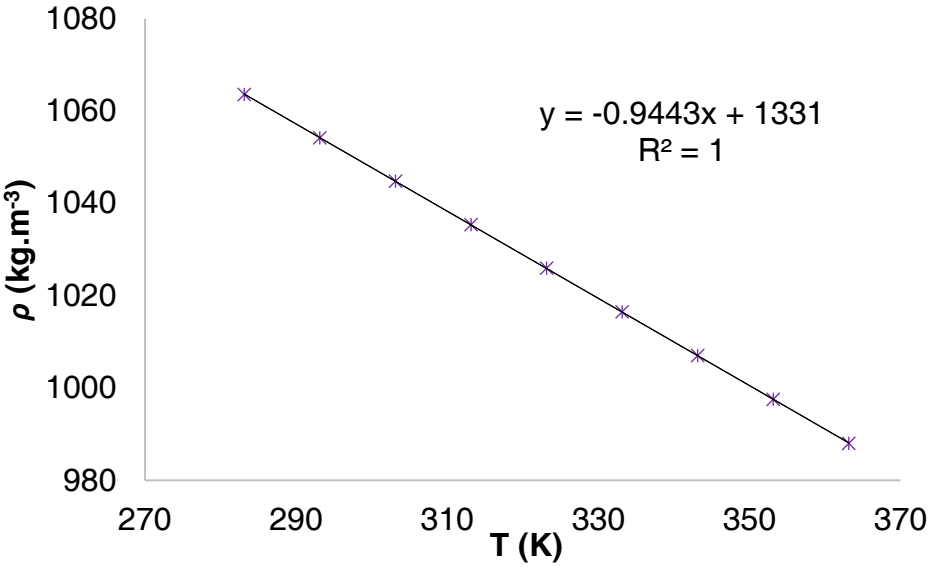

Figure 3.8. Evolution of GVL density with temperature.

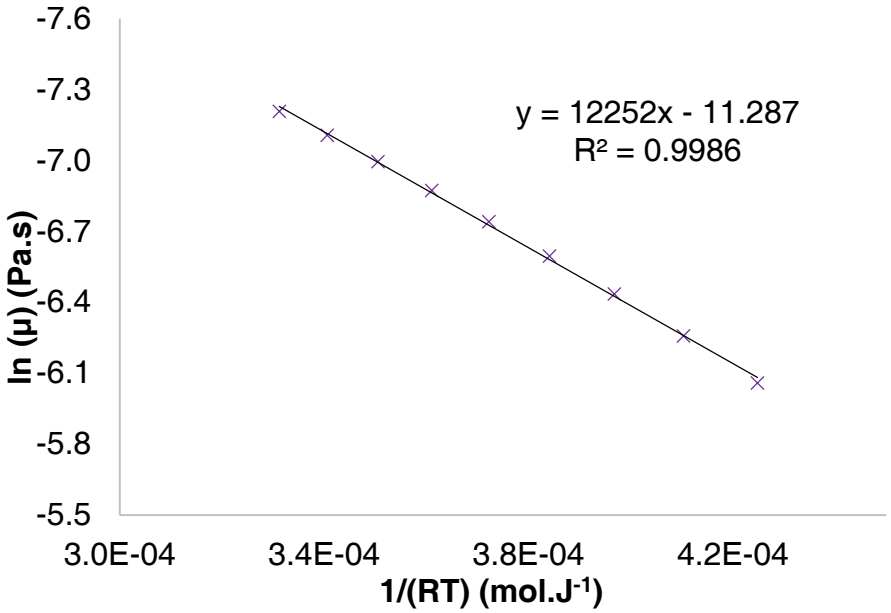

Figure 3.9. Arrhenius curve for GVL viscosity.

3.5.4 Validation of models

For the modeling stage, the software ModEst [141] was used. Ordinary differential equations were solved by using ODESSA algorithm.

For the mass transfer study, the number of moles of hydrogen in the liquid phase was used as an observable for $(k_L.\mathrm{a})_{modified}$ parameter estimation. For the kinetic study, the concentrations of substrate, intermediate and GVL were used as observable variables for parameter estimation. The objective function was defined as:

$$\omega = \sum_i (y_i - \hat{y}_i)^2 \tag{21}$$

where, y_i is the experimental value and $\hat{y}_i$ is the simulated one. The objective function was minimized by Simplex algorithm, then by Levenberg-Marquardt algorithm.

From the mass transfer experiments, it was found that $\Delta H_{Sol.H2} = 5936.8$ J.mol^{-1} and $He(T_{Ref} = 373.15K) = 1.86$ mol.m^{-3}.bar^{-1} as illustrated in Figure 3.10. Compared to the hydrogenation of levulinic acid in water [139], the absorption of hydrogen in GVL is an endothermic phenomenon. This endothermic behavior was also observed for other organic solvents [162-164]. This can be beneficial because, as the reaction temperature increases, the solubility of hydrogen and the kinetics of hydrogenation increase.

For mass transfer modeling, ODE (11) was solved in the absence of chemical reactions, i.e., R1=R2= 0 mol.m^{-3}.s^{-1}. The coefficient of explanation, defined as $R^2 = 1 - \left(\frac{y_i - \hat{y}_i}{y_i - \bar{y}_i}\right)^2$, was found to be 95% showing the reliability of the fitting to the experimental data. Table 3.4 shows the estimated values of $(k_L.\mathrm{a})_{modified}$. Figure 3.11 shows the fitting of the model to the experimental data. In general, one can say that the model fits well the experimental data.

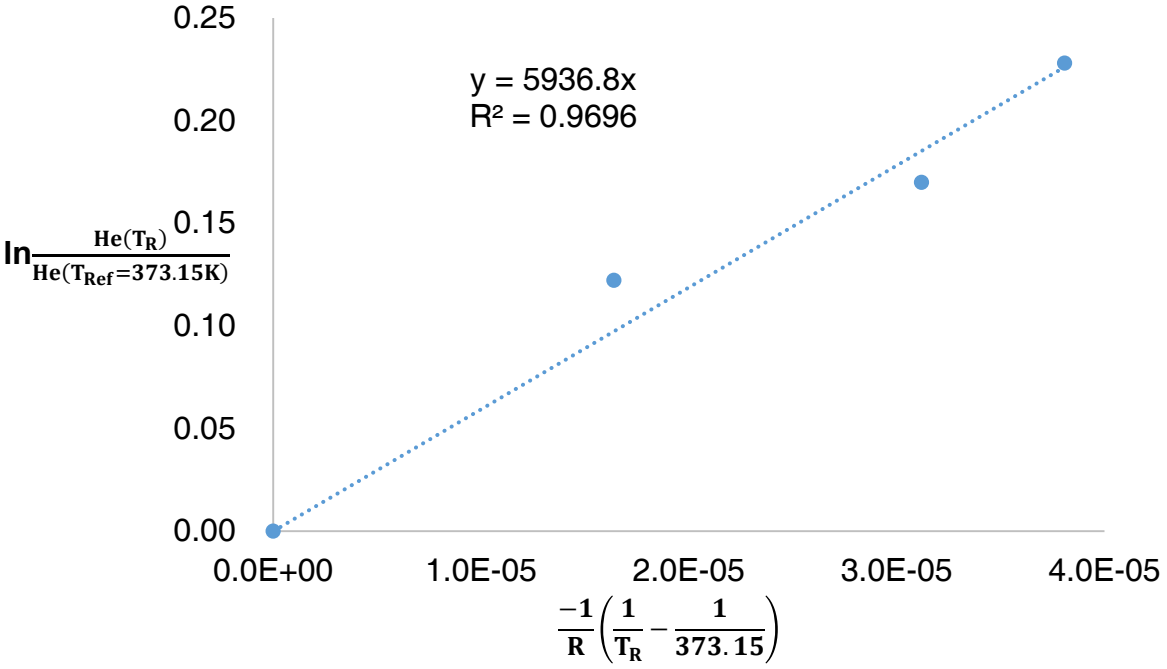

Figure 3.10. Van't Hoff plot for the absorption of hydrogen in GVL.

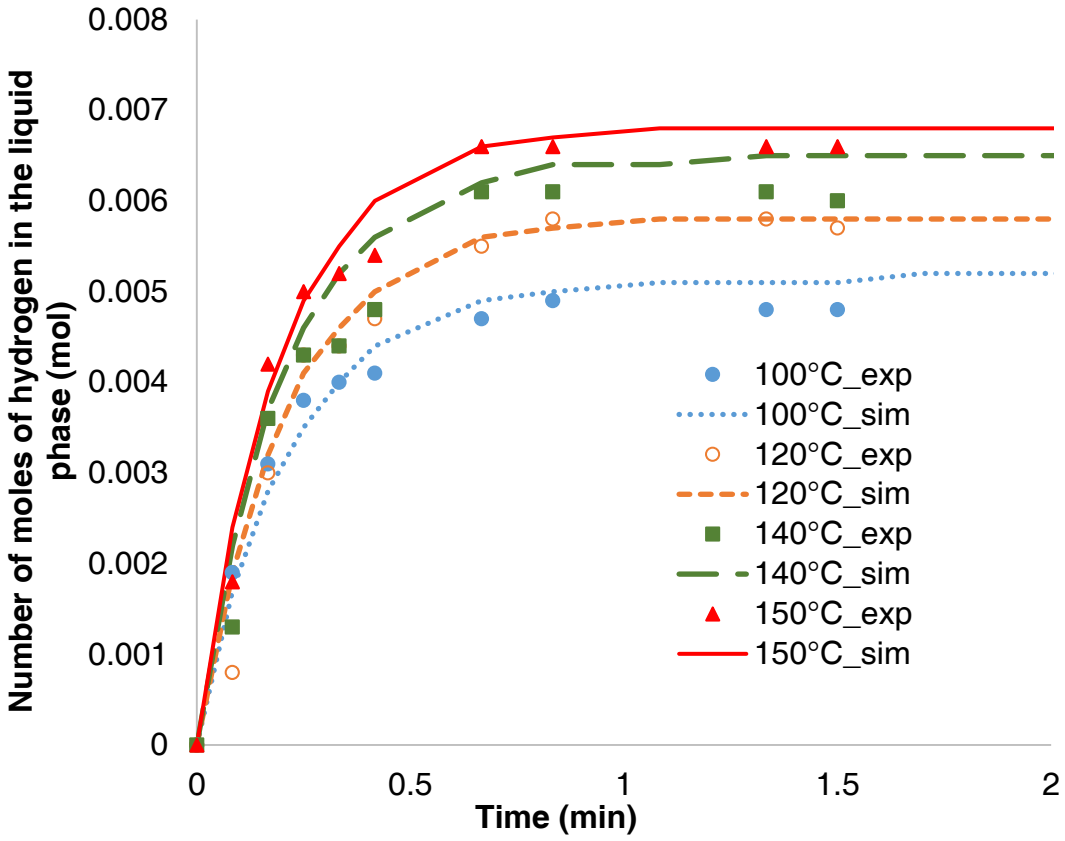

Figure 3.11. Fit of the model to the mass transfer experiments under a pressure of ca. 20 bars.

Table 3.4. Results of the mass transfer constant.

Parameter	Units	Value	Std error (%)
$(k_L.\mathrm{a})_{modified}$	$\left(\frac{\mathrm{Pa.\,s}}{\mathrm{K}}\right)^{0.5}.\left(\frac{\mathrm{Pa.\,s}}{kg.m^{-3}}\right)^{0.25}.s^{-1}$	2.22×10^{-6}	2.4

For the kinetic modeling, the value of $(k_L.\mathrm{a})_{modified}$ estimated previously was used. Rate constants of reactions 1 and 2 for the hydrogenation of ML were expressed by using modified Arrhenius equation:

$$k_i(T_R) = k_i(T_{Ref}) * exp\left(\frac{-Ea_i}{R} * \left(\frac{1}{T_R} - \frac{1}{T_{Ref}}\right)\right) \quad (22)$$

ODEs (10)-(14) were solved. Concentrations of substrate, intermediate and GVL were used as observables for the non-linear regression stage. The following parameters were estimated: kinetic constants $k_{1,ML}(T_{Ref})$, $Ea_{1,ML}$, $k_{2,MHP}(T_{Ref})$, $Ea_{2,MHP}$ and the parameters A_1, B_1, C_1, D_1, A_2, B_2, C_2 and D_2. The coefficient of explanation was found to be equal to 99.82%, showing the good fitting of the model to the experimental data. Table 4 displays the estimated parameters and the standard deviations.

Table 3.5 shows that standard deviation for kinetic constants are low. Nevertheless, the standard deviation for the Taft parameters are not low. This could be explained by the fact that equations (6)-(9) might not be the most appropriate to represent the evolution of ρ^* and δ with temperature.

Figure 3.12 shows some fitting of the model to the experimental data. In general, the fitting is correct. One can observe that the fitting of the model to the intermediate concentration is less accurate. This is due to the high reactivity of these species making their analysis less accurate, which is particularly pronounced for the intermediate HPA produced by hydrogenation of LA. The fitting of the model to the experimental concentration of HPA is lower compared to the other ones. This is due to the fact that this intermediate is very reactive making its analysis difficult. The parity plot (Figure 3.13) shows that the developed model is reliable.

Table 3.5. Estimated parameters and standard deviation at T_{Ref}= 403.15K.

Parameters	Units	Estimated values	Estimated Relative Standard Error (%)
$k_{1,ML}(T_{Ref})$	$m^6.mol^{-1}.kg^{-1}.s^{-1}$	3.79E-06	4.6
$Ea_{1,ML}$	$J.mol^{-1}$	15000.00	21.8
$k_{2,MHP}(T_{Ref})$	s^{-1}	8.92E-04	7.0
$Ea_{2,MHP}$	$J.mol^{-1}$	59300.00	6.4
A1	-	25.00	54.2
B1	K^{-1}	-0.07	51.5
C1	-	-10.00	54.6
D1	K^{-1}	0.03	51.3
A2	-	-22.00	50.4
B2	K^{-1}	0.06	46.7
C2	-	-8.40	49.2
D2	K^{-1}	0.02	44.9

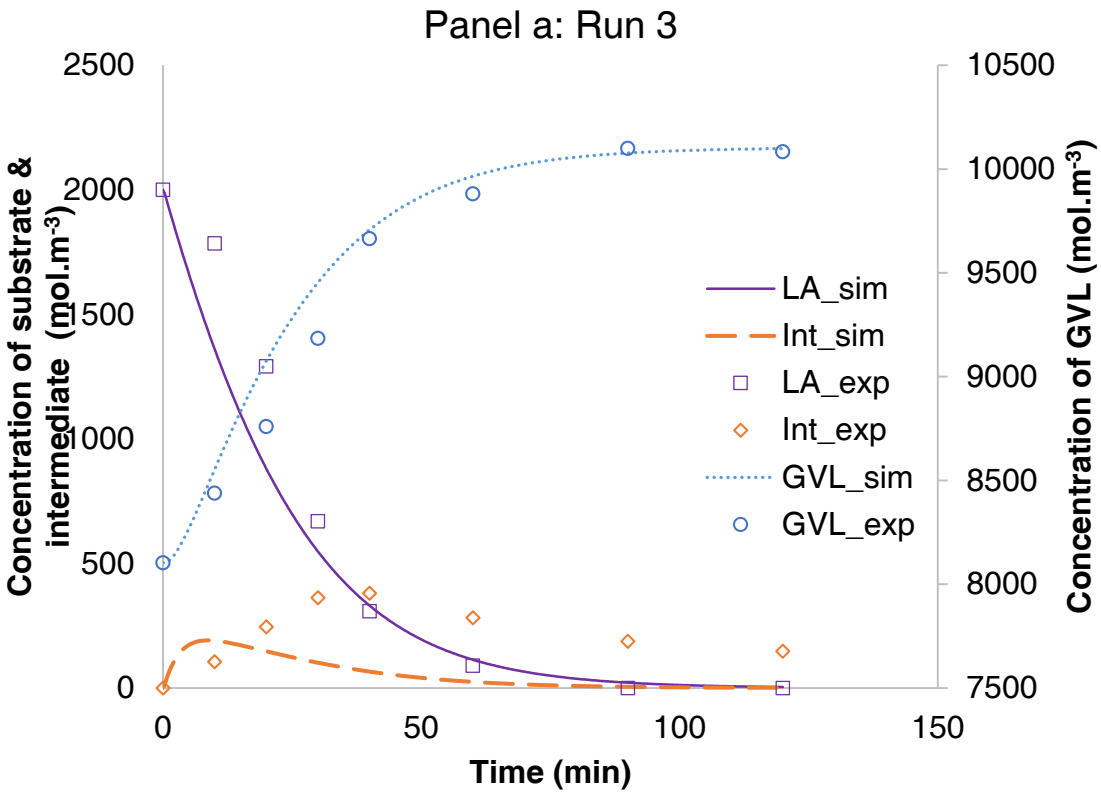

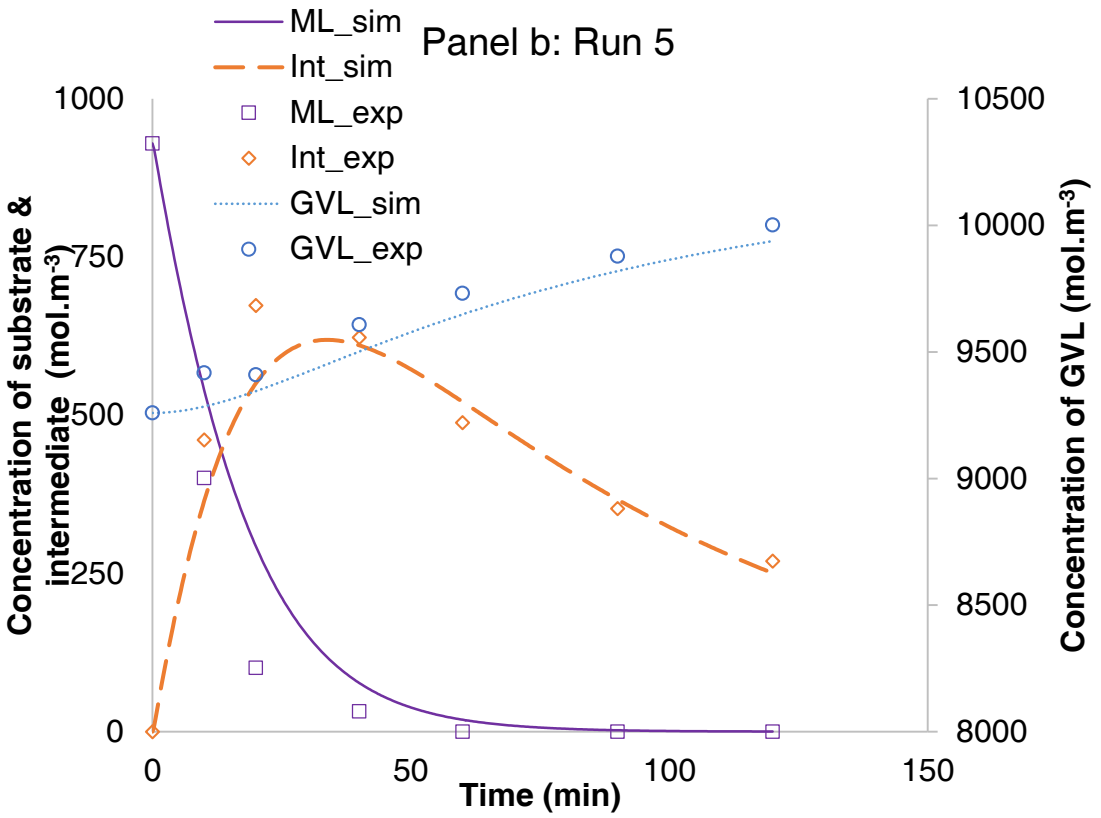
Panel b: Run 5
ML_sim
Int_sim
ML_exp
Int_exp
GVL_sim
GVL_exp
Concentration of substrate & intermediate (mol.m-3)
Concentration of GVL (mol.m-3)
Time (min)
1000
750
500
250
0
10500
10000
9500
9000
8500
8000
0
50
100
150

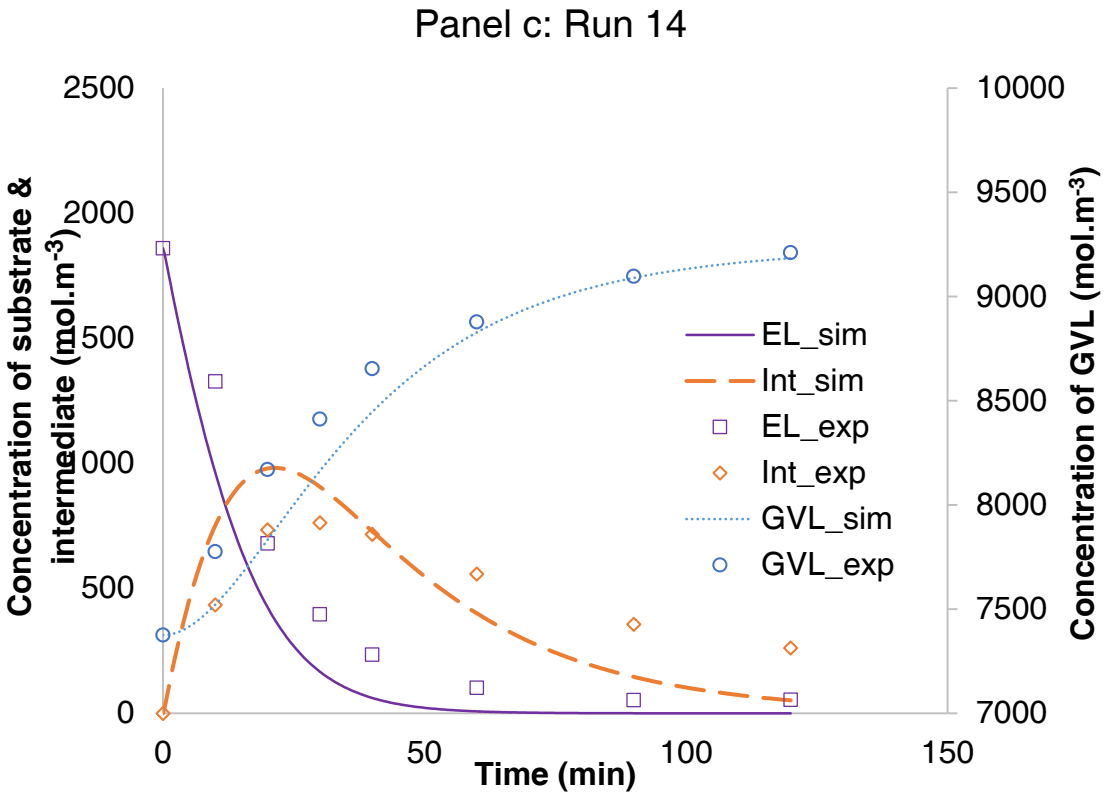
Panel c: Run 14
EL_sim
Int_sim
EL_exp
Int_exp
GVL_sim
GVL_exp
Concentration of substrate & intermediate (mol.m-3)
Concentration of GVL (mol.m-3)
Time (min)
2500
2000
1500
1000
500
0
10000
9500
9000
8500
8000
7500
7000
0
50
100
150

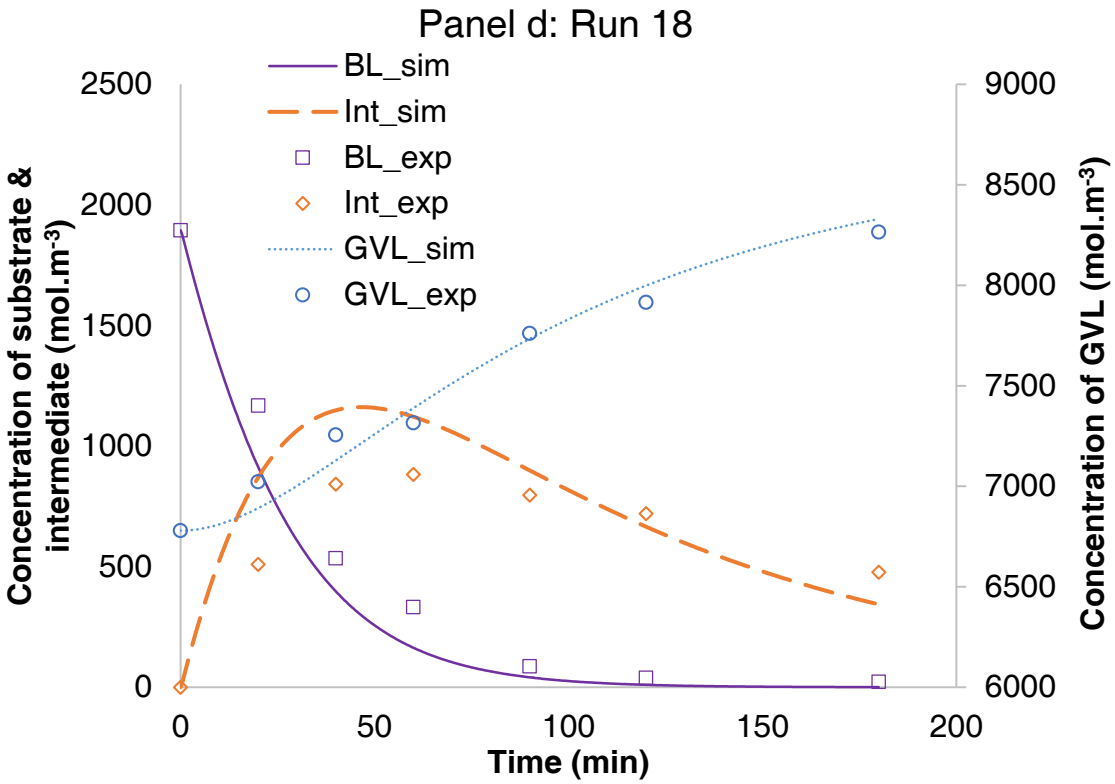

Figure 3.12. Fitting of the model to the experimental data for the different substrates: LA (panel a), ML (panel b), EL (panel c) and BL (panel d).

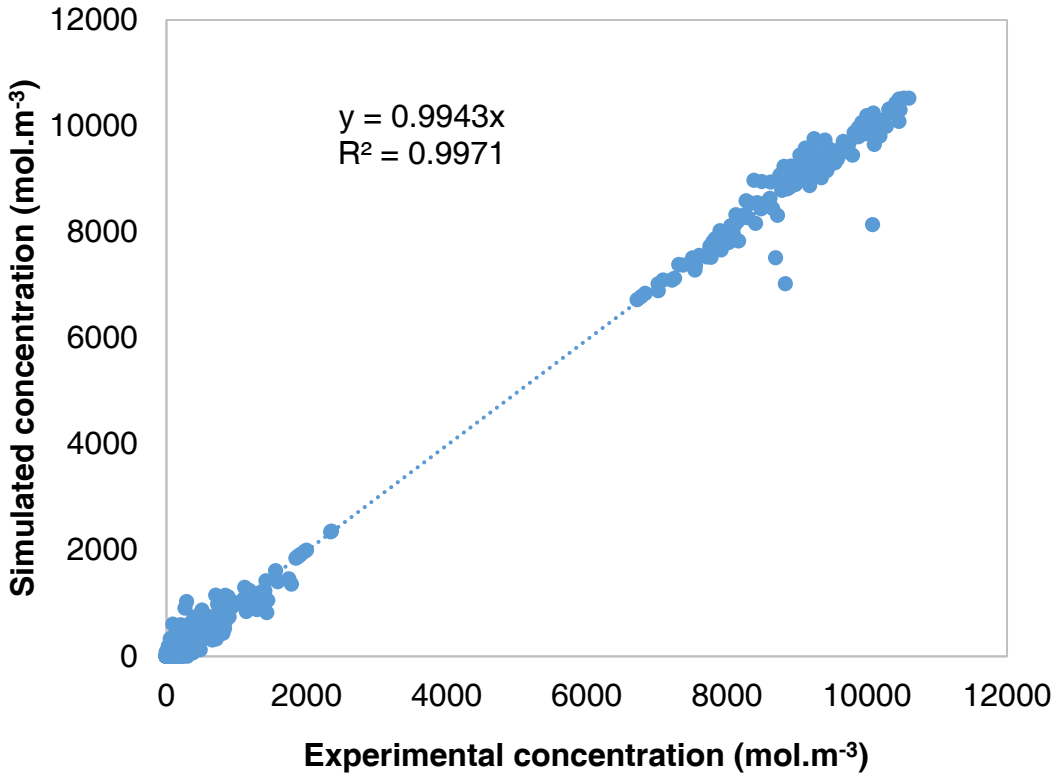

Figure 3.13. Parity plot.

3.5.5 Comparison of kinetics

Based on Table 3.5, it is possible to determine the kinetic constants for the different substrates (Table 3.6). From Table 3.6, it is possible to notice that the rate constants of hydrogenation of substrates in GVL are not proportional to the steric hindrance of the substituent alkyl groups, especially for reaction 1. The activation energy for the second ring-closure reaction of LA is very high maybe due to the different mechanism where the proton participates to catalyze and accelerate the second step. For a better comparison of rate constants for different substrates about the first reaction of hydrogenation and the second reaction of ring-closure at different temperature, graphs in Figures 3.14 and 3.15 were made and discussed below.

Table 3.6. Kinetic constants for the hydrogenation of LA, ML, EL and BL (T_{Ref} = 403.15K).

Constant	Unit	ML	EL	BL	LA
$k_{1,Subst.}(T_{Ref})$	$m^6.mol^{-1}.kg^{-1}.s^{-1}$	3.79×10^{-06}	5.17×10^{-06}	3.09×10^{-06}	5.13×10^{-06}
$Ea_{1,Subst.}$	$J.mol^{-1}$	15000	28931	9680	17029
$k_{2,Int.}(T_{Ref})$	s^{-1}	8.92×10^{-04}	4.45×10^{-04}	1.88×10^{-04}	1.92×10^{-01}
$Ea_{2,Int.}$	$J.mol^{-1}$	59300	37056	10250	228693

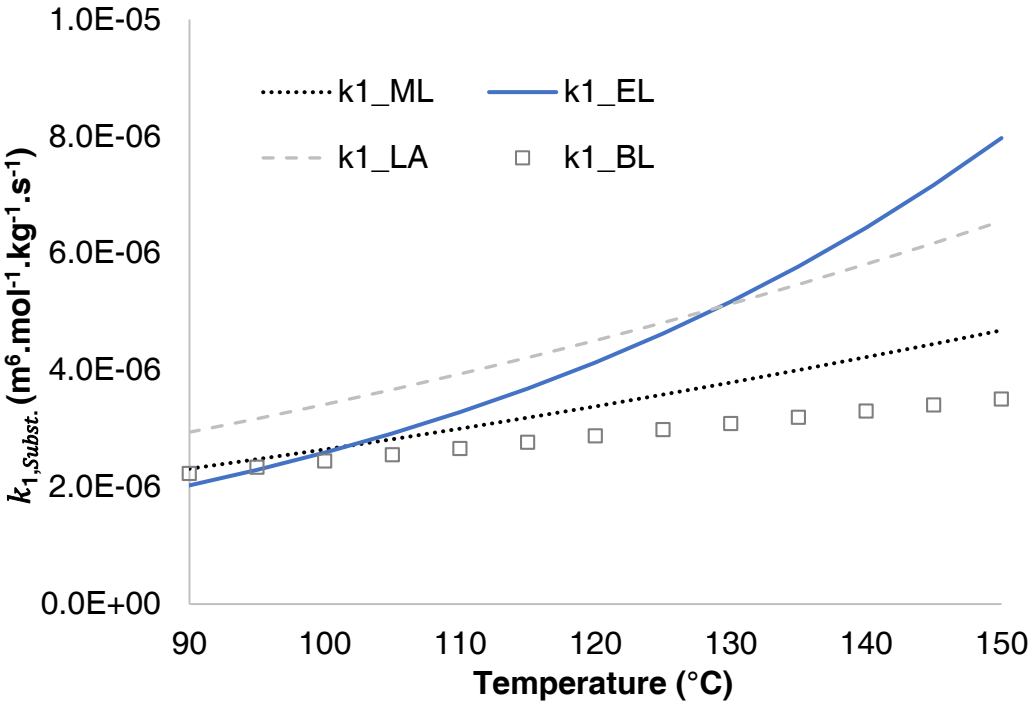

Figure 3.14. Evolution of rate constants 1 for different substrates with temperature.

From Figure 3.14, we can notice that rate constants 1 of hydrogenation of LA, EL, ML and BL to the intermediates are affected by the nature of the substituent and the temperature. This observation could be surprising because the substituent is relatively far from the ketone group. For reaction temperature lower than 135°C, the rate constant for the hydrogenation of LA is the highest one. Whereas, for reaction temperature higher than 135°C, the rate constants increase in the following order: $k_{1,EL} > k_{1,LA} > k_{1,ML} > k_{1,BL}$. This difference of reactivity is not in agreement with the steric hindrance induced by the substituent groups.

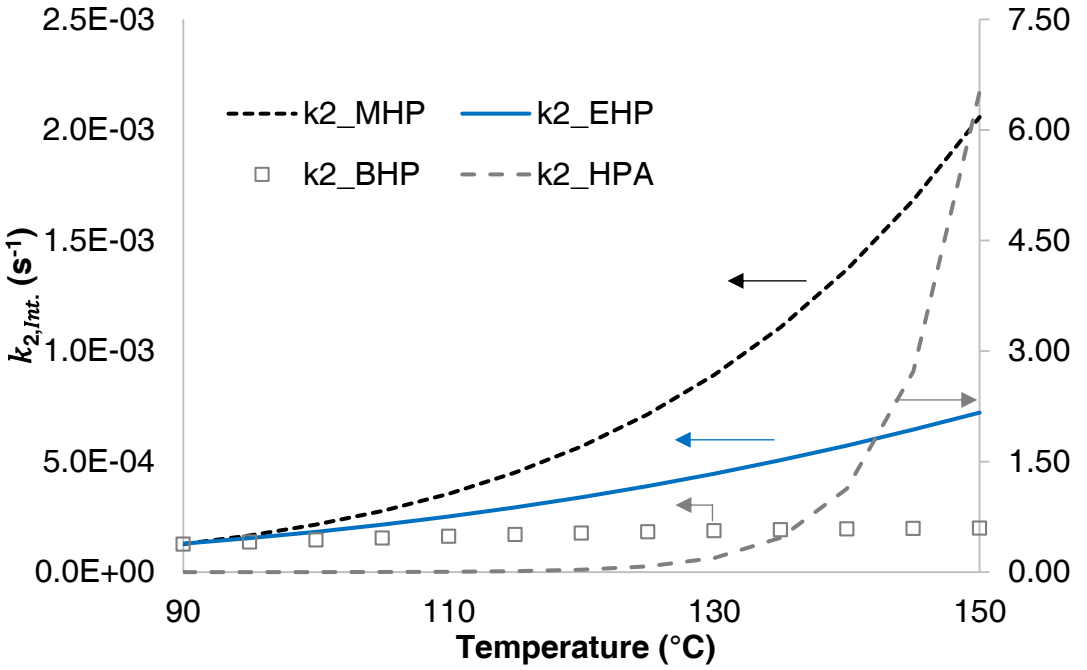

Figure 3.15. Evolution of rate constants 2 for different substrates with temperature.

From Figure 3.15, the influence of the substituent groups and temperature is more significant on rate constant 2 than for rate constant 1. This observation seems to be logical because the substituents are closer to the reaction center. In the temperature range 90-150°C, the rate constants increase in the following order: $k_{2,HPA} >> k_{2,MHP} > k_{2,EHP} > k_{2,BHP}$. When the steric hindrance is lower, then the reaction rate is faster. From Figures 3.14 and 3.15, it is possible to notice that steric hindrance could not explain properly the kinetic behavior of the hydrogenation of LA, ML, EL and BL. As Taft equation was introduced to this model with the possibility to quantify polar and

steric effect of the different substituent group, one can have a deep insight into the relationships between molecule structure and reactivity.

Figure 3.16 shows the evolution of the Taft parameters (ρ_1^*, ρ_2^*, δ_1 and δ_2) with temperature. The influence of the polar effect (ρ_1^* and ρ_2^*) on both reactions is higher than the steric effect, and this difference is more pronounced when the reaction temperature is higher than 110°C as ρ_1^* and ρ_2^* are much higher than 1.Steric effect can be considered as negligible for reaction temperature lower than 140°C for both reactions, i.e., δ_1 and δ_2 are lower than 1.

Furthermore, polar effect of reaction 1 starts to be significant when reaction temperature is ca. 115°C and 110°C for reaction 2. For reaction 1, the value of ρ_1^* is negative. From Taft definition, this means that the reaction is accelerated by electron donating group. As the temperature increases, the ethyl group increases the most the electron donor capacity of the group ROOC-CH_2-CH_2- on the ketone group. For reaction 2, the value of ρ_2^* is positive. From Taft definition, this means that the reaction is accelerated by electron withdrawing group. From the four substrates, the hydrogen group is the most electron withdrawing group explaining the fact that reaction 2 with hydrogen substituent is the fastest one.

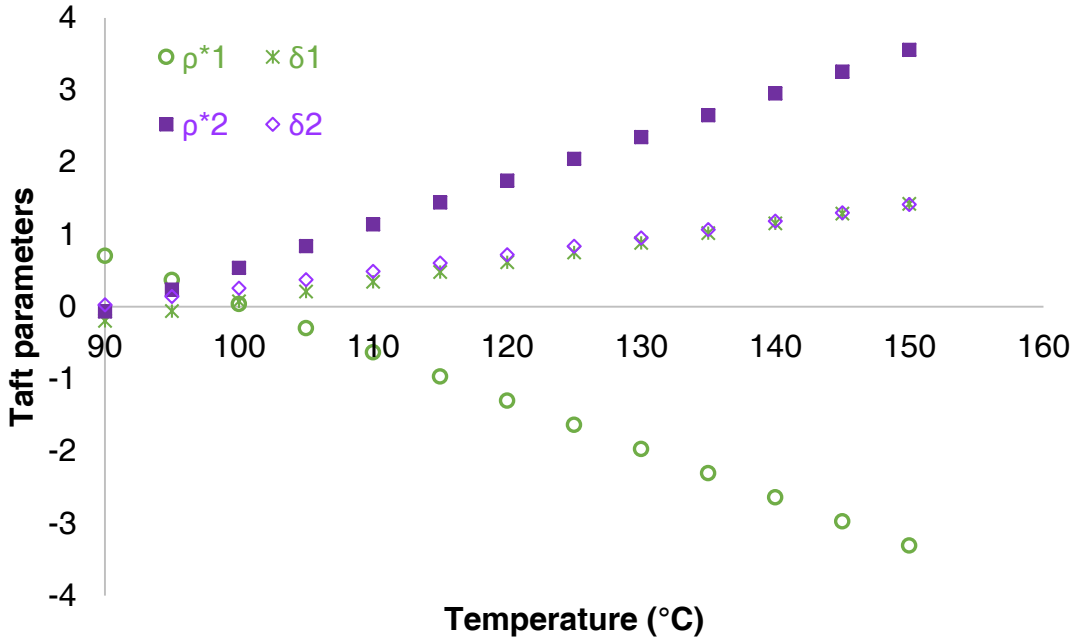

Figure 3.16. Influence of temperature on Taft parameters.

To have a full view of kinetic behaviors of different substrates, based on the estimated kinetic constants, it is possible to plot the kinetics of GVL production under the same operating conditions for LA, ML, EL and BL at two temperatures (Figures 3.17 and 3.18).

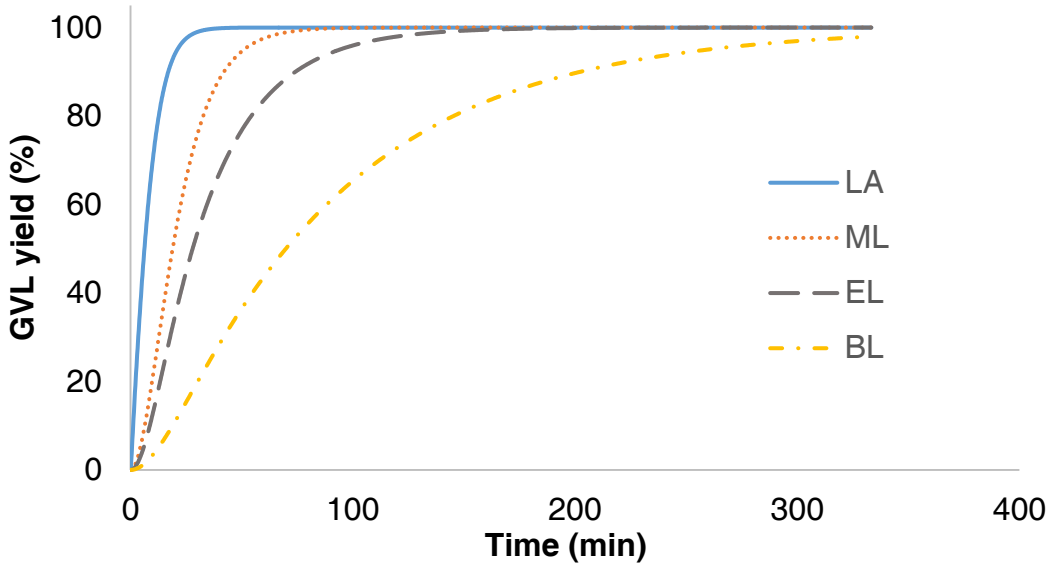

Figure 3.17. Kinetics of production of GVL from LA, ML, EL and BL at 140°C and 20 bar of H_2. $[Substrate]_0$ = 1000 mol.m^{-3}, $[GVL]_0$ = 7685-8250 mol.m^{-3} and $\omega_{Cat.}$ = 11.67 kg.m^{-3}.

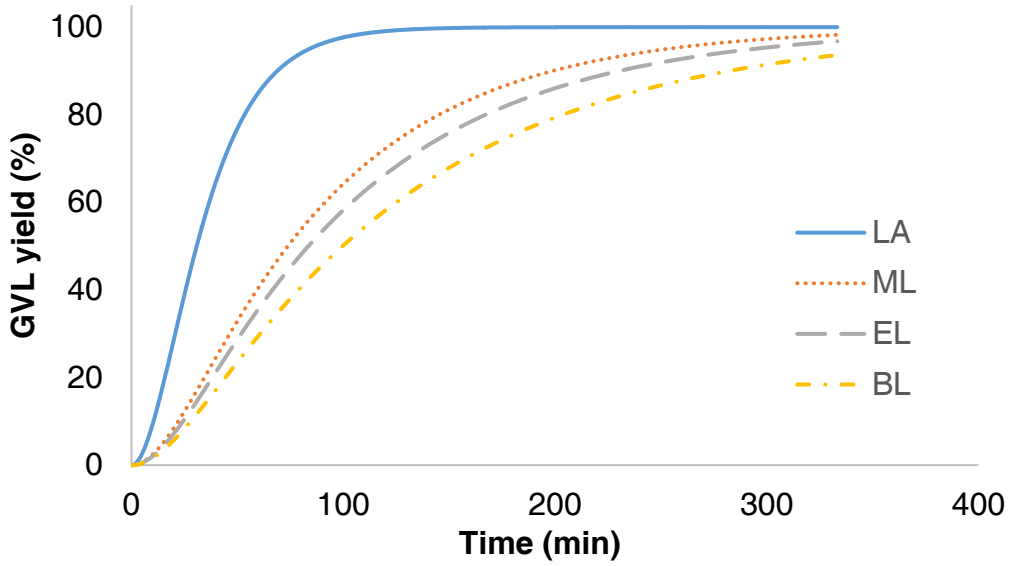

Figure 3.18. Kinetics of production of GVL from LA, ML, EL and BL at 100°C and 20 bar of H_2. $[Substrate]_0$= 1000 mol.m^{-3}, $[GVL]_0$ = 8064-8625 mol.m^{-3} and $\omega_{Cat.}$. = 11.67 kg.m^{-3}.

From Figures 3.17 and 3.18, one can notice that the total rates of GVL production increases in the following order: $r_{GVL\ from\ LA} > r_{GVL\ from\ ML} > r_{GVL\ from\ EL} > r_{GVL\ from\ BL}$. Reaction rate 2 is the governing reaction for ML, EL and BL which is not the case for LA (Figures 3.19 and 3.20). From Figures 3.19 and 3.20, one can notice that reaction rates 1 are faster than reaction rates 2 for the hydrogenation of alkyl levulinate, but for the hydrogenation of LA both reaction rates are similar.

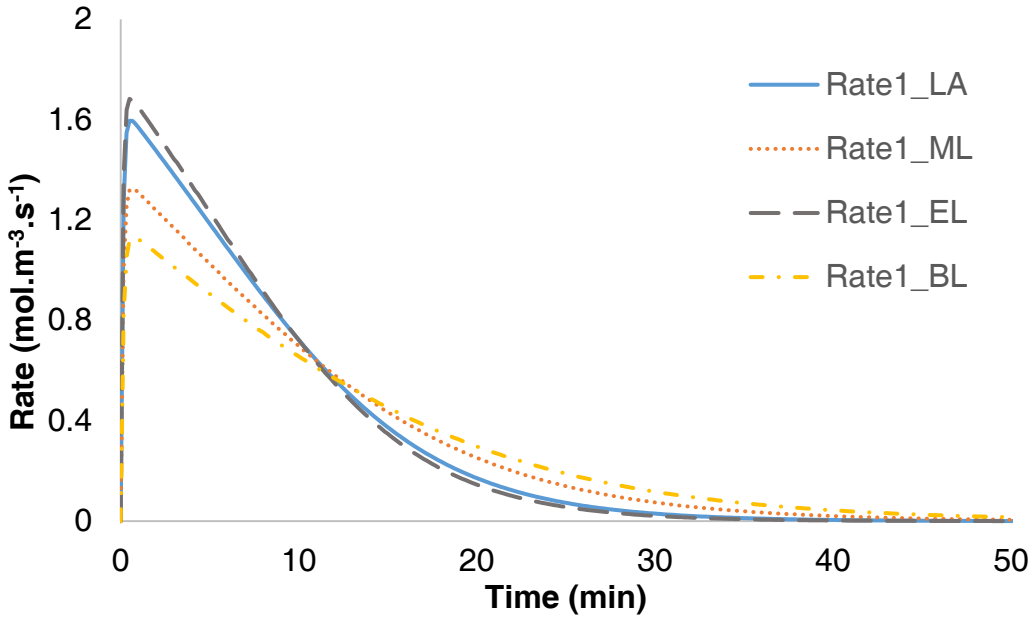

Figure 3.19. Reaction rate 1 at 140°C and 20 bar of H_2. $[Substrate]_0$ = 1000 mol.m^{-3}, $[GVL]_0$ = 7685-8250 mol.m^{-3} and $\omega_{Cat.}$ = 11.67 kg.m^{-3}.

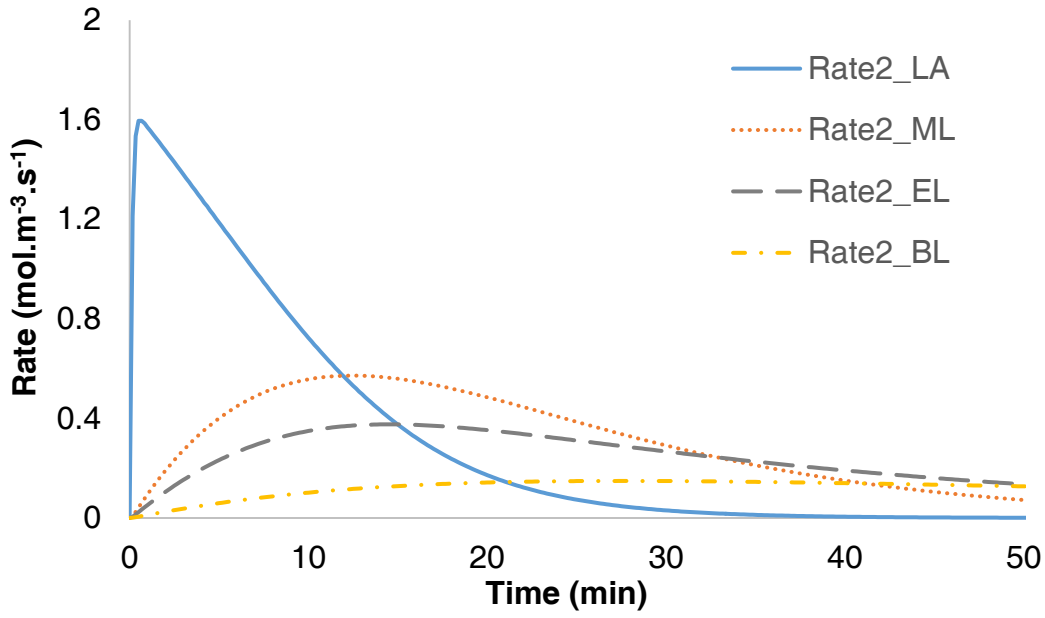

Figure 3.20. Reaction rate 2 at 140°C and 20 bar of H_2. $[Substrate]_0$ = 1000 mol.m^{-3}, $[GVL]_0$ = 7685-8250 mol.m^{-3} and $\omega_{Cat.}$ = 11.67 kg.m^{-3}.

3.6 Conclusion

In this chapter, structure-reactivity study for hydrogenation of levulinic acid (LA) and methyl (ML), ethyl (EL), n-butyl levulinate (BL) using Ru/C as catalyst to γ-valerolactone (GVL) was investigated. Two parts of experiments including gas-liquid mass transfer experiment and hydrogenation kinetic experiments were performed under isobaric and isothermal conditions and GVL was used as solvent to avoid liquid-liquid reaction system.

A mass transfer investigation was done to evaluate the gas-liquid mass transfer coefficient (k_L. a) for the transfer of hydrogen gas from the gas to the liquid phase. The influence of reaction temperature, solvent viscosity and density was taken into account to determine the value of k_L. a. Besides, it was found that Henry's constant for hydrogen absorption in GVL follows a van't Hoff law. This absorption was found to be endothermic meaning that temperature increase leads to increase the amount of absorbed hydrogen.

Then, a kinetic model including mass transfer parameters, was developed by varying the reactant concentration, hydrogen pressure, reaction temperature and catalyst loading. The originality of this model was the use of Taft equation to take into account the steric and polar effects of the substituents (H-, CH_3-, CH_3-CH_2-, CH_3-CH_2-CH_2-CH_2-) for the hydrogenation and ring-closure step reactions. We have demonstrated that the Taft parameters ρ^* (T) and $\delta(T)$ vary with temperature. It was found that the total reaction rate for production of GVL was: $r_{GVL\ from\ LA} > r_{GVL\ from\ ML} > r_{GVL\ from\ EL} > r_{GVL\ from\ BL}$.

For this reaction system, the steric effect was found to be negligible for both reactions. Nevertheless, the polar effects were found to be important for the ring-closure ones. The rate of GVL production is faster by using LA, because the electron withdrawing effect of the group H- increases the kinetics of reaction 2. The reaction 2 is slower for the hydrogenation for the other alkyl because alkyl groups are electron-donating groups.

This study opens new possibility in chemical reaction engineering, by knowing the Taft

parameters, it is possible to predict the rate constants with other substrates. The continuation of this work is to test the Taft equation on other substrates and have a better understanding on the evolution of Taft parameters with temperature.

Chapter IV. Experimental determination of reaction enthalpies for γ-valerolactone production

4.1 Introduction

Thermodynamic constant like reaction enthalpy is essential to take into account energy balance in chemical reaction processes. Hydrogenation reaction is normally an exothermic reaction, which needs an efficient cooling system to make sure that the reaction process is operated safely under isothermal conditions. Thus, it is necessary to obtain the reaction enthalpy for hydrogenation of levulinic acid or its esters to γ-valerolactone to be able to develop a process flow diagram and make a cost evaluation.

Herein, the hydrogenation of methyl levulinate (ML) to γ-valerolactone (GVL) was selected as an example for the reaction enthalpy determination in GVL solvent due to comparatively stable intermediate. The reaction enthalpy for this system was experimentally and preliminarily determined through reaction calorimeters and Gas-chromatography (GC) analysis (Figure 4.1). The calorimeters RC1 and Tian-Calvet calorimeter C80 were used for measurement of reaction heat release and GC analysis was employed for quantification of chemical compounds. Based on the two-step reaction mechanism, the reaction enthalpy for each step and overall reaction enthalpy were determined and summarized in this chapter.

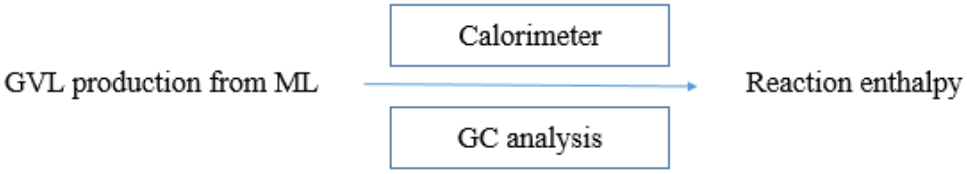

Figure 4.1. Experimental determination of reaction enthalpy for hydrogenation of ML to GVL by using calorimeter and GC analysis.

The methodology for reaction enthalpy determination is shown in detail in section 4.2, which links the calorimeter measurement and GC analysis to calculation of reaction enthalpy. Section 4.3 about experimental and analytical methods includes chemical

used in this study which is shown in section 4.3.1, RC1 introduction and experiment detail shown in section 4.3.2, C80 introduction and experiment detail shown in section 4.3.3 and analytical section 4.3.4.

RC1 results and C80 results are shown in detail and discussed in section 4.4.1 and section 4.4.2 respectively. The final determination of reaction enthalpy for each step and overall reaction is concluded in section 4.4.3 based on the methodology described in section 4.2. Section 4.5 gives the conclusion of this chapter.

4.2 Methodology of reaction enthalpy determination

As discussed in Chapter III, the mechanism for hydrogenation of ML to GVL was shown in Figure 4.2. This reaction includes two steps. The first step is hydrogenation of carbonyl group of ML to the intermediate MHP. The second step is the cyclization of the intermediate to GVL and methanol in equivalent mole ratio. Based on this mechanism and experimental observation, determination of reaction enthalpy of each step is necessary due to the existence of intermediate and incomplete conversion. Then, the enthalpy for overall reaction can be calculated based on the reaction enthalpy of these two steps.

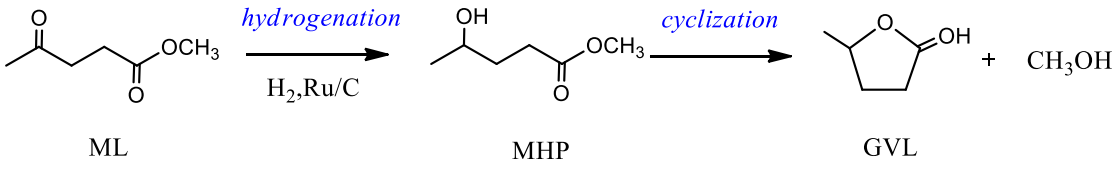

Figure 4.2. Mechanism of hydrogenation of ML to GVL.

Herein, reaction calorimeters RC1 and C80 were used to measure the heat flow of the reaction in combination with GC analysis to obtain more precise value of reaction enthalpies (more experimental detail in section 4.3). In RC1, ML, GVL, H_2 and Ru/C catalyst were mixed for the overall reaction, both of the steps occur. While in C80, only step 2 occur as the experiment in C80 used the final liquid obtained from RC1 without Ru/C catalyst and H_2. The definition of reaction enthalpy ΔH_R, $\Delta H_{R,1}$, $\Delta H_{R,2}$ are shown in Figure 4.3.

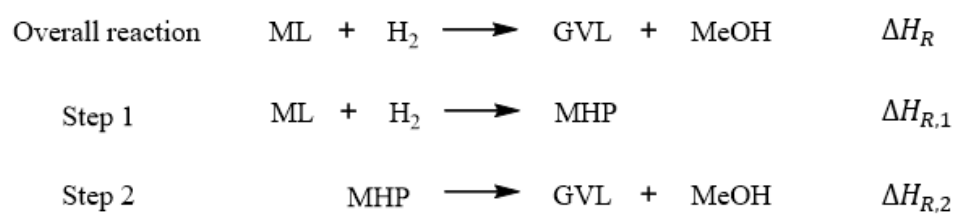

Figure 4.3. Definition of reaction enthalpy.

As shown above, the correlation of reaction enthalpies between overall reaction and two reaction steps can be concluded as below:

$$\Delta H_R = \Delta H_{R,1} + \Delta H_{R,2} \quad (1)$$

The heat release in RC1 (Q_{RC1}) includes the heat release from the step 1 (Q_1) and step 2 ($Q_{2\ from\ RC1}$) as these two steps occur together. However, in calorimeter C80, only step 2 occurs without hydrogen and catalyst. Thus, the heat release in C80 (Q_{C80}) is the heat release from step 2 ($Q_{2\ from\ C80}$). The heat release in RC1 (Q_{RC1}) and C80 (Q_{C80}) can be obtained from experimental measurement. The equations for energy balance are shown below:

$$Q_{RC1} = Q_1 + Q_{2\ from\ RC1} \quad (2)$$

$$Q_{C80} = Q_{2\ from\ C80} \quad (3)$$

It is worth noticing that Q_1, $Q_{2\ from\ RC1}$ and $Q_{2\ from\ C80}$ depends on the conversion extent of the reactant in different calorimeters and reaction enthalpy. Fortunately, the conversion extent of the reactant such as ML and MHP and yield of GVL can be determined by GC analysis, which can give us concentration of each compound in the liquid. By knowing the volume, the mole of each compound can be calculated. As there was no side reaction in these systems, the conversion of ML only leads to production of MHP and GVL, the equation of mass balance is shown as:

$$n_{ML,0} = n_{ML} + n_{MHP} + n_{GVL} - n_{GVL,0} \quad (4)$$

The heat release from step 1 (Q_1) depends on the first reaction enthalpy and mole conversion of substrate ML (eq. 5). The heat release of $Q_{2\ from\ RC1}$ depends on the second reaction enthalpy and mole yield of GVL (eq. 6). The heat release of $Q_{2\ from\ C80}$ depends on the second reaction enthalpy and mole conversion of the intermediate MHP (eq. 7).

$$Q_1 = (n_{ML,0} - n_{ML,final}) \times \Delta H_{R,1} \quad (5)$$

$$Q_{2\ from\ RC1} = (n_{GVL,final} - n_{GVL,0}) \times \Delta H_{R,2} \quad (6)$$

$$Q_{2\ from\ C80} = (n_{MHP,0} - n_{MHP,final}) \times \Delta H_{R,2} \quad (7)$$

Then, by integration of equations (2) and (3), we can finally obtain the equations for the calculation of reaction enthalpy:

$$\Delta H_{R,2} = \frac{Q_{C80}}{n_{MHP,0} - n_{MHP,final}} \quad (8)$$

$$\Delta H_{R,1} = \frac{Q_{RC1} - (n_{GVL,final} - n_{GVL,0}) \times \Delta H_{R,2}}{n_{ML,0} - n_{ML,final}} \quad (9)$$

As in C80 experiment, only step 2 occurs so the reaction enthalpy for the second step ($\Delta H_{R,2}$) can be calculated firstly. Then by applying the value of $\Delta H_{R,2}$, the reaction enthalpy for the first reaction ($\Delta H_{R,1}$) can be obtained. Finally, by using equation (1), the overall reaction enthalpy is gained easily. The methodology of reaction enthalpy determination by applying calorimeters RC1 and C80 and GC analysis is shown in Figure 4.4.

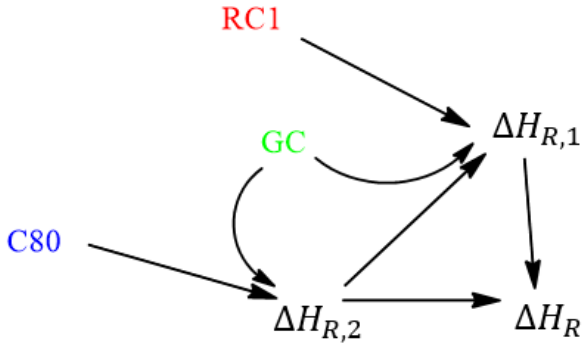

Figure 4.4. Scheme of reaction enthalpy determination by using RC1, C80 and GC analysis.

4.3 Experimental and analytical section

Reaction calorimeters has wide applications by allowing tracking the thermal behaviors reactions. The reaction calorimeter can be used for thermal safety analysis [153, 165-167], process development [168-172], reaction kinetics [173-175], physicochemical properties of reaction systems [161, 176], etc. due to the precise temperature control and heat flow measurement. And it becomes more efficient and precise by combining analytical methods to obtain thermodynamic parameters of the reaction [177]. Different reactions have been studied by reaction calorimeters, such as hydrogenation [178], nitration reactions [166, 168, 171].

As the production of GVL from ML includes two step reactions, the experiments were performed in two calorimetry reactors: Mettler Toledo RC1 and Tian-Calvet C80. The calorimeter RC1 was used to measure the total heat release from this reaction. The Tian-Calvet calorimeter C80 was applied to measure the heat of the second step ring-closure reaction. Combined with the GC analysis, the reaction enthalpies of these two steps are possible to be determined.

4.3.1 Chemicals

Methyl levulinate (wt% ≥ 98%) and γ-valerolactone (wt% ≥ 99%) were purchased from Sigma-Aldrich. Furfural (wt% ≥ 99%) were supplied by Acros Organics. Ru/C (5 wt % ruthenium on activated carbon powder, reduced and 50% water wet) were provided by the Alfa Aesar. H2 (>99.999%) was supplied by Linde. Acetone (Analytical grade) was bought from VWR. Sulfuric acid (wt% ≥ 98%) was obtained from Fisher chemicals. All the chemicals were used without further treatment.

4.3.2 RC1 experiments

Experiment on hydrogenation of ML to GVL catalyzed by Ru/C in GVL solvent was performed in RC1 which includes pressure system, temperature system and process control system (Figure 4.5). The picture of RC1 reactor used actually is shown in Figure 4.6. This reaction was performed under isothermal and isobaric conditions assured by process control system and jacket temperature control system. The aim of this experiment was to measure the total heat release from this reaction.

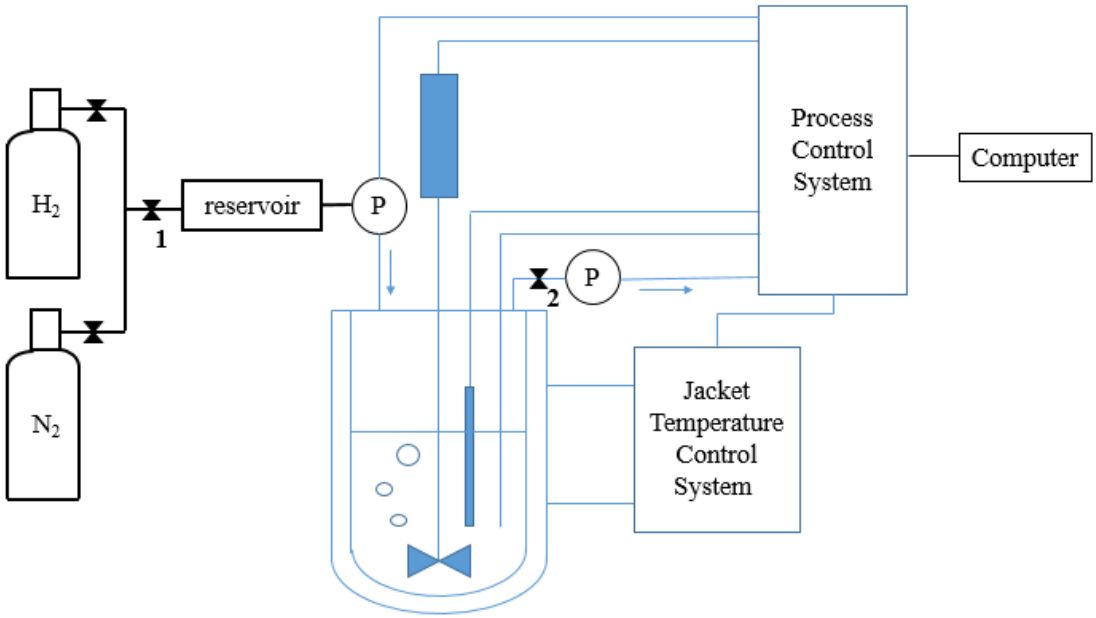

Figure 4.5. RC1 for hydrogenation of ML to GVL.

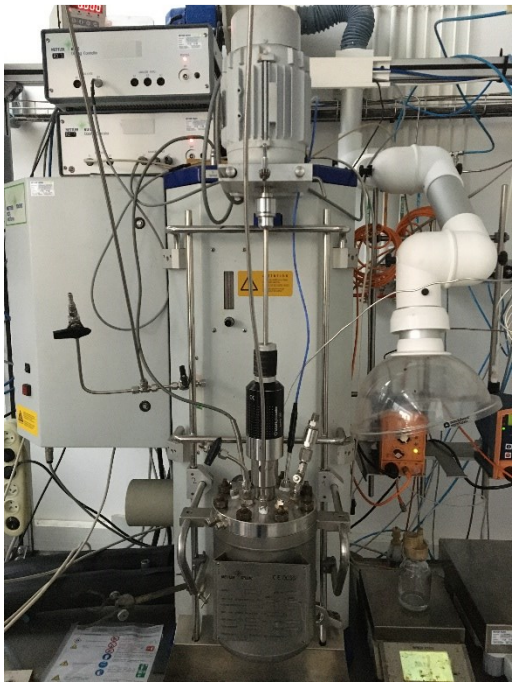

Figure 4.6. RC1 used in this study.

At first, ca. 5mol.L^{-1} ML solution (total mass 566.6g, volume 0.54L) was introduced to the reactor with 6.3g Ru/C catalyst. Then, the sealed reactor was purged with nitrogen for three times before increasing temperature in the reactor to 130°C. The stirring was stopped and valve 2 was closed when the reactor temperature reached 130 °C. After that,

valve 1 was open and ca. 35 bar of hydrogen was injected to the reactor. When reaching 35 bar in the reactor, valve 1 was closed and the pressure in reservoir is around 70 bar. In this way, the storage gas in the reservoir could make sure the pressure in the reactor is constant during the reaction by the automatic pressure control system. The stirring was restarted to 800rpm to start the reaction and the reaction was kept for 3.5h. The temperature in the liquid and jacket and heat flow of the system were recorded and measured. During the reaction time, no sampling was taken to avoid interfering the signals. After 3.5h, the experiment was stopped and cooled down by process control system.

The initial mixture sample was got before the liquid mixture was put into the reactor. The final mixture sample was obtained after cooling down the system and the rest mixture was filtered and stored in fridge for further C80 measurement. Both of these samples were filtered for further GC analysis.

4.3.3 C80 experiments

Experiment on ring-closure of MHP was performed in Tian-Calvet calorimeter C80 (Figure 4.7). The aim of this experiment was to determine the enthalpy of the second ring-closure reaction. The calorimeter C80 is a differential calorimeter which can be operated under isothermal condition. For this study, the experiment was kept at 60 ^{o}C to avoid extreme evaporation. It includes two Hastelloy cells inside the calorimeter: reference cell and measurement cell. The temperature and heat flow were recorded and measured during the experiment.

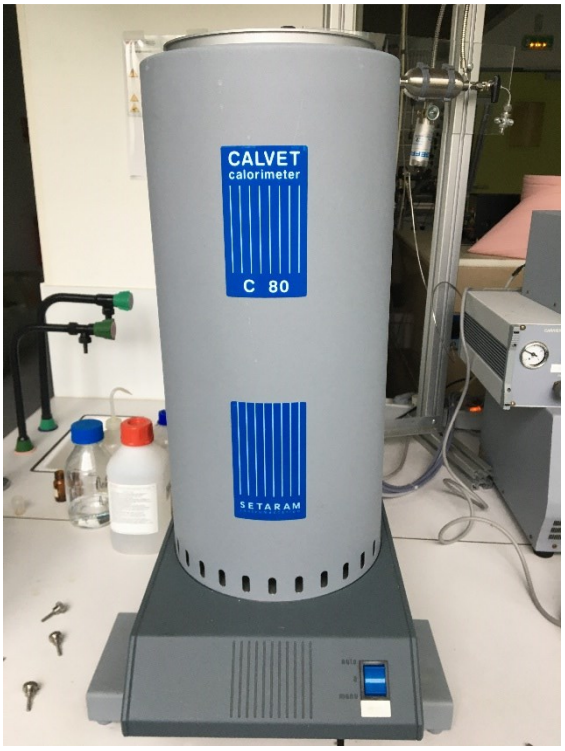

Figure 4.7. C80 used for this study.

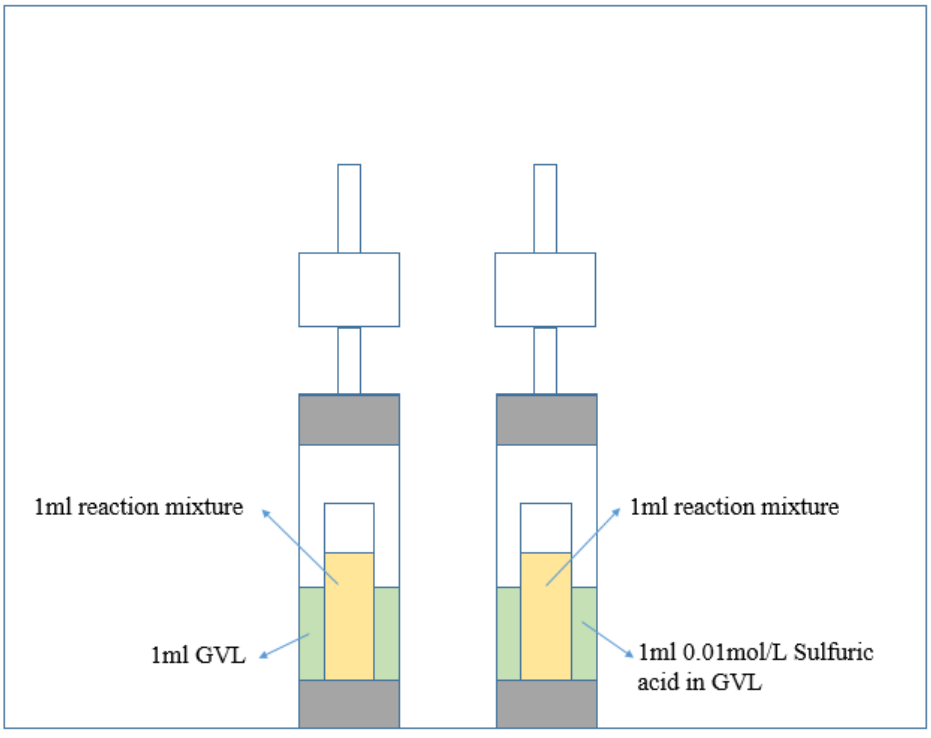

Figure 4.8. C80 for the ring closure reaction.

The cell contains two major parts: inside open tube and outside sealed container (Figure 4.8). For this study, in the inside tube of reference cell, 1ml of reaction mixture was put

in. And in the outside container of the reference cell, 1ml of pure GVL was injected in to avoid reaction and keep the similar heat capacity with the measurement cell. In the inside tube of measurement cell, 1ml of reaction mixture was also put in, while in the outside container of the measurement cell, 1ml 0.01mol.L^{-1} sulfuric acid in GVL solvent was injected. Because sulfuric acid is common used as catalyst for esterification reaction, for this study it was used for acceleration of the ring-closure reaction.

After injection of the liquids, the two cells were put inside the C80 calorimeter vertically and the temperature of this calorimeter was increased to 60ºC. When the temperature reached 60ºC and the recording curve was stable, the calorimeter started to rotate continuously. The upper of the calorimeter rotated to the bottom position (180º angle change) and the bottom of the calorimeter rotated to the upper position and then returned back for the next time rotating. When this rotating process started, the liquids in the inside tube and outside container were mixed and the reaction started. After 3h reaction, the rotating was stopped and the calorimeter was cooled down.

For the GC analysis, the initial sample was gotten from the mixture sample stored. The final samples including the sample from reference cell and the sample from measurement cell were obtained after the experiment.

4.3.4 Analytical section

The concentration of ML, intermediate MHP, GVL was quantified by GC-FID analysis. The method used for GC analysis was the same as shown in the analytical section in Chapter III.

4.4 Results and discussion

4.4.1 RC1 results

From Figure 4.9, the temperature variation of jacket (Tj) and inside reactor (Tr) demonstrated the exothermic behavior of this reaction and the jacket process control system was trying to keep the temperature constant at 130ºC. The heat flow for production of GVL from ML in RC1 was measured every 2 second (Figure 4.10). The time zero was set when the stirring was started. It is worth noticing that at the beginning

2000s, the heat flow increased sharply and then fell down, resulting in an extreme exothermic behavior. However, after 2000s, the heat flow turned be constant until the end of this experiment.

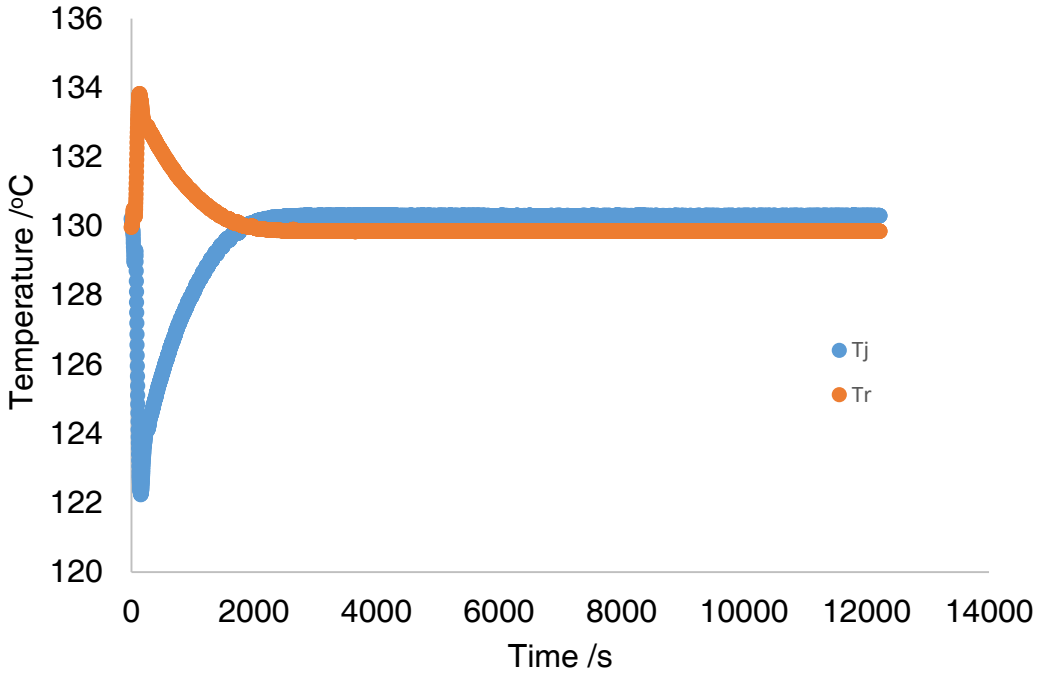

Figure 4.9. Temperature of Tj and Tr for hydrogenation of ML to GVL in RC1.

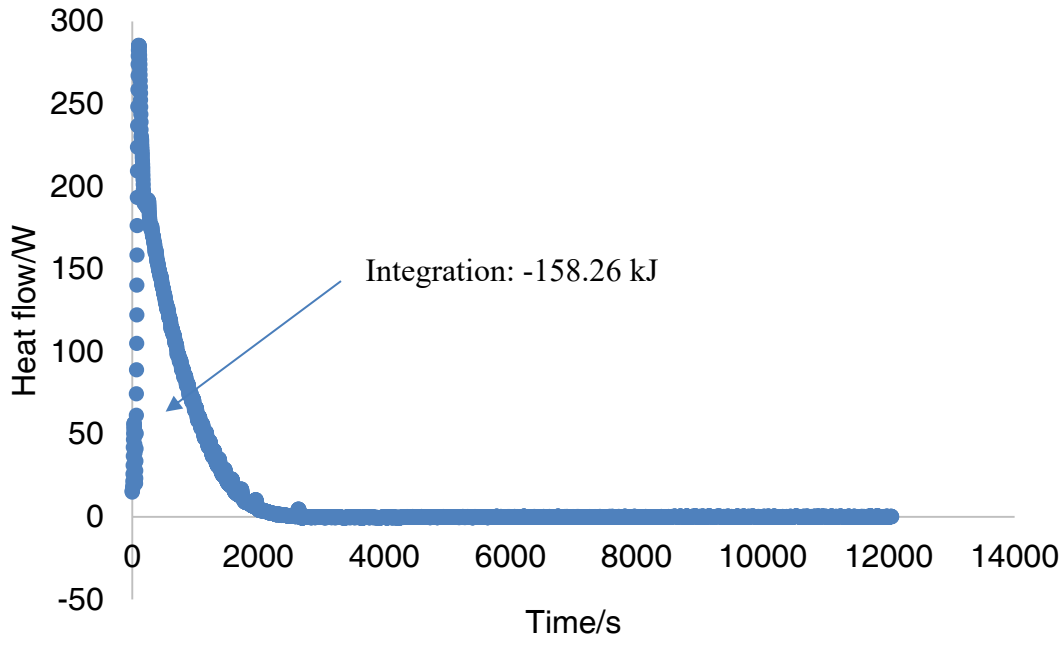

Figure 4.10. Heat flow for hydrogenation of ML to GVL in RC1.

By integrating the peak area from time 0 to the end of experiment, the total energy released (Q_{RC1}) from this reaction can be obtained from RC1 software and shown below:

$$Q_{RC1} = -158.26\ kJ$$

As energy released from reaction depends on the conversion extent of the chemicals, it is necessary to know the concentration of each compound in the liquid. The initial mixture before experiment and after experiment were analyzed by GC and the quantification results were shown in Table 4.1. It was found there was no side reaction by checking the mass balance of the reaction. The substrate ML was converted totally while at the end there was still huge amount of intermediate MHP exists. In the other words, the first step of reaction finished rapidly while the second step of reaction goes more slowly. By corresponding to the heat flow recording during a long period, it can be concluded that the overall reaction is an exothermic reaction step and the second step reaction ran moderately without significant heat flow change.

Table 4.1. GC analysis result for RC1 experiment.

Samples	Compounds	Concentration mol.L^{-1}
Initial	ML	5.15
	MHP	0
	GVL	3.90
Final	ML	0
	MHP	3.40
	GVL	5.16

4.4.2 C80 results

As the final mixture liquid from RC1 includes MHP, GVL, Ru/C catalyst and n-butanol, after filtration of this mixture, the liquid was further used for C80 measurement. 0.01 mol.L^{-1} sulfuric acid in GVL was used as the acid catalyst to accelerate the second step ring-closure reaction and the heat flow for the second step is shown in Figure 4.11. The endothermic phenomenon was observed in this measurement obviously with a significant peak. Furthermore, the reaction occurred rapidly with a sharp peak of heat flow by using low concentration sulfuric acid as the catalyst, which can be further

employed to optimize the overall process.

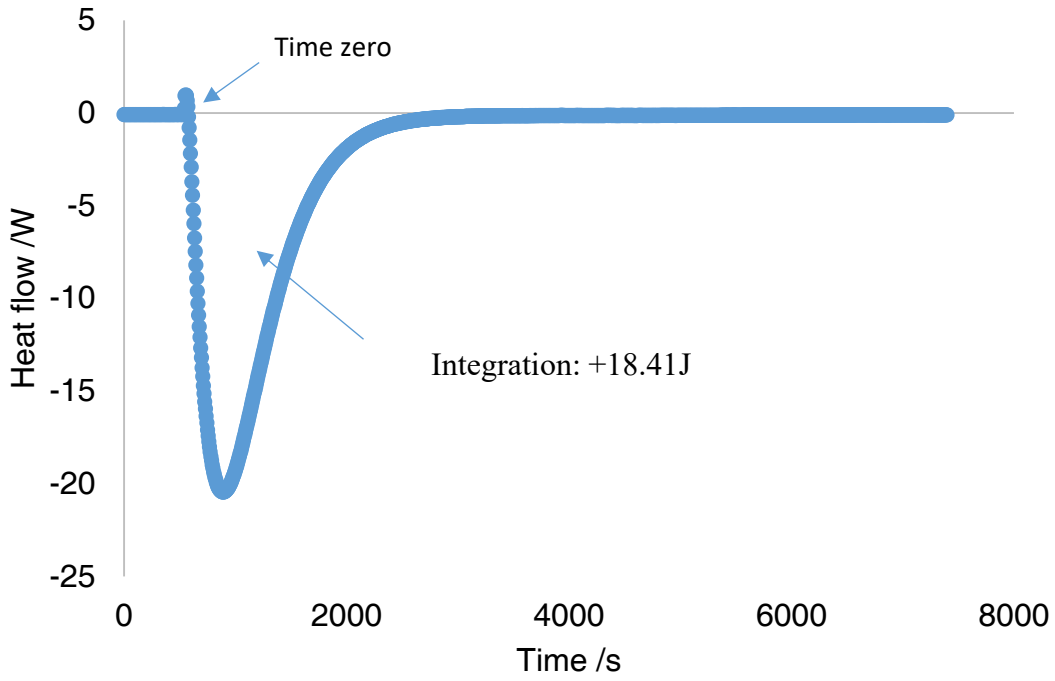

Figure 4.11. Heat flow for ring-closure reaction in C80.

By integration the peak of heat flow, the total energy absorbed by the reaction was:

$$Q_{C80} = +18.41 \text{ J}$$

As the energy absorbed by the reaction also depends on the conversion extent of the intermediate, it is necessary to get the concentration of each compound in the solution. The concentrations of compound in reference cell and measurement cell are shown in Table 4.2. Due to the differential calorimetry principal, the reference cell was used as background for this measurement and the analysis shown there was no reaction observed in the reference cell as the concentrations did not change. So the heat flow peak was due to ring-closure reaction using low concentration of sulfuric acid as the acid catalyst. The conversion of intermediate MHP was 75.8% after the experiment and it was found there was no side reaction.

Table 4.2. GC analysis result for C80 experiment.

Samples	Compounds	Concentration mol.L^{-1}
Reference cell	ML	0
	MHP	1.70
	GVL	7.80
Measurement cell	ML	0
	MHP	0.41
	GVL	9.00

4.4.3 Reaction enthalpy determination

Based on the measurement result from RC1 and C80, the reaction enthalpy for each step and overall reaction can be calculated by employing the method described in section 4.2. Depending on equation (3) and equation (8), the reaction enthalpy for the second ring-closure step can be calculated as:

$$\Delta H_{R,2} = \frac{18.41\ J}{1.70 \times 0.002\ mol - 0.41 \times 0.002\ mol} = +7.16\ kJ/mol$$

Then, by equation (9), the reaction enthalpy for the first step hydrogenation can be calculated as:

$$\Delta H_{R,1} = \frac{-158.26\ kJ - (5.16 \times 0.54 - 3.90 \times 0.54)\ mol \times 7.16\ kJ/mol}{5.15 \times 0.54\ mol - 0} = -58.66\ kJ/mol$$

Finally, by using equation (1), the reaction enthalpy for the overall reaction was:

$$\Delta H_R = -58.66\ kJ/mol + 7.16\ kJ/mol\ = -51.5\ kJ/mol$$

It is worthy noticing that the two steps have two different thermal behaviors as the first step for hydrogenation is exothermic reaction and the second step for ring-closure is endothermic reaction. Meanwhile, the heat released from the first step is much higher

than the energy absorbed by the second step, which causes huge heat release and it need be considered in the process safety design and optimization of the process. Reaction enthalpies for each step and overall reaction are summarized in the Table 4.3.

Table 4.3. Reaction enthalpies for each step and overall reaction.

Reaction enthalpy in GVL	Values kJ.mol^{-1}
$\Delta H_{R,1}$	-58.66
$\Delta H_{R,2}$	+7.16
$\Delta H_{R,for\ overall\ reaction}$	-51.50

4.5 Conclusion

In this chapter, experimental determination of reaction enthalpy for production of GVL from hydrogenation of ML was performed. As reaction enthalpy is an important thermodynamic property for process design and optimization, the reaction enthalpies for the overall reaction and two step reactions-hydrogenation and cyclization were determined by using calorimeters RC1 and Tian-Calvet C80 and GC analysis. An original method for this reaction enthalpy determination was proposed.

It was found that the overall reaction enthalpy was -51.5 kJ/mol, which indicated that the reaction for production of GVL from ML was exothermic and certain safety control should be involved for this process. Furthermore, the thermal behavior of each step was different with each other according to calorimetry measurement and calculation. The reaction enthalpy for the first hydrogenation step was -58.66 kJ/mol as an exothermic reaction and the reaction enthalpy for the second ring-closure step was 7.16 kJ/mol as an endothermic reaction. These reaction enthalpies can be employed for process optimization and design.

Further study will be expanded to other common levulinate esters such as ethyl levulinate and n-butyl levulinate and the comparison of thermal behavior between different substrates. Cost evaluation and process flow diagram design could also be involved depending on energy and mass balance of this system.

Conclusions and Perspectives

Based on the work of this thesis, thermal risk assessment, structure-reactivity and reaction enthalpy were studied for production of γ-valerolactone (GVL) from hydrogenation of levulinic acid (LA) and its esters including methyl levulinate (ML), ethyl levulinate (EL) and n-butyl levulinate (BL). Study by coupling of mass and energy balance for this reaction system has been performed for thermal risk assessment and reaction enthalpy determination. Structure-reactivity for this reaction has given a deeper sight into the relationships between reaction kinetics and structures. All of these three parts can be further used and guide the chemical process design and optimization for this reaction.

In the part of thermal risk assessment, hydrogenation reaction of LA to GVL catalyzed by Ru/C in water was studied. A kinetic model under near-adiabatic condition was built. Experiments at different operating conditions were performed in calorimeter ARSST (advanced reactive system screening tool). The kinetic constants were estimated by using the reaction temperature as an observable through a non-linear regression method. Good agreement between data of experiments and the model was obtained. Based on the model, two risk parameters ΔT_{ad} which characterize the severity of thermal runaway and TMR_{ad} which characterize the probability of thermal runaway were obtained by simulation and used for thermal risk assessment with aid of a risk matrix. Different operating conditions such as LA concentration, process temperature, catalyst loading and hydrogen pressure were examined. It is worth noticing that when the catalyst is within the loading range of 0.0014-0.014 $kg.L^{-1}$, LA within the concentration in range of 0.62-6.75 $mol.L^{-1}$, temperature in the range of 100-130°C and under 35 bar hydrogen pressure, the thermal risk is medium in the majority of cases and safety barriers should be included to prevent a thermal runaway. Elevating hydrogen pressure can also increase the thermal risk. Form this thermal risk assessment, safe operating conditions can be obtained for further optimization of the process for this reaction system.

For the study of structure-reactivity relationship for hydrogenation of LA and its esters to GVL, LA, ML, EL and BL were used as the substrates for this reaction catalyzed by Ru/C catalyst in GVL solvent. Experiments were performed under isothermal and

isobaric conditions by varying the conditions of reactant concentration, reaction temperature, hydrogen pressure and catalyst loading. By using GVL as the solvent, all of the substrates can be solubilized to avoid liquid-liquid reaction system and ease the downstream process. The mass transfer coefficient (k_L.a) for the transfer of hydrogen from the gas to the liquid phase was evaluated by taking into account the influence of process temperature, solvent viscosity and density. It was found that Henry's constant for hydrogen absorption in GVL follows van't Hoff law. This absorption was found to be endothermic meaning that temperature increase leads to increase the amount of absorbed hydrogen. A kinetic model by including mass transfer parameters was developed and by integrating with Taft equation, the steric and polar effects of substituents (H-, CH_3-, CH_3-CH_2-, CH_3-CH_2-CH_2-CH_2-) on the two-step reaction, hydrogenation step and ring-closure step, were investigated with kinetic study. For this reaction system, the steric effect was found to be negligible for both step reactions. Nevertheless, the polar effects were found to be important for the ring-closure ones. The rate of GVL production is faster by using LA because the electron withdrawing effect of the group H- increases the kinetics of reaction 2. The reaction 2 is slower for the other alkyl levulinates as alkyl groups are electron-donating groups. The overall reaction rate follows the order: $r_{GVL\ from\ LA} > r_{GVL\ from\ ML} > r_{GVL\ from\ EL} > r_{GVL\ from\ BL}$. By knowing Taft parameters, it is possible to predict the rate constants with other substrates.

Then, as reaction enthalpy is an important thermodynamic property for process design and optimization, experimental determination of reaction enthalpy from hydrogenation of ML catalyzed by Ru/C in GVL solvent was performed. An original method of determination of reaction enthalpy for this reaction was proposed. The reaction enthalpies for the overall reaction and two step reactions including hydrogenation and cyclization were determined by using calorimeters RC1 and Tian-Calvet C80. GC analysis was used to quantify the concentration of substrates, intermediates and GVL product. By calculation, it was found that the overall reaction enthalpy was -51.5 $kJ.mol^{-1}$ of GVL produced, which indicates that the overall reaction for production of GVL from ML is exothermic. Certain safety control operation should be designed for this process. The reaction enthalpy for the first hydrogenation step was calculated to be -58.66 $kJ.mol^{-1}$, and the reaction enthalpy for the second ring-closure step was calculated to be +7.16 $kJ.mol^{-1}$. Thermal behavior of these two steps are different and the exothermic step is much more pronounced than the endothermic step.

Perspectives of this doctoral thesis work could be focused on:

- Development of an intrinsic kinetic model taking into account internal and external mass transfer under adiabatic mode and the influence of the main inlet parameters such as catalyst particle size distribution and rotating speed on thermal risk.
- Test Taft equation on other alkyl substrates and have a better understanding on the evolution of Taft parameters with temperature.
- Enthalpy determination for other alkyl substrates, such as EL and BL and comparison of thermal risk for different substrates.
- Measurement of physicochemical properties of this reaction system for development of process flow diagram and cost-evaluation.
- Model descrimination for the kinetics of GVL production.

References

[1] F. Cherubini, The biorefinery concept: using biomass instead of oil for producing energy and chemicals, Energy Convers. Manage. 51(7) (2010) 1412-1421.

[2] R.D. Perlack, L.L. Wright, A.F. Turhollow, R.L. Graham, B.J. Stokes, D.C. Erbach, Biomass as feedstock for a bioenergy and bioproducts industry: the technical feasibility of a billion-ton annual supply, DTIC Document, 2005.

[3] S.K. Maity, Opportunities, recent trends and challenges of integrated biorefinery: Part I, Renewable Sustainable Energy Rev. 43 (2015) 1427-1445.

[4] BP company, BP energy outlook 2017.

[5] G.W. Huber, S. Iborra, A. Corma, Synthesis of transportation fuels from biomass: Chemistry, catalysts and engineering, Chem. Rev. 106(9) (2006) 4044-4098.

[6] A. Corma, S. Iborra, A. Velty, Chemical routes for the transformation of biomass into chemicals, Chem. Rev. 107(6) (2007) 2411-2502.

[7] P. Gallezot, Catalytic Conversion of Biomass: Challenges and Issues, ChemSus-Chem 1(8-9) (2008) 734-737.

[8] B. Kamm, P. Gruber, M. Kamm, Biorefineries-Industrial Processes and Products; Status Quo and Futute Directions, Wiley Online Library, 2006.

[9] L. Petrus, M.A. Noordermeer, Biomass to biofuels, a chemical perspective, Green Chem. 8(10) (2006) 861-867.

[10] S. Liu, Z. Zhang, G.M. Scott, The biorefinery: Sustainably renewable route to commodity chemicals, energy, and materials: Selected papers from the Second International Biorefinery Conference (IBC 2009) Syracuse, New York, October 6-9, 2009, Biotechnol. Adv. 28(5) (2010) 541-542.

[11] A.J. Ragauskas, C.K. Williams, B.H. Davison, G. Britovsek, J. Cairney, C.A. Eckert, W.J. Frederick, J.P. Hallett, D.J. Leak, C.L. Liotta, The path forward for biofuels and biomaterials, science 311(5760) (2006) 484-489.

[12] G. Taylor, Biofuels and the biorefinery concept, Energy Policy 36(12) (2008) 4406-4409.

[13] M. FitzPatrick, P. Champagne, M.F. Cunningham, R.A. Whitney, A biorefinery processing perspective: Treatment of lignocellulosic materials for the production of value-added products, Bioresour. Technol. 101(23) (2010) 8915-8922.

[14] D.M. Alonso, S.H. Hakim, S. Zhou, W. Won, O. Hosseinaei, J. Tao, V. Garcia-

Negron, A.H. Motagamwala, M.A. Mellmer, K. Huang, Increasing the revenue from lignocellulosic biomass: Maximizing feedstock utilization, Sci. Adv. 3(5) (2017) e1603301.
[15] F.H. Isikgor, C.R. Becer, Lignocellulosic biomass: a sustainable platform for the production of bio-based chemicals and polymers, Polym. Chem. 6(25) (2015) 4497-4559.
[16] D.W. Rackemann, W.O.S. Doherty, The conversion of lignocellulosics to levulinic acid, Biofuels Bioproducts & Biorefining-Biofpr 5(2) (2011) 198-214.
[17] S. Fernando, S. Adhikari, C. Chandrapal, N. Murali, Biorefineries: current status, challenges, and future direction, Energy & Fuels 20(4) (2006) 1727-1737.
[18] E. de Jong, G. Jungmeier, Biorefinery concepts in comparison to petrochemical refineries, Industrial Biorefineries & White Biotechnology (2015) 3-33.
[19] X. Tang, X.H. Zeng, Z. Li, L. Hu, Y. Sun, S.J. Liu, T.Z. Lei, L. Lin, Production of gamma-valerolactone from lignocellulosic biomass for sustainable fuels and chemicals supply, Renewable Sustainable Energy Rev. 40 (2014) 608-620.
[20] E.I. Gürbüz, S.G. Wettstein, J.A. Dumesic, Conversion of hemicellulose to furfural and levulinic acid using biphasic reactors with alkylphenol solvents, ChemSusChem 5(2) (2012) 383-387.
[21] D. Zhao, P. Prinsen, Y. Wang, W. Ouyang, F. Delbecq, C. Len, R. Luque, Continuous flow alcoholysis of furfuryl alcohol to alkyl levulinates using zeolites, ACS Sustainable Chem. Eng. 6(5) (2018) 6901-6909.
[22] J.J. Bozell, G.R. Petersen, Technology development for the production of biobased products from biorefinery carbohydrates-the US Department of Energy's "Top 10" revisited, Green Chem. 12(4) (2010) 539-554.
[23] L. Yan, Q. Yao, Y. Fu, Conversion of levulinic acid and alkyl levulinates into biofuels and high-value chemicals, Green Chem. 19(23) (2017) 5527-5547.
[24] S. Dutta, K. Iris, D.C. Tsang, Y.H. Ng, Y.S. Ok, J. Sherwood, J.H. Clark, Green synthesis of gamma-valerolactone (GVL) through hydrogenation of biomass-derived levulinic acid using non-noble metal catalysts: A critical review, Chem. Eng. J. 372 (2019) 992-1006.
[25] Z. Zhang, Synthesis of γ-Valerolactone from Carbohydrates and its Applications, ChemSusChem 9(2) (2016) 156-171.
[26] A. Osatiashtiani, A.F. Lee, K. Wilson, Recent advances in the production of γ-valerolactone from biomass-derived feedstock by heterogeneous catalytic transfer

hydrogenation, J. Chem. Technol. Biotechnol. 92 (2017) 1125-1135.
[27] C. Moreno-Marrodan, F. Liguori, P. Barbaro, Sustainable processes for the catalytic synthesis of safer chemical substitutes of N-methyl-2-pyrrolidone, Molecular Catalysis 466 (2019) 60-69.
[28] A. Démolis, N. Essayem, F. Rataboul, Synthesis and applications of alkyl levulinates, ACS Sustainable Chem. Eng. 2(6) (2014) 1338-1352.
[29] D. Fernandes, A. Rocha, E. Mai, C.J. Mota, V.T. Da Silva, Levulinic acid esterification with ethanol to ethyl levulinate production over solid acid catalysts, Appl. Catal., A 425 (2012) 199-204.
[30] K.C. Maheria, J. Kozinski, A. Dalai, Esterification of levulinic acid to n-butyl levulinate over various acidic zeolites, Catal. Lett. 143(11) (2013) 1220-1225.
[31] J. Yang, G. Li, L. Zhang, S. Zhang, Efficient production of n-butyl levulinate fuel additive from levulinic acid using amorphous carbon enriched with oxygenated groups, Catalysts 8(1) (2018) 14.
[32] S. Zhou, X. Liu, J. Lai, M. Zheng, W. Liu, Q. Xu, D. Yin, Covalently linked organo-sulfonic acid modified titanate nanotube hybrid nanostructures for the catalytic esterification of levulinic acid with n-butyl alcohol, Chem. Eng. J. 361 (2019) 571-577.
[33] K.Y. Nandiwale, V.V. Bokade, Environmentally benign catalytic process for esterification of renewable levulinic acid to various alkyl levulinates biodiesel, Environ. Prog. Sustainable Energy 34(3) (2015) 795-801.
[34] S. Dharne, V. Bokade, Esterification of levulinic acid to n-butyl levulinate over heteropolyacid supported on acid-treated clay, J. Nat. Gas Chem. 20(1) (2011) 18-24.
[35] M.M. Zainol, N.A.S. Amin, M. Asmadi, Kinetics and thermodynamic analysis of levulinic acid esterification using lignin-furfural carbon cryogel catalyst, Renewable Energy 130 (2019) 547-557.
[36] E. Christensen, A. Williams, S. Paul, S. Burton, R.L. McCormick, Properties and performance of levulinate esters as diesel blend components, Energy fuels 25(11) (2011) 5422-5428.
[37] J.J. Bozell, L. Moens, D.C. Elliott, Y. Wang, G.G. Neuenscwander, S.W. Fitzpatrick, R.J. Bilski, J.L. Jarnefeld, Production of levulinic acid and use as a platform chemical for derived products, Resour. Conserv. Recycl. 28(3-4) (2000) 227-239.
[38] A. Mukherjee, M.-J. Dumont, V. Raghavan, Sustainable production of hydroxymethylfurfural and levulinic acid: Challenges and opportunities, Biomass Bioenergy 72 (2015) 143-183.

[39] K.C. Badgujar, V.C. Badgujar, B.M. Bhanage, A review on catalytic synthesis of energy rich fuel additive levulinate compounds from biomass derived levulinic acid, Fuel Process. Technol. 197 (2020) 106213.
[40] J. Sadhukhan, K.S. Ng, E. Martinez-Hernandez, Novel integrated mechanical biological chemical treatment (MBCT) systems for the production of levulinic acid from fraction of municipal solid waste: A comprehensive techno-economic analysis, Bioresour. Technol. 215 (2016) 131-143.
[41] Q. Fang, M.A. Hanna, Experimental studies for levulinic acid production from whole kernel grain sorghum, Bioresour. Technol. 81(3) (2002) 187-192.
[42] A.M.R. Galletti, C. Antonetti, V. De Luise, D. Licursi, N. Nassi, Levulinic acid production from waste biomass, BioResources 7(2) (2012) 1824-1835.
[43] R. Le Van Mao, Q. Zhao, G. Dima, D. Petraccone, New process for the acid-catalyzed conversion of cellulosic biomass (AC3B) into alkyl levulinates and other esters using a unique one-pot system of reaction and product extraction, Catal. Lett. 141(2) (2011) 271-276.
[44] S. Van de Vyver, J. Thomas, J. Geboers, S. Keyzer, M. Smet, W. Dehaen, P.A. Jacobs, B.F. Sels, Catalytic production of levulinic acid from cellulose and other biomass-derived carbohydrates with sulfonated hyperbranched poly (arylene oxindole) s, Energy Environ. Sci. 4(9) (2011) 3601-3610.
[45] D.J. Hayes, S. Fitzpatrick, M.H. Hayes, J.R. Ross, The biofine process-production of levulinic acid, furfural, and formic acid from lignocellulosic feedstocks, Biorefineries-Industrial Processes and Product 1 (2006) 139-164.
[46] C.-H. Kuo, A.S. Poyraz, L. Jin, Y. Meng, L. Pahalagedara, S.-Y. Chen, D.A. Kriz, C. Guild, A. Gudz, S.L. Suib, Heterogeneous acidic TiO_2 nanoparticles for efficient conversion of biomass derived carbohydrates, Green Chem. 16(2) (2014) 785-791.
[47] X. Hu, S. Wang, R.J. Westerhof, L. Wu, Y. Song, D. Dong, C.-Z. Li, Acid-catalyzed conversion of C6 sugar monomer/oligomers to levulinic acid in water, tetrahydrofuran and toluene: Importance of the solvent polarity, Fuel 141 (2015) 56-63.
[48] B.C. Redmon, Process for the production of levulinic acid, Google Patents, 1956.
[49] R.A. Schraufnagel, H.F. Rase, Levulinic acid from sucrose using acidic ion-exchange resins, Ind. Eng. Chem. Prod. Res. Dev. 14(1) (1975) 40-44.
[50] X. Qi, M. Watanabe, T.M. Aida, R.L. Smith Jr, Efficient one-pot production of 5-hydroxymethylfurfural from inulin in ionic liquids, Green Chem. 12(10) (2010) 1855-1860.

[51] Y. Zuo, Y. Zhang, Y. Fu, Catalytic Conversion of Cellulose into Levulinic Acid by a Sulfonated Chloromethyl Polystyrene Solid Acid Catalyst, ChemCatChem 6(3) (2014) 753-757.
[52] D.M. Alonso, J.M.R. Gallo, M.A. Mellmer, S.G. Wettstein, J.A. Dumesic, Direct conversion of cellulose to levulinic acid and gamma-valerolactone using solid acid catalysts, Catal. Sci. Technol. 3(4) (2013) 927-931.
[53] P.P. Upare, J.-W. Yoon, M.Y. Kim, H.-Y. Kang, D.W. Hwang, Y.K. Hwang, H.H. Kung, J.-S. Chang, Chemical conversion of biomass-derived hexose sugars to levulinic acid over sulfonic acid-functionalized graphene oxide catalysts, Green Chem. 15(10) (2013) 2935-2943.
[54] L.C. Peng, L. Lin, J.H. Zhang, J.P. Zhuang, B.X. Zhang, Y. Gong, Catalytic Conversion of Cellulose to Levulinic Acid by Metal Chlorides, Molecules 15(8) (2010) 5258-5272.
[55] V. Choudhary, S.H. Mushrif, C. Ho, A. Anderko, V. Nikolakis, N.S. Marinkovic, A.I. Frenkel, S.I. Sandler, D.G. Vlachos, Insights into the interplay of Lewis and Brønsted acid catalysts in glucose and fructose conversion to 5-(hydroxymethyl) furfural and levulinic acid in aqueous media, J. Am. Chem. Soc. 135(10) (2013) 3997-4006.
[56] M. Brasholz, K. Von Kaenel, C.H. Hornung, S. Saubern, J. Tsanaktsidis, Highly efficient dehydration of carbohydrates to 5-(chloromethyl) furfural (CMF), 5-(hydroxymethyl) furfural (HMF) and levulinic acid by biphasic continuous flow processing, Green Chem. 13(5) (2011) 1114-1117.
[57] X. Hu, C.Z. Li, Levulinic esters from the acid-catalysed reactions of sugars and alcohols as part of a bio-refinery, Green Chem. 13(7) (2011) 1676-1679.
[58] X. Hu, Y. Song, L. Wu, M. Gholizadeh, C.-Z. Li, One-pot synthesis of levulinic acid/ester from C5 carbohydrates in a methanol medium, ACS Sustainable Chem. Eng. 1(12) (2013) 1593-1599.
[59] M. Mascal, E.B. Nikitin, Comment on processes for the direct conversion of cellulose or cellulosic biomass into levulinate esters, ChemSusChem 3(12) (2010) 1349-1351.
[60] R. Liu, J. Chen, X. Huang, L. Chen, L. Ma, X. Li, Conversion of fructose into 5-hydroxymethylfurfural and alkyl levulinates catalyzed by sulfonic acid-functionalized carbon materials, Green Chem. 15(10) (2013) 2895-2903.
[61] Y. Hirose, T. Kinoshita, T. Masawa, M. Otsuka, Manufacture of levulinic acid,

Google Patents, 1973.
[62] L. Peng, R. Tao, Y. Wu, Catalytic upgrading of biomass-derived furfuryl alcohol to butyl levulinate biofuel over common metal salts, Catalysts 6(9) (2016) 143-155.
[63] L. Peng, X. Gao, K. Chen, Catalytic upgrading of renewable furfuryl alcohol to alkyl levulinates using $AlCl_3$ as a facile, efficient, and reusable catalyst, Fuel 160 (2015) 123-131.
[64] J.P. Lange, W.D. van de Graaf, R.J. Haan, Conversion of furfuryl alcohol into ethyl levulinate using solid acid catalysts, ChemSusChem 2(5) (2009) 437-441.
[65] S.S. Enumula, K.S. Koppadi, V.R.B. Gurram, D.R. Burri, S.R.R. Kamaraju, Conversion of furfuryl alcohol to alkyl levulinate fuel additives over Al_2O_3/SBA-15 catalyst, Sustainable Energy Fuels 1(3) (2017) 644-651.
[66] P. Neves, S. Lima, M. Pillinger, S.M. Rocha, J. Rocha, A.A. Valente, Conversion of furfuryl alcohol to ethyl levulinate using porous aluminosilicate acid catalysts, Catal. Today 218 (2013) 76-84.
[67] G. Wang, Z. Zhang, L. Song, Efficient and selective alcoholysis of furfuryl alcohol to alkyl levulinates catalyzed by double SO_3H-functionalized ionic liquids, Green Chem. 16(3) (2014) 1436-1443.
[68] D. Ren, J. Fu, L. Li, Y. Liu, F. Jin, Z. Huo, Efficient conversion of biomass-derived furfuryl alcohol to levulinate esters over commercial α-Fe_2O_3, RSC Adv. 6(26) (2016) 22174-22178.
[69] G.M.G. Maldonado, R.S. Assary, J. Dumesic, L.A. Curtiss, Experimental and theoretical studies of the acid-catalyzed conversion of furfuryl alcohol to levulinic acid in aqueous solution, Energy Environ. Sci. 5(5) (2012) 6981-6989.
[70] M. Hronec, K. Fulajtárová, T. Soták, Kinetics of high temperature conversion of furfuryl alcohol in water, J. Ind. Eng. Chem. 20(2) (2014) 650-655.
[71] H. Van Dam, A. Kieboom, H. Van Bekkum, The conversion of fructose and glucose in acidic media: formation of hydroxymethylfurfural, Starch, 38(3) (1986) 95-101.
[72] J.Q. Bond, D.M. Alonso, D. Wang, R.M. West, J.A. Dumesic, Integrated Catalytic Conversion of gamma-Valerolactone to Liquid Alkenes for Transportation Fuels, Science 327(5969) (2010) 1110-1114.
[73] J.C. Serrano-Ruiz, D. Wang, J.A. Dumesic, Catalytic upgrading of levulinic acid to 5-nonanone, Green Chem. 12(4) (2010) 574-577.
[74] J.M. Tukacs, B. Fridrich, G. Dibó, E. Székely, L.T. Mika, Direct asymmetric reduction of levulinic acid to gamma-valerolactone: synthesis of a chiral platform

molecule, Green Chem. 17(12) (2015) 5189-5195.
[75] I.T. Horváth, H. Mehdi, V. Fábos, L. Boda, L.T. Mika, γ-Valerolactone-a sustainable liquid for energy and carbon-based chemicals, Green Chem. 10(2) (2008) 238-242.
[76] W.R. Wright, R. Palkovits, Development of heterogeneous catalysts for the conversion of levulinic acid to γ-valerolactone, ChemSusChem 5(9) (2012) 1657-1667.
[77] U. Omoruyi, S. Page, J. Hallett, P.W. Miller, Homogeneous Catalyzed Reactions of Levulinic Acid: To γ-valerolactone and Beyond, ChemSusChem 9(16) (2016) 2037-2047.
[78] L. Qi, I.n.T. Horváth, Catalytic Conversion of Fructose to γ-Valerolactone in γ-Valerolactone, ACS Catal. 2(11) (2012) 2247-2249.
[79] C. Sener, A.H. Motagamwala, D.M. Alonso, J.A. Dumesic, Enhanced Furfural Yields from Xylose Dehydration in the γ-Valerolactone/Water Solvent System at Elevated Temperatures, ChemSusChem 11(14) (2018) 2321-2331.
[80] S.G. Wettstein, D.M. Alonso, Y. Chong, J.A. Dumesic, Production of levulinic acid and gamma-valerolactone (GVL) from cellulose using GVL as a solvent in biphasic systems, Energy Environ. Sci. 5(8) (2012) 8199-8203.
[81] M.A. Mellmer, D.M. Alonso, J.S. Luterbacher, J.M.R. Gallo, J.A. Dumesic, Effects of γ-valerolactone in hydrolysis of lignocellulosic biomass to monosaccharides, Green Chem. 16(11) (2014) 4659-4662.
[82] Y. Rodenas, R. Mariscal, J. Fierro, D.M. Alonso, J. Dumesic, M.L. Granados, Improving the production of maleic acid from biomass: TS-1 catalysed aqueous phase oxidation of furfural in the presence of γ-valerolactone, Green Chem. 20(12) (2018) 2845-2856.
[83] J.S. Luterbacher, J.M. Rand, D.M. Alonso, J. Han, J.T. Youngquist, C.T. Maravelias, B.F. Pfleger, J.A. Dumesic, Nonenzymatic sugar production from biomass using biomass-derived γ-valerolactone, Science 343(6168) (2014) 277-280.
[84] D.M. Alonso, S.G. Wettstein, M.A. Mellmer, E.I. Gurbuz, J.A. Dumesic, Integrated conversion of hemicellulose and cellulose from lignocellulosic biomass, Energy Environ. Sci. 6(1) (2013) 76-80.
[85] D.M. Alonso, S.G. Wettstein, J.A. Dumesic, Gamma-valerolactone, a sustainable platform molecule derived from lignocellulosic biomass, Green Chem. 15(3) (2013) 584-595.
[86] E. Ahmad, M.I. Alam, K. Pant, M.A. Haider, Catalytic and mechanistic insights

into the production of ethyl levulinate from biorenewable feedstocks, Green Chem. 18(18) (2016) 4804-4823.
[87] C. Fellay, P.J. Dyson, G. Laurenczy, A Viable Hydrogen-Storage System Based On Selective Formic Acid Decomposition with a Ruthenium Catalyst, Angew. Chem. Int. Ed. 120 (21) 4030-4032.
[88] H. Mehdi, V. Fabos, R. Tuba, A. Bodor, L.T. Mika, I.T. Horvath, Integration of homogeneous and heterogeneous catalytic processes for a multi-step conversion of biomass: From sucrose to levulinic acid, gamma-valerolactone, 1,4-pentanediol, 2-methyl-tetrahydrofuran, and alkanes, Top. Catal. 48(1-4) (2008) 49-54.
[89] L. Deng, J. Li, D.M. Lai, Y. Fu, Q.X. Guo, Catalytic conversion of biomass-derived carbohydrates into γ-valerolactone without using an external H_2 supply, Angew. Chem. Int. Ed. 48(35) (2009) 6529-6532.
[90] H. Heeres, R. Handana, D. Chunai, C.B. Rasrendra, B. Girisuta, H.J. Heeres, Combined dehydration/(transfer)-hydrogenation of C6-sugars (D-glucose and D-fructose) to γ-valerolactone using ruthenium catalysts, Green Chem. 11(8) (2009) 1247-1255.
[91] L. Deng, Y. Zhao, J. Li, Y. Fu, B. Liao, Q.X. Guo, Conversion of Levulinic Acid and Formic Acid into γ-Valerolactone over Heterogeneous Catalysts, ChemSusChem 3(10) (2010) 1172-1175.
[92] J. Yuan, S.-S. Li, L. Yu, Y.-M. Liu, Y. Cao, H.-Y. He, K.-N. Fan, Copper-based catalysts for the efficient conversion of carbohydrate biomass into γ-valerolactone in the absence of externally added hydrogen, Energy Environ. Sci. 6(11) (2013) 3308-3313.
[93] C. Ortiz-Cervantes, J.J. García, Hydrogenation of levulinic acid to γ-valerolactone using ruthenium nanoparticles, Inorg. Chim. Acta 397 (2013) 124-128.
[94] P.A. Son, S. Nishimura, K. Ebitani, Production of γ-valerolactone from biomass-derived compounds using formic acid as a hydrogen source over supported metal catalysts in water solvent, RSC Adv. 4(21) (2014) 10525-10530.
[95] A.M. Ruppert, M. Jędrzejczyk, O. Sneka-Płatek, N. Keller, A.S. Dumon, C. Michel, P. Sautet, J. Grams, Ru catalysts for levulinic acid hydrogenation with formic acid as a hydrogen source, Green Chem. 18(7) (2016) 2014-2028.
[96] A.M. Hengne, A.V. Malawadkar, N.S. Biradar, C.V. Rode, Surface synergism of an Ag-Ni/ZrO_2 nanocomposite for the catalytic transfer hydrogenation of bio-derived platform molecules, RSC Adv. 4(19) (2014) 9730-9736.

[97] X.L. Du, L. He, S. Zhao, Y.M. Liu, Y. Cao, H.Y. He, K.N. Fan, Hydrogen-Independent Reductive Transformation of Carbohydrate Biomass into γ-Valerolactone and Pyrrolidone Derivatives with Supported Gold Catalysts, Angew. Chem. Int. Ed. 123(34) (2011) 7961-7965.
[98] V. Fabos, L.T. Mika, I.T. Horvath, Selective Conversion of Levulinic and Formic Acids to gamma-Valerolactone with the Shvo Catalyst, Organometallics 33(1) (2014) 181-187.
[99] T. Miyazawa, S. Koso, K. Kunimori, K. Tomishige, Glycerol hydrogenolysis to 1, 2-propanediol catalyzed by a heat-resistant ion-exchange resin combined with Ru/C, Appl. Catal., A 329 (2007) 30-35.
[100] M. Osada, N. Hiyoshi, O. Sato, K. Arai, M. Shirai, Subcritical water regeneration of supported ruthenium catalyst poisoned by sulfur, Energy Fuels 22(2) (2008) 845-849.
[101] M. Chia, J.A. Dumesic, Liquid-phase catalytic transfer hydrogenation and cyclization of levulinic acid and its esters to gamma-valerolactone over metal oxide catalysts, Chem. Commun. 47(44) (2011) 12233-12235.
[102] X. Tang, L. Hu, Y. Sun, G. Zhao, W. Hao, L. Lin, Conversion of biomass-derived ethyl levulinate into γ-valerolactone via hydrogen transfer from supercritical ethanol over a ZrO_2 catalyst, RSC Adv. 3(26) (2013) 10277-10284.
[103] J. He, H. Li, Y.-M. Lu, Y.-X. Liu, Z.-B. Wu, D.-Y. Hu, S. Yang, Cascade catalytic transfer hydrogenation-cyclization of ethyl levulinate to γ-valerolactone with Al-Zr mixed oxides, Appl. Catal., A 510 (2016) 11-19.
[104] J. Song, L. Wu, B. Zhou, H. Zhou, H. Fan, Y. Yang, Q. Meng, B. Han, A new porous Zr-containing catalyst with a phenate group: an efficient catalyst for the catalytic transfer hydrogenation of ethyl levulinate to γ-valerolactone, Green Chem. 17(3) (2015) 1626-1632.
[105] X. Tang, X. Zeng, Z. Li, W. Li, Y. Jiang, L. Hu, S. Liu, Y. Sun, L. Lin, In Situ Generated Catalyst System to Convert Biomass-Derived Levulinic Acid to γ-Valerolactone, ChemCatChem 7(8) (2015) 1372-1379.
[106] J. Song, B. Zhou, H. Zhou, L. Wu, Q. Meng, Z. Liu, B. Han, Porous zirconium-phytic acid hybrid: a highly efficient catalyst for Meerwein-Ponndorf-Verley reductions, Angew. Chem. Int. Ed. 54(32) (2015) 9399-9403.
[107] Y. Kuwahara, W. Kaburagi, Y. Osada, T. Fujitani, H. Yamashita, Catalytic transfer hydrogenation of biomass-derived levulinic acid and its esters to γ-valerolactone over ZrO_2 catalyst supported on SBA-15 silica, Catal. Today 281 (2017) 418-428.

[108] S.S. Enumula, V.R.B. Gurram, M. Kondeboina, D.R. Burri, S.R.R. Kamaraju, ZrO_2/SBA-15 as an efficient catalyst for the production of γ-valerolactone from biomass-derived levulinic acid in the vapour phase at atmospheric pressure, RSC Adv. 6(24) (2016) 20230-20239.
[109] H. Li, Z. Fang, S. Yang, Direct conversion of sugars and ethyl levulinate into γ-valerolactone with superparamagnetic acid-base bifunctional $ZrFeO_x$ nanocatalysts, ACS Sustainable Chem. Eng. 4(1) (2015) 236-246.
[110] H. Li, Z. Fang, S. Yang, Direct Catalytic Transformation of Biomass Derivatives into Biofuel Component γ-Valerolactone with Magnetic Nickel-Zirconium Nano-particles, ChemPlusChem 81(1) (2016) 135-142.
[111] D. Xianlong, L. Yongmei, W. Jianqiang, C. Yong, F. Kangnian, Catalytic conversion of biomass-derived levulinic acid into γ-valerolactone using iridium nanoparticles supported on carbon nanotubes, Chin. J. Catal. 34(5) (2013) 993-1001.
[112] L.E. Manzer, Catalytic synthesis of α-methylene-γ-valerolactone: a biomass-derived acrylic monomer, Appl. Catal., A 272(1) (2004) 249-256.
[113] M. Sudhakar, M.L. Kantam, V.S. Jaya, R. Kishore, K. Ramanujachary, A. Venugopal, Hydroxyapatite as a novel support for Ru in the hydrogenation of levulinic acid to γ-valerolactone, Catal. Commun. 50 (2014) 101-104.
[114] W. Luo, U. Deka, A.M. Beale, E.R. van Eck, P.C. Bruijnincx, B.M. Weckhuysen, Ruthenium-catalyzed hydrogenation of levulinic acid: Influence of the support and solvent on catalyst selectivity and stability, J. Catal. 301 (2013) 175-186.
[115] A.M. Hengne, C.V. Rode, Cu-ZrO_2 nanocomposite catalyst for selective hydrogenation of levulinic acid and its ester to γ-valerolactone, Green Chem. 14(4) (2012) 1064-1072.
[116] J.Y. Park, M.A. Kim, S.J. Lee, J. Jung, H.M. Jang, P.P. Upare, Y.K. Hwang, J.-S. Chang, J.K. Park, Preparation and characterization of carbon-encapsulated iron nanoparticles and their catalytic activity in the hydrogenation of levulinic acid, J. Mater. Sci. 50(1) (2015) 334-343.
[117] K.-i. Shimizu, S. Kanno, K. Kon, Hydrogenation of levulinic acid to γ-valerolactone by Ni and MoO_x co-loaded carbon catalysts, Green Chem. 16(8) (2014) 3899-3903.
[118] M.L. Testa, L. Corbel-Demailly, V. La Parola, A.M. Venezia, C. Pinel, Effect of Au on Pd supported over HMS and Ti doped HMS as catalysts for the hydrogenation of levulinic acid to γ-valerolactone, Catal. Today 257 (2015) 291-296.

[119] M.G. Al-Shaal, W.R. Wright, R. Palkovits, Exploring the ruthenium catalysed synthesis of γ-valerolactone in alcohols and utilisation of mild solvent-free reaction conditions, Green Chem. 14(5) (2012) 1260-1263.
[120] A. Piskun, H. Van de Bovenkamp, C. Rasrendra, J. Winkelman, H. Heeres, Kinetic modeling of levulinic acid hydrogenation to γ-valerolactone in water using a carbon supported Ru catalyst, Appl. Catal., A 525 (2016) 158-167.
[121] L. Negahdar, M.G. Al-Shaal, F.J. Holzhäuser, R. Palkovits, Kinetic analysis of the catalytic hydrogenation of alkyl levulinates to γ-valerolactone, Chem. Eng. Sci. 158 (2017) 545-551.
[122] L. Vernieres-Hassimi, V. Casson-Moreno, M.-A. Abdelghani-Idrissi, S. Leveneur, Cooling Configuration Effect on the Thermal Risk of Tubular Reactor, Chemical Engineering Transactions 67 (2018) 37-42.
[123] E. Marco, S. Cuartielles, J. Pena, J. Santamaria, Simulation of the decomposition of di-cumyl peroxide in an ARSST unit, Thermochim. Acta 362(1) (2000) 49-58.
[124] W. Tang, M. Sarvestani, X. Wei, L.J. Nummy, N. Patel, B. Narayanan, D. Byrne, H. Lee, N.K. Yee, C.H. Senanayake, Formation of 2-trifluoromethylphenyl Grignard reagent via magnesium-halogen exchange: process safety evaluation and concentration effect, Org. Process Res. Dev. 13(6) (2009) 1426-1430.
[125] S. Leveneur, Thermal Safety Assessment through the Concept of Structure-Reactivity: Application to Vegetable Oil Valorization, Org. Process Res. Dev. 21(4) (2017) 543-550.
[126] S. Veedhi, A. Sawant, Designing a safer process for the reaction of TFA with sodium borohydride in THF by calorimetric technique, J. Therm. Anal. Calorim. 111(2) (2013) 1093-1097.
[127] S. Veedhi, V. Mishra, S. Kulkarni, R. Gorthi, Incident investigation on thermal instability of an intermediate using adiabatic calorimeter, J. Therm. Anal. Calorim. 115(1) (2014) 909-914.
[128] S. Shimizu, Y. Imamura, T. Ueki, Incompatibilities between N-Bromo-succinimide and Solvents, ACS Publications, 2014.
[129] A.E. Theis, J.P. Burelbach, C.F. Askonas, Safely scale-up processes and accommodate recipe changes, Process Saf. Prog. 28(2) (2009) 135-140.
[130] L. Vernières-Hassimi, A. Dakkoune, L. Abdelouahed, L. Estel, S. Leveneur, Zero-Order Versus Intrinsic Kinetics for the Determination of the Time to Maximum Rate under Adiabatic Conditions (TMRad): Application to the Decomposition of Hydrogen

Peroxide, Ind. Eng. Chem. Res. 56(45) (2017) 13040-13049.
[131] H.K. Fauske, Managing chemical reactivity-Minimum best practice, Process Saf. Prog. 25(2) (2006) 120-129.
[132] S. Mannan, Lees' Process Safety Essentials: Hazard Identification, Assessment and Control, Butterworth-Heinemann, 2013.
[133] O.A. Abdelrahman, A. Heyden, J.Q. Bond, Analysis of kinetics and reaction pathways in the aqueous-phase hydrogenation of levulinic acid to form γ-valerolactone over Ru/C, ACS Catal. 4(4) (2014) 1171-1181.
[134] E.W. Washburn, C.J. West, International critical tables of numerical data, physics, chemistry and technology, National Academies, 1930.
[135] E.C. Carlson, Don't gamble with physical properties, Chem. Eng. Prog. 92 (10) (1996) 35-46.
[136] H.T. Chua, A. Chakraborty, X.L. Wang, The Specific Heat Capacity of Adsorbate-Adsorbent System, 2004.
[137] M. Vasiliu, K. Guynn, D.A. Dixon, Prediction of the thermodynamic properties of key products and intermediates from biomass, J. Phys. Chem. C 115(31) (2011) 15686-15702.
[138] M. Chase, Jr.,, NIST-JANAF Thermochemical, J. Phys. Chem. Ref. Data (1998) 1-1951.
[139] A. Piskun, J. de Haan, E. Wilbers, H. van de Bovenkamp, Z. Tang, H. Heeres, Hydrogenation of levulinic acid to γ-valerolactone in water using millimeter sized supported Ru catalysts in a packed bed reactor, ACS Sustainable Chem. Eng. 4(6) (2016) 2939-2950.
[140] J.R. Leis, M.A. Kramer, Algorithm 658: ODESSA-an ordinary differential equation solver with explicit simultaneous sensitivity analysis, ACM Transactions on Mathematical Software (TOMS) 14(1) (1988) 61-67.
[141] H. Haario, MODEST User's guide, Profmath Oy, Helsinki, 1994.
[142] F. Stoessel, Thermal safety of chemical processes: risk assessment and process design, John Wiley & Sons, 2008.
[143] P. Baybutt, Guidelines for designing risk matrices, Process Saf. Prog. 37(1) (2018) 49-55.
[144] P. Daoutidis, W.A. Marvin, S. Rangarajan, A.I. Torres, Engineering biomass conversion processes: a systems perspective, AlChE J. 59(1) (2013) 3-18.
[145] R.W. Taft Jr, Polar and steric substituent constants for aliphatic and o-Benzoate

groups from rates of esterification and hydrolysis of esters1, J. Am. Chem. Soc. 74(12) (1952) 3120-3128.
[146] R.W. Taft Jr, The separation of relative free energies of activation to three basic contributing factors and the relationship of these to structure, J. Am. Chem. Soc. 75(18) (1953) 4534-4537.
[147] R.W. Taft Jr, Linear steric energy relationships, J. Am. Chem. Soc. 75(18) (1953) 4538-4539.
[148] R.W. Taft Jr, The general nature of the proportionality of polar effects of substituent groups in organic chemistry, J. Am. Chem. Soc. 75(17) (1953) 4231-4238.
[149] J. Lilja, D.Y. Murzin, T. Salmi, J. Aumo, P. Mäki-Arvela, M. Sundell, Esterification of different acids over heterogeneous and homogeneous catalysts and correlation with the Taft equation, J. Mol. Catal. A: Chem. 182 (2002) 555-563.
[150] S. Leveneur, D.Y. Murzin, T. Salmi, Application of linear free-energy relationships to perhydrolysis of different carboxylic acids over homogeneous and heterogeneous catalysts, J. Mol. Catal. A: Chem. 303(1-2) (2009) 148-155.
[151] J. Vojtko, P. Tomčík, A Method for Esterification Reaction Rate Prediction of Aliphatic Monocarboxylic Acids with Primary Alcohols in 1, 4-Dioxane Based on Two Parametrical Taft Equation, Int. J. Chem. Kinet. 46(3) (2014) 189-196.
[152] P.R. Wells, Linear Free Energy Relationships, Chem. Rev. 63(2) (1963) 171-219.
[153] Y. Wang, L. Vernières-Hassimi, V. Casson-Moreno, J.-P. Hébert, S.b. Leveneur, Thermal risk assessment of levulinic acid hydrogenation to γ-valerolactone, Org. Process Res. Dev. 22(9) (2018) 1092-1100.
[154] J.-C. Charpentier, Mass-transfer rates in gas-liquid absorbers and reactors, Advances in chemical engineering, Elsevier (1981) 1-133.
[155] N. Frikha, E. Schaer, J.-L. Houzelot, Methodology of multiphase reaction kinetics and hydrodynamics identification: Application to catalyzed nitrobenzene hydrogenation, Chem. Eng. J. 124(1-3) (2006) 19-28.
[156] N. Gemo, P. Biasi, P. Canu, T.O. Salmi, Mass transfer and kinetics of H_2O_2 direct synthesis in a batch slurry reactor, Chem. Eng. J. 207 (2012) 539-551.
[157] X. Cai, J.L. Zheng, J. Wärnå, T. Salmi, B. Taouk, S. Leveneur, Influence of gas-liquid mass transfer on kinetic modeling: Carbonation of epoxidized vegetable oils, Chem. Eng. J. 313 (2017) 1168-1183.
[158] X. Cai, M. Matos, S.b. Leveneur, Structure-Reactivity: Comparison between the Carbonation of Epoxidized Vegetable Oils and the Corresponding Epoxidized Fatty

Acid Methyl Ester, Ind. Eng. Chem. Res. 58(4) (2019) 1548-1560.
[159] Y. Kawase, Volumetric mass transfer coefficients in aerated stirred tank reactors with Newtonian and non-Newtonian media, Chem. Eng. Res. Des. 66 (1988) 284-288.
[160] C. Wilke, P. Chang, Correlation of diffusion coefficients in dilute solutions, AlChE J. 1(2) (1955) 264-270.
[161] X. Cai, K. Ait Aissa, L. Estel, S.b. Leveneur, Investigation of the Physicochemical Properties for Vegetable Oils and Their Epoxidized and Carbonated Derivatives, J. Chem. Eng. Data 63(5) (2018) 1524-1533.
[162] E. Brunner, Solubility of Hydrogen in 10 Organic Solvents at 298.15, 323.15, and 373.15 K, J. Chem. Eng. Data 30(3) (1985) 269-273.
[163] J.V.H. d 'Angelo, A.Z. Francesconi, Gas-Liquid Solubility of Hydrogen in n-Alcohols at Pressures from 3.6 MPa to 10 MPa and Temperatures from 298.15 K to 525.15 K, J. Chem. Eng. Data 46(3) (2001) 671-674.
[164] S. Raeissi, C.J. Peters, Understanding temperature dependency of hydrogen solubility in ionic liquids, including experimental data in [bmim][Tf2N], AlChE J. 58(11) (2012) 3553-3559.
[165] J. Jiang, F. Cui, S. Shen, X. Guo, L. Ni, Y. Pan, New Thermal Runaway Risk Assessment Methods for Two Step Synthesis Reactions, Org. Process Res. Dev. 22(12) (2018) 1772-1781.
[166] K. Emerson, D. Muzzio, E. Fisher, Identification of Significant Process Safety Risks in the Preparation of Methyl-N-cyanocarbamate, Org. Process Res. Dev. 23(7) (2019) 1352-1358.
[167] C. Guinand, M. Dabros, B. Roduit, T. Meyer, F. Stoessel, Thermal Process Safety Based on Reaction Kinetics and Reactor Dynamics, Chemical Engineering Transactions 48 (2016) 19-24.
[168] D. Am Ende, P. Clifford, D. Northrup, The role of reaction calorimetry in the development and scale-up of aromatic nitrations, Thermochim. Acta 289(2) (1996) 143-154.
[169] B. Grob, R. Riesen, Reaction calorimetry for the development of chemical reactions, Thermochim. Acta 114(1) (1987) 83-90.
[170] F. Stoessel, O. Ubrich, Safety assessment and optimization of semi-batch reactions by calorimetry, J. Therm. Anal. Calorim. 64(1) (2001) 61-74.
[171] A. Diop, I.B. Talouba, L. Balland, N. Mouhab, Thermal characterization of a biodiesel nitration: bio-additive's synthesis by calorimetric methods, Thermochim.

Acta (2019).
[172] W.Y. Pérez-Sena, X. Cai, N. Kebir, L. Vernières-Hassimi, C. Serra, T. Salmi, S. Leveneur, Aminolysis of cyclic-carbonate vegetable oils as a non-isocyanate route for the synthesis of polyurethane: a kinetic and thermal study, Chem. Eng. J. 346 (2018) 271-280.
[173] Y.-S. Duh, C.-C. Hsu, C.-S. Kao, S.W. Yu, Applications of reaction calorimetry in reaction kinetics and thermal hazard evaluation, Thermochim. Acta 285(1) (1996) 67-79.
[174] W. Hoffmann, Y. Kang, J.C. Mitchell, M.J. Snowden, Kinetic data by nonisothermal reaction calorimetry: a model-assisted calorimetric evaluation, Org. Process Res. Dev. 11(1) (2007) 25-29.
[175] A. Zogg, F. Stoessel, U. Fischer, K. Hungerbühler, Isothermal reaction calorimetry as a tool for kinetic analysis, Thermochim. Acta 419(1-2) (2004) 1-17.
[176] Y. Wang, M. Cipolletta, L. Vernières-Hassimi, V. Casson-Moreno, S. Leveneur, Application of the concept of Linear Free Energy Relationships to the Hydrogenation of Levulinic acid and its corresponding esters, Chem. Eng. J. 374 (2019) 822-831..
[177] A. Zogg, U. Fischer, K. Hungerbühler, A new approach for a combined evaluation of calorimetric and online infrared data to identify kinetic and thermodynamic parameters of a chemical reaction, Chemom. Intell. Lab. Syst. 71(2) (2004) 165-176.
[178] F. Stoessel, Experimental study of thermal hazards during the hydrogenation of aromatic nitro compounds, J. Loss Prev. Process Ind. 6(2) (1993) 79-85.

Nomenclature

Notations

C_P	Specific heat-capacity [J.(kg.K)$^{-1}$]
Ea	Activation energy [J.mol^{-1}]
ΔH_R	Reaction enthalpy [J.mol^{-1}]
k	Rate constant
K_{HPA}	Adsorption coefficient of HPA [L.mol^{-1}]
K_{LA}	Adsorption coefficient of LA [L.mol^{-1}]
K_{GVL}	Adsorption coefficient of GVL [L.mol^{-1}]
K_{LA}^{diss}	Dissociation constant of LA [mol.L^{-1}]
K_{HPA}^{diss}	Dissociation constant of HPA [mol.L^{-1}]
K_2	Equilibrium constant
V_{liq}	Volume of liquid [L]
m_{insert}	Insert mass [kg]
m_j	Mass of compound j [kg]
n_j	Number of moles of compound j [mol]
P	Pressure [bar]
q_{el}	Electrical heating-rate [J.s^{-1}]
q_{rx}	Heat-flow rate due to chemical reactions [J.s^{-1}]
R	Gas constant [J.(K.mol)$^{-1}$]
R^2	Coefficient of explanation [%]
ΔT_{ad}	Adiabatic temperature rise [°C]
T_1	Temperature of the reaction mixture [°C]
T_2	Temperature in the gas phase [°C]
T_{Ref}	Reference temperature [°C]
$T_{R,exp}$	Experimental observable value
$T_{R,model}$	Simulated observable value
D_j	molecular diffusion coefficient of *j* [m^2.s^{-1}]
Ea_i	activation energy of reaction *i* [J.mol^{-1}]
Es_i	near-quantitative measure of the steric effect of a substituent i
He	Henry's coefficient [mol.m^{-3}.bar^{-1}]

ΔH_{sol}	dissolution enthalpy [J.mol^{-1}]
k_i	Rate constant of reaction *i*
$k_L.a$	volumetric mass transfer coefficient [s^{-1}]
$(k_L.a)_{modified}$	modified volumetric mass transfer coefficient $[\left(\frac{\text{Pa.s}}{\text{K}}\right)^{0.5} . \left(\frac{\text{Pa.s}}{\text{kg.m}^{-3}}\right)^{0.25} . s^{-1}]$
r_j	rate of formation or disappearance of compound *j* [mol.m^{-3} .s^{-1}]
R_i	reaction rate *i* [mol.m^{-3}.s^{-1}]
R^2	coefficient of explanation [%]
T	temperature [K]
V_{molar}	molar volume [cm^3.mol^{-1}]
w_i	weight percent
y_i	experimental observable
$\bar{y}$	mean value of the experimental observables
$\hat{y}_i$	observable simulated by the model

Greek letters

β	Background heating rate [°C/min]
ω	Objective function
δ	sensitivity factor of a reaction series to steric effects
μ	liquid viscosity [Pa.s]
σ_i^*	near-quantitative measure of the polar effect of a substituent i
ξ	energy dissipation rate per unit mass [W.kg^{-1}]
ρ	mass density [kg.m^{-3}]
ρ^*	sensitivity factor of a reaction series to polar effects
ψ	resonance effect between the substituent & the reaction center
$\omega_{Cat.}$	catalyst loading [kg.m^{-3}]
ϕ	association factor

Subscripts and superscripts

ave	average
Ref	reference

*	interfacial value

Abbreviations

ARSST	Advanced Reactive System Screening Tool
BL	butyl levulinate
BHP	butyl 4-hydroxypentanoate
EL	ethyl levulinate
EHP	ethyl 4-hydroxypentanoate
GVL	γ-valerolactone
HMF	Hydroxymethylfurfural
HPA	4-hydroxypentanoic acid
LA	Levulinic acid
LCB	Lignocellulosic biomass
ML	methyl levulinate
MHP	methyl 4-hydroxypentanoate
ROH	co-product of the second reaction (water, methanol, ethanol or butanol)
TMR_{ad}	Time-to-maximum rate under adiabatic conditions at T_P [hrs]

List of tables

List of figures